THE UNIVERSITY
of EDINBURGH

Analysis of Developmental and Regenerative Spinal Motor Neuron Generation in Zebrafish Larvae

Yujie Yang

Doctor of Philosophy

The University of Edinburgh

2016

Statement of originality

Unless stated otherwise, the research work contained in this thesis has been performed by the candidate, Yujie Yang. I declare that the text presented in this document is original and that no sources other than those mentioned in the text and its references have been used in creating it.

Neither this thesis nor the original work therein has been submitted for academic merit at another educational institution. Data within this thesis have been submitted for the following publication:

[1]equally contributing first authors.

Jochen Ohnmacht[1] , Yu-jie Yang (杨宇婕)[1] , Gianna W. Maurer, Antón Barreiro-Iglesias, Themistoklis M. Tsarouchas, Daniel Wehner, Dirk Sieger, Catherina G. Becker, Thomas Becker (2016). Spinal Motor Neurons are Regenerated after Mechanical Lesion and Genetic Ablation in Larval Zebrafish. Development. doi: 10.1242/dev.129155

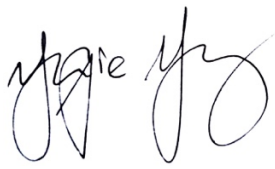

Yujie Yang (杨宇婕)

24th August 2016

Abstract

In contrast to mammals, adult zebrafish are able to regenerate motor neurons and regain swimming ability within 6 weeks after a spinal cord injury. During this regenerative process, a range of developmental signals such as dopamine and serotonin are found to be re-deployed. This makes the research of embryonic signals become essential for the promotion of regeneration in the future. In my research, I am interested in identifying genes that are important for motor neuron development and motor axon differentiation. I also aimed to study the ability of zebrafish larvae to regenerate spinal motor neurons, and whether they can be used to study the essential developmental cues and the mechanisms underlying successful functional recovery.

Motor axons grow out of the spinal cord in a motor neuron subtype specific manner and innervate different muscle groups to facilitate locomotor movements. To find genes and important pathways involved in motor neuron generation and axon development in zebrafish, we conducted an ENU-induced mutagenesis screen in islet-1:GFP transgenic zebrafish, in which a subset of dorsally projecting motor neurons are labelled. We have discovered 6 mutants displaying delayed or inhibited appearance of secondary motor neurons and/or motor axon deficits among 111 F2 families screened. Through subsequent mutant phenotypical analysis, I focused my study in two mutant lines manifesting a lack of islet-1:GFP motor neurons, and an absence of islet-1:GFP motor axons. I used various molecular markers to characterise the mutant phenotypes and observed several additional anatomical defects. I also initiated the study of causative mutation analysis based on the candidate gene list generated from Next Generation Sequencing (NGS). To gain an insight of the genes' role in motor neuron development and axonal differentiation, I started functional analyses in order to confirm genes that are responsible for the observed motor neuron/axon phenotypes, and I have achieved some promising preliminary results.

Motor neurons are generated from the motor neuron progenitor domain (pMN). This neurogenesis process sharply declines at 48 hours post-fertilisation (hpf), while pMN progenitor cells continue to proliferate to produce oligodendrocytes. By inflicting a

mechanical lesion in the spinal cord of zebrafish larvae, we demonstrated that they are capable of regenerate new motor neurons and achieve full functional recovery within 48 hours following the injury, sharing similar mechanisms to that of the adult zebrafish. I further studied oligodendrocyte generation and found that pMN domain is able to switch from oligodendrogenesis to motor neuron generation after a spinal lesion. This demonstrates the high plasticity of the pMN domain. Interestingly, the generation of dorsal Pax2-positive interneurons was not altered after the lesion, suggesting that the regenerative potential differs in different progenitor domains. This study showed that the motor neuron regenerative process in zebrafish larvae is robust and they can be used for studying motor neuron regeneration.

Taken together, the discovery of the genes from our screen will provide insights to the developmental cues that are involved in motor neuron generation and axon growth. Furthermore, spinal cord lesion in larval zebrafish larvae is established as a regenerative model that can be utilized to dissect the roles and mechanisms of these signals and pathways in the promotion of motor neuron regeneration.

Lay summary

Motor neurons are the cells in the spinal cord that communicate with muscles and are responsible for all movement. In humans, motor neuron diseases and spinal cord injuries often cause a loss of these neurons which cannot be replaced, and consequently lead to life-long paralysis and death. In contrast to mammals, adult zebrafish are able to regenerate spinal motor neurons and regain their ability to swim within weeks of an injury. This process requires the reactivation of the signals that are important for producing motor neurons during the development of embryos. More importantly, these signals are found to promote the generation of motor neurons in human stem cells, demonstrating that studies in zebrafish may be applicable to humans. If we understand the developmental signals and pathways that are essential for making motor neurons, we might be able to promote the regeneration of motor neurons in the future in injury and disease. In my research, I study (1) which genes control the generation of motor neurons and their path to contact muscle targets; (2) whether we can use larval zebrafish as an animal model to study the essential signals and mechanisms underlying successful functional recovery.

In order to dissect the underlying gene pathways for motor neuron generation, I performed a screen for gene defects that lead to abnormal development of motor neurons. Zebrafish were chemically treated to produce random gene defects. In the screen, I have successfully discovered 6 mutant fish lines manifesting abnormal motor neuron and axon development. I focused my study in two mutants displaying a lack of motor neurons and an absent of motor axons. I investigated the anatomy of these two mutants and found various defects. I started investigating which genes are responsible for the observed abnormalities in the motor neurons.

Previous work within the research group has found that larval zebrafish are able to remake new motor neurons after a spinal cord injury like the adult zebrafish, and the regenerative process is robust and fast as they regain full functional recovery within 48 hours.

Taken together, the discovery of these genes will shed light on important signals during the development of the nervous system, and by establishing larval zebrafish as a regenerative model organism, we can apply these discovered developmental cues in the lesioned zebrafish larvae to study their roles in promoting motor neuron regeneration. The findings may ultimately be used to regenerate spinal cell types in spinal injury and human motor neuron diseases.

Acknowledgements

First and foremost, I would like to express my sincerest gratitude to my supervisors, Professor Catherina Becker and Dr. Thomas Becker, who have supported and guided me throughout my PhD as well as my Masters for the past 5 years with their encouragement, patience and insightful discussions.

I thank the University of Edinburgh for funding my work through the award of a PhD scholarships. I am also very grateful to my supervisor Professor Catherina Becker for her support.

I would like to thank my supervisor Professor David Lyons for his valuable guidance throughout my genetic screening project. A special thank you also goes to Dr. Richard Poole from University College London for kindly performing the Bioinformatics analysis, as well as Dr. Antón Barreiro-Iglesias and Dr. Karolina Mysiak for their assistance with the phenotypic screen. My thanks also go to Linde Kegel, Anna Klingseisen, Maria Rubio and Rafael Almeida from the Lyons group for sharing their expertise and valuable advice.

I have been blessed with a group of cheerful colleagues and friends in my daily work - thank you to all the members of the Becker lab and Kelda Chia for your support, friendship and kindness.

Finally, I would like to thank my family for their unconditional love and Peter for his support and encouragement at every step of the way.

Table of Contents

Chapter 1 General Introduction

Overall aims of my PhD

In contrast to mammals, zebrafish possess a high regenerative capacity of the central nervous system. It has shown that adult zebrafish are able to regenerate motor neurons after a spinal cord injury, and embryonic signals such as dopamine and serotonin are found to be reactivated during the regenerative process (Reimer et al. 2008; Reimer et al. 2013; Barreiro-Iglesias et al. 2015). This makes the studies of developmental cues become essential for the promotion of regeneration in the future. I wondered what controls motor neuron development – which genes and signalling pathways participate in the generation of motor neurons during development? Also, I wondered whether larval zebrafish would be able to regenerate motor neurons following injury like the adults, and could be used as a model organism to dissect developmental signals and mechanisms underlying successful functional regeneration. In chapter 3 of this thesis, 1) I described an unbiased genetic screen to look for genes that are important for motor neuron and axon differentiation; 2) I characterised the mutants displaying motor neuron and axon phenotypes discovered in a screen, and I investigated the potential candidate genes that are responsible for the mutant phenotypes observed. In chapter 4, I analysed the lesion-induced spinal motor neuron regeneration in zebrafish larvae and the regenerative potential of different cell types.

In the following introduction part, I will introduce briefly the formation of zebrafish spinal cord, the generation of motor neurons and the known signalling pathways involved in this process. I will discuss the regenerative ability of mammals and zebrafish, and elucidate the features of the zebrafish as a model in connecting research on neurodevelopment with disease research.

1.1 Development of zebrafish spinal cord

1.1.1 The formation of neural tube

In central nervous system (CNS), brain and spinal cord are derived from the neural tube. Fertilized eggs go through cell divisions to reach the gastrulation stage during

zebrafish embryogenesis, from there three germ layers are formed: endoderm, mesoderm and ectoderm (Stifani 2014). The mesoderm gives rise to a narrow rod structure called notochord. The nervous system such as brain and spine are derived from the ectoderm. The initial structure of the neural tube is a flat sheet of the ectodermal epithelium cells that thickens into a columnar shape called neural plate (Kimmel et al. 1995) (Fig 1.1). During neurulation, epithelial cells in the neural plate infolds at the midline to create a fish-specific structure, the neural keel (Araya et al. 2016). The neural keel develops to form a more cylindrical-like structure called the neural nod, which cavitates at the ventro-dorsal midline to generate a lumen and form the neural tube (Kimmel et al. 1995; Araya et al. 2016). The neural tube sits dorsal to the notochord. The caudal part of the neural tube later develops into the spinal cord (Yamada et al. 1993). The inner layer (ependymal layer) adjacent to the lumen is known as the ventricular zone. The central canal of the spinal cord is continuous with the ventricular zones of the brain (Gilbert 2000). The ventricular zone is lined with multi-ciliated neuroepithelial cells. Neuroepithelial cells generate ependymal cells, neuroblasts and glioblasts that divide into neurons and glia cells. Therefore, neuroepithelial cells are the stem cells/progenitor cells in the CNS (Patestas & Gartner 2013). For the purpose of this thesis, stem cells refer to self-renewable undifferentiated cells that give rise to different neural cell types. Progenitor cells refer to specified stem cells that differentiate into specific cell types. For instance, motor neuron progenitor cells develop into motor neurons. In the injured spinal cord, ependymal cells act as stem cells in response to injury (Panayiotou & Malas 2013). Motor neurons that reside in the ventral part of the spinal cord are generated from ventral neuroepithelial cells, while other types of neurons that lie in more dorsal areas of the cord are derived from more dorsal parts of the neuroepithelium.

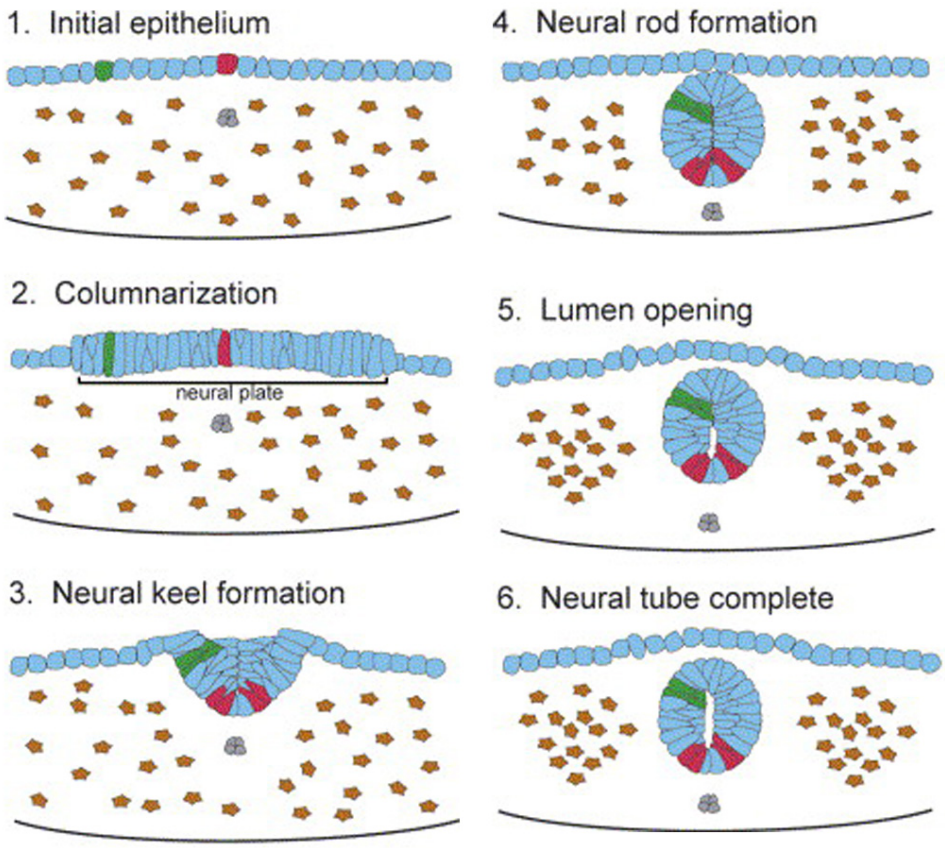

Fig 1.1 Zebrafish neurulation. In zebrafish, an initial epithelium layer thickens to form the neural plate. Epithelial cells in the neural plate converges at the midline to form a neural keel and then subsequently a neural rod. Through cavitation, a lumen opens from ventral to dorsal midline of the neural rod which then transforms into a neural tube. Adapted from (Lowery & Sive 2004).

1.1.2 Formation of the motor neuron progenitor domain (pMN)

Multiple molecules and transcription factors are reported to be involved in the organization of cells in neural tube to create distinct cell-type specific progenitor zones. Notably, sonic hedgehog (Shh) is found to provide positional information for the generation of different neuron types and stereotypical patterning along the neural tube (Francius & Clotman 2014). Shh is first secreted by notochord and later expressed by floor plate from the ventral spinal cord (Yamada et al. 1993). The floor plate of the spinal cord is positioned dorsal to the notochord. It consists of a layer of specialised glia cells and serves as a source of inductive signals (Jessell 2000). Along

the ventral to dorsal axis of the neural tube, Shh displays a ventral-high to dorsal-low level concentration gradient which controls the fate of interneurons and motor neurons (Yamada et al. 1993; Pfaff & Kintner 1998; Francius & Clotman 2014), whereas other molecules such as Bone Morphogenetic Proteins (BMPs) and Wnt secreted from the roof plate in the dorsal neural tube show a ventral-low to dorsal-high level gradient that contribute to the generation of sensory interneurons (Fig 1 A; Stifani 2014; Shirasaki & Pfaff 2002). This polarized signal expression of Shh, together with homeodomain (HD) transcription factors, divide neuronal progenitor into five cell-type specific progenitor domains in ventral spinal cord: p0, p1, p2, pMN, p3 (Fig 1 B, Stifani 2014). Depending on their interaction with Shh, HD factors can be divided into two classes (Stifani 2014; Davis-Dusenbery et al. 2014). Class I is repressed by Shh, which includes Irx3, Dbx1, Dbx2, and Pax6. On the contrary, Shh induces Class II factors such as Nkx6.2, Nkx6.1, Nkx2.2, and Olig2 which belongs to basic helix-loop-helix (bHLH) family. The cross-repressive interaction between class I and class II transcription factors following the graded Shh signalling level define the boundaries of each progenitor domain, while the restricted combination of two classes refine the neuronal type produced from each progenitor zone. For example, the pMN domain forms in the ventral part of the neural tube where the level of Shh is high and exposure is long. pMN cells uniquely co-express homeodomain proteins Nkx6.1, Pax6 and Olig2 and give rise to motor neurons (Reimer et al. 2009). Each progenitor domain specifies distinct neuronal types that are bilaterally distributed along the dorso-ventral axis of the spinal cord. p0, p1, p2 and p3 progenitors give rise to interneuron types V0-V3 (Fig 1 C, Stifani 2014).

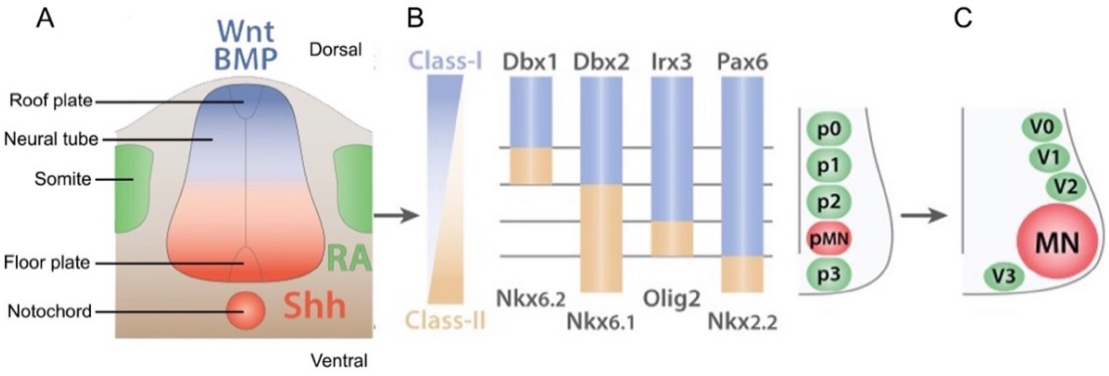

Fig 1.2 Shh gradient and the patterning of neuronal subtypes on the ventral neural tube. (A) Schematic cross section of neural tube. shh shows a high to low level concentration gradient from ventral to dorsal neural tube. **(B)** Interaction of two classes of HD factor with Shh in determine 5 progenitor zones. **(C)** Each progenitor domain gives rise to a distinct cell type. Motor neurons are generated from the pMN domain of the ventral spinal cord. Adapted and modified from Stifani (2014).

1.1.3 From progenitor cells to mature motor neurons

The progress from the formation of the pMN domain to the maturation of motor neurons that project motor axons into periphery is regulated by various signals and transcription factors. The fate of progenitor cells in pMN zone is in part determined by Olig2 transcription factor inducing differentiation of first motor neurons and later oligodendrocytes (Francius & Clotman 2014; Allan & Thor 2003; Briscoe & Novitch 2008). In mammals such as mouse, Olig2 interacts with another bHLH protein Neurogenin2 (Neurog2) to promote motor neuron generation. When Neurog2 is down regulated, Olig2 acts with Nkx2.2 and Sox10 to give rise to oligodendrocytes (Allan & Thor 2003). After progenitor cells exit from cell cycles, they acquire and consolidate motor neuron identity by expressing LIM-HD factors downstream of Olig2 (Shirasaki & Pfaff 2002; Allan & Thor 2003). For instance, a homeobox gene – motor neuron and pancreas homeobox 1 (*mnx1;* also known as *hb9*) is expressed primarily in post-mitotic motor neurons (Francius & Clotman 2014). A LIM homeobox gene *islet-1* is initially expressed in all early post-mitotic cells but later restricted in a subtype of motor neurons (Pfaff & Kintner 1998). Therefore, Hb9 and Islet-1 have been used as early markers for motor neurons. Fully differentiated motor neurons are cholinergic and express choline acetyltransferase (ChAT) enzyme (Shirasaki & Pfaff 2002).

During development, motor neurons that share similar functions group together to form motor neuron pools (Stifani 2014). Based on the locations and axon connections, motor neurons can be categorized into two general classes: Upper class motor neurons located in the cortex of the brain that extend axons into the spinal cord; lower class motor neurons which cell bodies reside in the spinal cord are the only

type of neurons that grow axons out of the CNS into the skeletal muscles in the periphery (Davis-Dusenbery et al. 2014). The zebrafish has two main types of spinal motor neurons according to the time of birth and innervated muscle types. They are primary motor neurons and secondary motor neurons (Patrick J. Babin et al. 2014). Three identifiable primary motor neurons per hemisegment control fast muscle fibres. The rostral, middle and caudal primary motor neurons innervate muscles in ventral-lateral, dorsal and ventral part of the body, respectively. Secondary motor neurons are born later than the primary motor neurons. They are a type of abundant cells with small somas that extend axons to innervate both fast and slow muscle fibres.

As part of the neuronal differentiation programme, post-mitotic motor neurons initiate axon outgrowth and their stereotypical pathfinding (Shirasaki & Pfaff 2002). Motor axons at first follow a common pathway to grow ventrally as they leave the spinal cord. Once they reach the horizontal myeseptom, the axonal growth cones of motor neurons follow specific guidace cues and choose their distinc pathway to project into the perihery. Coordinated locomotor movements rely on the correct connection between motor aoxns and their final skeletalmuscle targets. Based on their eventual projection targets, Bonanomi & Pfaff (2010) divided motor axons into two general categories: dorsally projecting axons and ventrally projecting axons. For example, in chicks, motor neurons at medial motor column (MMC) extend axons dorsally to innervate the dermomyotome, whereas axons of lateral motor column (LMC) neurons project ventro-laterally to the limbs (Bonanomi & Pfaff 2010; Jessell 2000). In zebrafish spinal cord, based on the motor neuron types, there are two main types of motor axons - primary motor axons and secondary motor axons (Myers et al. 1986). Both types of motor axons extend dorsal and ventral projections for muscle innervation.

The exit points of motor axons from the spinal cord and the recognition of the correct targets at different locations in the periphery are regulated by different transcription factors (Eisen 1994). A combination of LIM homeodomain (LIM-HD) transcription factors expressed in post-mitotic motor neurons first acts as a determinant of motor neuron subtype identity prior to the initiation of their axon outgrowth, and then as a

decision making code in axon pathway selection (Appel et al. 1995). For example, LIM-HD gene *lim3* and *islet-1* are expressed in dorsally and ventro-laterally projecting primary motor neurons, whereas *lim3* and *islet-2* expression are detected in primary motor neurons that project ventrally. Axon guidance molecules are also regulated by LIM-HDs. Zhong et al (2012) found that *chondrolectin* (*chodl*) gene downstream of LIM-HD is expressed in primary motor neurons. Knockdown of *chodl* leads to a specific phenotype of shorter CaP motor axons at the horizontal myoseptum, suggesting the role of *chodl* in the target recognition for axon pathfinding (Zhong et al. 2012).

In summary, the effects of polarised signals such as Shh, Wnt and BMPs on the unspecified epithelium cells along the ventro-dorsal axis of the neural tube, in collaboration with HD transcription factors and bHLH factors to define pMN domain specifies the fate of progenitor cells. When progenitor cell proliferation is complete, progenitor cells acquire motor neuron identity by expressing LIM-HD factors such as Hb9 and Islet-1. Further regulation of LIM-HD genes consolidates the motor neuron subtypes and initiate cell-type specific axonogenesis.

1.2 Neurodegeneration – disease and injury

Motor neuron disease (MND) is one of the most common forms of neurodegenerative disease. It manifests as a progressive neuronal death – especially of lower motor neurons in the spinal cord and brainstem, and upper motor neurons in the brain motor cortex, which leads to progressive muscle weakening and eventually failure of the respiratory system (Shaw 1999). Motor neuron disease is incurable, and current treatments are mainly symptomatic. For instance, genetic mutations in the gene encoding the enzyme Cu/Zn superoxide dismutase 1 (SOD1) were identified to account for 20% of family inherited MND (Shaw 1999); mutation of the *survival of motor neuron* 1 (*smn1*) gene was found to associate with spinal muscular atrophy (SMA), in which lower motor neurons located in the anterior horn of the spinal cord were selectively degenerated (Kolb & Kissel 2011). Environmental factors such as oxidative stress and glutamate excitotoxicity were also found to increase the vulnerability of motor neurons to neuronal damage and death (Shaw 1999). Ferrante

et al (1997) showed that in both sporadic and familial amyotrophic lateral sclerosis (ALS) patients, the level of immunostaining for 8-hydroxy-2'-deoxyguanosine (OH^8dG) was significantly increased in the spinal cord of both types of ALS patients. OH^8dG is a marker for oxidative free radical damage to nuclear DNA (Ferrante et al. 1997). Excessive Ca+ influx though the glutamate receptor AMPA (alpha-amino-3-hydroxy-5-methyl-4-isoxazole propionic acid) was found contribute to excitotoxic death of neurons in motor neuron cultures from mouse spinal cord (van Den Bosch et al. 2000). However, the precise genetic and neurobiological mechanisms underlying the motor neuron injury, and why some populations of motor neurons are more vulnerable to the disease are still uncertain.

Another common form of neurological disorder that leads to motor neuron death is spinal cord injury (SCI). Every year 1,000 of people suffer spinal cord injury in the UK and Ireland. The traumatic injury of the spinal cord damages the vasculature, leading to glutamate excitotoxicity, inflammation as well as a cascade of cell death of motor neurons and interneurons, as well as oligodendrocytes (Thuret et al. 2006). In the injured spinal cord, a glia scar composed of astrocytes, microglia and glia progenitor cells forms after the injury. Cells in the scar secrete molecular inhibitors that prevented axons from sprouting across the injury site, causing disrupted descending and ascending axon tracts which eventually result in the degeneration of the caudal axons (Thuret et al. 2006; Silva et al. 2014). Moreover, the loss of oligodendrocytes often causes demyelination, which subsequently affects the remaining axons. These chains of events contribute to the poor functional recovery post-injury, and often leads to disabilities, neurological deficit and even complications of the other systems. The aim of spinal cord injury research is to find out what can be done to interfere with the degenerative process, and to promote the regeneration of motor neurons and axons, therefore to provide an effective therapy for functional recovery. However, this cannot be achieved without understanding the mechanisms underlying the motor neuron degeneration and regeneration. To do this, it is necessary to establish an animal model with robust regenerative capacity, as the findings may shed light to potential therapeutic applications.

1.3 Regeneration: An overview

1.3.1 Regeneration paradigm

Poss (2010) and Vervoort (2011) classified regeneration into two general types: homeostatic regeneration and injury-induced regeneration. Homeostatic regeneration (physiological regeneration) is the regular physiological turnover of limited numbers of cells due to natural cell death and ageing, or a replacement of body parts such as teeth during the life-cycle (Vervoort 2011). Injury-induced regeneration (restorative regeneration) is the repair of tissues caused by an insult such as amputation, ablation or disease (Poss 2010). For the purpose of this thesis, the term regeneration refers to injury-induced regeneration.

Regeneration is a biological phenomenon involving a series of events including initiation by injury, activation of quiescent tissue to generate new cells in response toinsult, as well as maintenance and integration of these cells into a functional network. Different experimental paradigms and injury models have been used for regeneration study. Mechanical injury and chemically-induced injury are commonly used injury models. Mechanical injury is usually induced by surgical procedures such as transection, cryoinjury, stab lesion and so forth. Transection is inflicted by using a sharp instrument such as an injection gauge, micro-scissors or a scalpel to make a partial or full disassociation between the rostral and caudal side of the structure (Cheriyan et al. 2014). It has been used extensively for the study of spinal cord regeneration in many animal models including mice and zebrafish (Lukovic et al. 2015; Becker et al. 1997; Reimer et al. 2008). Transection model is easy to reproduce, however, it can be difficult to apply consistent partial injury (Cheriyan et al. 2014). Cryoinjury involves an acutely damage to tissue or organ by applying a dry ice-cooled steel probe or copper filament. This method is precise and experimentally controllable. lez-Rosa & Mercader (2012) established a cryoinjury technique to induce myocardial infraction in adult zebrafish heart. Injury induces cell death via apoptosis or necrosis, which is similar to the cell death mechanism found in myocardial infraction (Chablais & Jaźwińska 2012). The chemically induced injury model is often performed by the injection or direct exposure of a chemical agent or a toxin (Kuyinu et al. 2016). For instance, cuprizone is a toxin that targets mature

oligodendrocytes (Torkildsen et al. 2008). Administration of cuprizone in mice lead to oligodendrocytes apoptosis and demyelination, which are the clinical features of multiple sclerosis (Torkildsen et al. 2008). This model has been used and well characterised for multiple sclerosis research. It has been shown that alterations in surrounding environment as well as regenerative response varies depending on the nature of the injury. Hardy et al (2016) compared different muscle injury models that are commonly used for the study of skeletal muscle regeneration in mice, such as freeze injury (cryoinjury), chemical and toxin models. The study found a massive loss of muscle stem cells following the chemical/toxin-induced injury compared with freeze injury. Moreover, freeze injury caused muscle damage is usually focal, whereas chemical/toxin model has an impact on the entire muscle (Hardy et al. 2016). Therefore, one must have a careful consideration based on the goals and expected outcomes of the study when it comes to the selection of an optimal injury model.

In response to injury, new cells are re-produced during regeneration and tissue repair. Newly regenerated cells arise from either resident stem cells/progenitor cells, or through de-differentiation or trans-differentiation of tissue cells (Tanaka & Reddien 2011). Stem cells are self-renewable and can produce one or more cell types. Progenitor cells are the precursors of a mature cell type. An example of stem cell/progenitor based regeneration is planarians. Study has shown that adult dividing pluripotent stem cells, neoblasts, are the source for new cells and contribute to blastema formation in amputated planarians (Tanaka & Reddien 2011). Blastema is a growth zone consisting of a mass of accumulated proliferative progenitor cells that eventually form newly re-produced structures. Different types of tissue regeneration involve specific lineage-restricted progenitors. In vertebrate, satellite cells are the skeletal muscle progenitors and express Pax3 and Pax7 markers (Kang & Krauss 2010). In regenerative myogenesis, quiescent satellite cells are reactivated upon injury and fuse into impaired muscle fibres (Kang & Krauss 2010). Regenerative spinal motor neurons are derived from a distinct population of cells located in ventral motor neuron progenitor domain (Reimer et al. 2009). New cells can also be regenerated through de-differentiation. De-differentiation is a process by which changes in genetic level revert fully mature cells to proliferate again and re-

differentiate within its own lineage (Jopling et al. 2011). Using 4-hydroxy-tamoxifen (4-OHT)-inducible Cre/lox system, Jopling et al (2010) lineage-traced regenerating cardiomyocytes in zebrafish heart. The study found pre-existing cardiomyocytes undergo limited de-differentiation to drive heart muscle cell regeneration. This proliferation of terminally differentiated cardiomyocytes correlates with the change in *plk1* gene expression (Jopling et al. 2010). Another route to regeneration is via trans-differentiation. Trans-differentiation is an irreversible switch of a cell lineage into another new cell type (Jopling et al. 2011; Shen et al. 2003). For example, vertebrate radial glial cells are originated from ectodermal tissues, whereas muscle and cartilage are derived from mesoderm (Echeverri & Tanaka 2002). During axolotl tail regeneration, radio glial cells are found not only contribute to the functional repair of the spinal cord, but also convert their cell phenotype to muscle cells to promote the regeneration of surrounding tissues (Echeverri & Tanaka 2002).

1.3.2 Regeneration and development

Development and regeneration in animals is the result of complicated genetic interactions and regulatory networks. Studies have shown similar mechanisms underlie development and regeneration (Key 2016; Wilken & Reh 2016; Mercola et al. 2011). For instance, there is a re-access of embryonic programmes and reactivation of developmental gene expression during the cell damage repair in regeneration (Tanaka & Ferretti 2009; Wang et al. 2007; Burton & Finnerty 2009). Transcription factor Pax6 is expressed in developing retinal progenitors and retinal neurons (Karl et al. 2008). In mice retina, a majority of newly regenerated retinal progenitor cells express Pax6 marker following a N-methyl-D-aspartic acid (NMDA) induced damage. In chicks, fish and Xenopus, Pax6 is also detected in retinal neuronal progenitors during retinal growth and found to be re-expressed during lens regeneration (Fischer & Reh 2001; Hitchcock et al. 1996; Henry et al. 2008). Proneural genes such as *Ascl1* regulate the specification and differentiation of neural progenitor cells during retina formation (Castro et al. 2011). *Ascl1a* expression can be detected in proliferating Müller glial cells after retinal injury in chick and zebrafish (Fausett et al. 2008). In mice retina, stimulation of *Ascl1*converted quiescent Müller glia to a proliferating neural progenitor state after injury (Wilken &

Reh 2016). In vertebrate limb and tail development, mesenchymal progenitor cell proliferation necessary for limb formation is regulated by Wnt/β-catenin signalling (Kawakami et al. 2006). This developmental signal is reactivated after Xenopus tail and zebrafish caudal fin amputation and promotes regeneration (Lin & Slack 2008; Kawakami et al. 2006). It has shown that *wnt10a* can activate Wnt/β-catenin signalling during limb development (Stoick-Cooper et al. 2007). Following fin amputation, *wnt10a* was upregulated from 3 to 6 days after injury. Blockage of Wnt/β-catenin signalling resulted in decreased blastema progenitor proliferation, whereas enhanced Wnt/β-catenin signalling augments fin regeneration. In the developing cerebellum, fibroblast growth factor (FGF) genes are expressed and involved in many neurogenesis processes such as neuronal precursor production, granule cell proliferation, differentiation and migration in the brain (Yaguchi et al. 2009). In differentiating cerebellum, FGF signalling is required for the cerebellum neuronal cells regeneration and anterior hindbrain re-patterning after the cerebellum ablation in zebrafish (Koster & Fraser 2006). Sox2 belongs to the SoxB1 family and is expressed in neural stem cells as well as progenitor cells in adult brain (Gaete et al. 2012). In Xenopus larvae, Sox2 cells are also observed in the ependymal zone of the developing and regenerative spinal cord (Muñoza et al. 2015; Gaete et al. 2012). Gaete et al (2012) detected an increased level of both *sox2* mRNA and Sox2 protein in ventral ependymal canal in the injured spinal cord of Xenopus tadpoles. Sox2 cells are activated and proliferate in response to spinal cord transection (Gaete et al. 2012). They also migrate to the ablation gap to contribute to axonal regeneration (Gaete et al. 2012). Block Sox2 function leads to disrupted spinal cord repair, supporting the positive role of Sox2 in spinal cord and tail regeneration in tadpoles. Taken together, there is a recapitulation of embryonic signals during the regeneration. Also, many of these genes are evolutionally conserved and therefore likely to share similar regeneration mechanisms across species.

However, studies also show differences exist between the genetic requirement for development and regeneration (Vervoort 2011; Burton & Finnerty 2009). Mizuno et al (1999) compared the expression of three classes of *crystallin* genes (*αA, βB1 and γ-crystallin*) during lens formation and regeneration in Xenopus embryos. In

embryonic Xenopus lens, positive signals for the expression of all three *αA*, *βB1*, and *γ-crystallin* genes can be detected simultaneously in lens placode at embryonic development stage 26-27, and later expressed in lens fibre cells. However, during the lens regeneration, only *αA* and *βB1-crystallin* signals were observed at Freeman's stage 3 before lens fibre differentiation can be distinguished. The expression of *γ-crystallin* was detected after the beginning of the lens fibre differentiation at Freeman's stage 4 (Mizuno et al. 1999). This indicates that although similar developmental genes were reactivated, the requirement for the timing of *crystallin* genes expression could be different during the lens regeneration. In *Nematostella*, the *Hox-like* gene *anthox6* is expressed in pharyngeal during larval development. However, *anthox6* signal is not detected during physa regeneration (Burton & Finnerty 2009). A member of FGF family Fgf20, which is not required for limb development during embryogenesis, has been identified to be able to regulate blastema formation and initiate fin regeneration in zebrafish (Whitehead et al. 2005; Vervoort 2011). These studies demonstrate that at least some partial distinct mechanisms are involved in regeneration.

To learn how to reactivate these intrinsic regeneration programs in future research, the challenge lies in exploring and systematically comparing the similarities and differences between the two processes.

1.3.3 Regeneration across species

Regeneration occurs at different levels such as a cell type, an organ, a body structure or even a whole organism (Rinkevich & Rinkevich 2013; Tanaka & Reddien 2011). There is a great diversity of regenerative capability exhibit across species. Some organisms can regrow a whole body, others only have some form of ability to replace a body part, or are even incapable of regeneration (Bely & Nyberg 2010). It also varies in the same animal in different body parts. For instance, a lizard can regenerate a new tail but fails to regrow a limb (Alibardi & Toni 2005). Regeneration differs at different stages of life-cycle amongst animals. Salamander limb regeneration occurs throughout the life, whereas regeneration in animals like chicks and Xenopus is largely age-dependent (Martino et al. 2013).

While regeneration in some simple invertebrate organisms such as *Drosophila melanogaster* and *C. elegans* is poor, planaria and hydras possess powerful regenerative abilities (Alvarado & Tsonis 2006). Planarians are fresh water flatworms and have been used as an animal model to study regeneration (Baguna 2001). Planarians regenerate through the proliferation of pre-existing pluripotent stem cells (Tanaka & Reddien 2011). They are able to regenerate all cell types and regrow body parts including the head and tail. Remarkably, even an entire animal can be regenerated from a small piece of body fragment. Hydras have very simple body structure: a foot, a polarized body axis and a head (Alvarado & Tsonis 2006). They also can regenerate hydra polyps from a tiny piece of tissue or even from dissociated cells (Poss 2010). Three types of stem cells are found to play a role in the hydra regenerative process: ectodermal epithelial cells, endodermal epithelial cells, and interstitial stem cells (Tanaka & Reddien 2011). It has shown that pre-existing interstitial cells might be able to transdifferentiate to another cell type during regeneration. Hydra orthologues of developmental genes and signalling pathways such as *Hox* genes, Wnt and FGF have been identified during the regeneration process (Alvarado & Tsonis 2006).

Although not be able to regenerate the whole organism, amphibians such as newts and salamanders can regrow limbs, tail, heart and spinal cord (Mchedlishvili et al. 2012; Alvarado & Tsonis 2006). In newts, epithelial cells cover the wound and provide signals for the cells to re-enter the cell cycle, to proliferate and differentiate into new cells. FGFs and SHH signalling are found to be reactivated during the limb regeneration. Salamanders are capable of regenerating retina, optic tectum and muscles. The formation of blastemal cells, a cluster of de-differentiated cells, contributes to their epimorphic regeneration (Mchedlishvili et al. 2012; Becker & Becker 2015).

A Xenopus tadpole tail consists of a spinal cord, a notochord and segmented myotomes with surrounding tissues (Slack et al. 2008). Amputation of the tadpole tail triggers ependymal cells in the spinal cord and the notochord to proliferate and

migrate to the wound site, forming an ependymal epithelium structure called neural ampulla which leads to a full tail regeneration in 20 days (Gaete et al. 2012; Slack et al. 2008). In Xenopus larvae, a spinal cord is necessary for the tail regeneration (Taniguchi et al. 2008). Ablating spinal cord in tadpoles resulted in decreased proliferation and differentiation of the notochord cells, and leads to regeneration of a shorter and twisted tail. Tadpoles can repair their cornea within 1 to 2 weeks (Beck et al. 2009; Slack et al. 2008). Cells of the inner layer of outer cornea transdifferentiate into new lens cells and eventually develop into a new lens. However, the regenerative ability in Xenopus larvae is limited to pre-metamorphic stages, little or no regenerate is observed after the onset of metamorphosis following an amputation.

Zebrafish have a robust capacity of re-generating a variety of organs and tissues including the fin, spinal cord, retina, and heart. Poss et al (2002) suggested that the ventricular myocardium of an adult zebrafish heart can recover in 1 week after a mechanical injury without scaring. The regenerated heart showed no obvious difference from the heart of an un-injured fish. During the zebrafish cardiac regeneration, undifferentiated progenitor cells acquires cardiac fate by expressing transcriptional activators such as NKX2.5, TBX20 and HAND2, and then differentiate into new proliferative cardiomyocytes (Lepilina et al. 2006). In a recent study, Mokalled et al (2016) analysed transcription factors that are up-regulated during the zebrafish spinal cord regeneration and found an increased level of connective tissue growth factor a (ctgfa). They found *ctgfa* is expressed in the ventral ependymal cells at 1 to 2 weeks post injury and promotes early glial bridging across the lesion site. ctgfa mutant displayed reduced axon regeneration across the lesion site and diminished swimming ability, whereas the overexpression of *ctgfa* leads to increased glial bridging and axon regeneration (Mokalled et al. 2016).

Birds in their embryonic stage display some capacity for retinal regeneration. In chick retinas, Müller glial cells serve as the source of neural regeneration (Fischer & Reh 2001). It has shown that neurotocxin injection to the retina triggers Müller glia at the central retina to re-enter their mitotic cycle, de-differentiate into progenitor fate and produce new neurons and glial cells. In young mice and rats, injury-induced

proliferative response of Muller glia was also observed (Wilken & Reh 2016). Neonatal mouse heart retains significant cardiac regenerative potential (Porrello et al. 2013). They are able to produce new cardiomyocytes through proliferation of existing cardiomyocytes after inducing ischemic myocardial infarction. However, the regenerative ability in birds, mice and rats sharply declines after the embryonic stage and becomes extremely low in adulthood.

1.3.4 Regeneration in mammals and limitations

In comparison with other well studied regeneration models, adult mammalian species have very little ability to replace lost cells after an insult or under pathological conditions. Humans show some regenerative response to fingertips amputation but only restrictedly limited to the distal end or the terminal phalanx (Muneoka et al. 2008). In adult human and mouse heart, in vitro studies showed that cardiac progenitor cells have the potential to differentiate into fully mature cardiomyocytes and cardiomyocytes was likely to be replenished by precursor cells after injury (Laugwitz et al. 2005; Hsieh et al. 2007; Wu et al. 2008). However, the limited regeneration in human hearts suggested that it is clearly insufficient to restore heart function. Although it was believed that mammals do not regenerate new nerve cells after an insult or under pathological conditions, studies have shown increased new born ependymal cells, astrocytes and oligodendrocyte progenitor cells restricted to the lesion site in the injured mice spinal cord (Mothe & Tator 2005; Barnabé-Heider et al. 2010). This suggests a degree of plasticity in mammalian CNS progenitor cells. However, only very limited neurogenesis occurred in the injured mammalian CNS. The regeneration efficiency is also extremely low and incomplete. For instance, in brain regions that are regarded as neurogenic such as the subgranular zone (SGZ) of the hippocampus and subventricular zone (SVZ), in which neurogenesis is active throughout life, an injury leads to increased proliferation of progenitor cells and generation of new neurons (Arvidsson et al. 2002). The study investigated newly formed neurons after a stroke and found that some were able to differentiate into mature neurons and migrate from SVZ to damaged area. However, over 80% of the newborn neurons died between 2 to 6 weeks post-ischemia, and eventually lead to only 0.2% neuronal replacement of the lost cells by the new born neurons. In the

injured adult mice spinal cord, although endogenous neural progenitors response to the injury with increased proliferation, no newly generated neurons were detected (Yamamoto et al. 2001). Similarly, a study in adult rats following minimal spinal cord injury showed increased ependymal stem cells that primarily differentiate into astrocytes but not neurons (Mothe & Tator 2005). Mammals display spontaneous sprouting of spared axons after the CNS injury, however, regenerated axons that bridge the lesion site are extremely rare. This is primarily due to the formation of the glia scar at the injury site and the secreted axon growth inhibitors, such as Nogo-A, myelin-associated glycoprotein (Mag) and oligodendrocyte myelin glycoprotein (Omgp) were identified to provide a non-permissive environment in axon regrowth (Filbin 2003). For example, Nogo-A expressed by oligodendrocytes leads to growth cone collapses and prevents axon outgrowth from the glia scar (GrandPré et al. 2000). The lack of neurogenesis and axonal regeneration may collectively limit the potential of functional recovery of injured CNS in mammals.

1.4 Zebrafish: connecting development and disease

1.4.1 Zebrafish as a forward genetic model

A forward genetic study is a laboratory method to identify the function of a gene through phenotypes of interest in an experimentally manipulated animal organism. (Moresco et al. 2013). Two complementary genetic approaches are often used: Forward genetics and reverse genetics (Acevedo-Arozena et al. 2008).

Forward genetics is a phenotypic-driven approach. It is an unbiased method through the identification of mutant phenotypes of interest from a large number of individuals by inducing random mutations to a large population of genomes, in searching for a gene or genes that are responsible for the phenotypes of interest (Griffiths et al. 2005). Forward genetics do not require prior knowledge of the causative gene. The phenotype-to-genotype approach often leads to the discovery of novel genes or uncover the novel function of a known gene, and provide opportunities to dissect the pathway involved and reveal the underlying mechanisms (Moresco et al. 2013; Griffiths et al. 2005).

Reverse genetics, on the other hand, is a gene-driven approach. The study involves a known gene. Through altering its sequence or its expression, the range of associated phenotypic effects such a manipulation causes can be studied, in order to investigate the function of a gene of interest (Nagy et al. 2003). Reverse genetic methods such as transgenic techniques, genome editing techniques like TALENs (Clark et al. 2011) and more recently CRISPR-Cas9 system to specifically knockout a gene of interest (Sander & Joung 2014), and knock-down have been widely used in experimental organism models to mimic human diseases (Argmann et al. 2006; Griffiths et al. 2005; Tierney & Lamour 2005). Reverse genetics can provide a deep insight of the roles and mechanisms of genes assessed. However, such a gene-to-phenotype approach often requires previous knowledge of the genes, such as protein or DNA sequences, and limited by the assumption of the functions they may have (Nguyen et al. 2011; Moresco et al. 2013).

In a forward genetic screen, animal models such as yeast (*S. cerevisiae*), fly (*Drosophila melanogaster*) and worm (*C. elegans*) have been widely used in isolating genes that are important for embryonic development. Mammalian models such as mice, which share a high degree of gene conservation and physiological similarities with human, have also been used in forward genetic screens and provided great insights into biological processes that relate to human diseases (Nguyen et al. 2011). However, a forward genetic screen is laborious, timely and costly. It involves several generations of breeding procedure and screening large numbers of individual animals (Argmann et al. 2006). For example, in a large-scale genetic screen using zebrafish, Driever et al. 1996) screened nearly 500,000 embryos from more than 30,000 crosses. Many factors have to be taken into account when selecting an experimental animal organism for genetic screen in order to balance the cost, time as well as the genetic similarities between human and animal models. Lower organisms like yeast, fly and worm are suitable for high-throughput in vivo screens because of their small size and simple structure. However, their lack of vertebrate-specific organs limits their suitability in modelling human disease (Dooley & Zon 2000). Although the mouse genome is 99% similar to that of humans, it has not been proven that they can reliably and accurately predict results of studies in humans. Obstacles

such as the cost for maintenance and the high demand for space limits its power to carry out large scale screen. It is also difficult to perform in vivo assessment for phenotypes and requires antibody staining, surgical intervention and post-mortem examination (Lieschke & Currie 2007).

The need of a model organism with a high degree of similarity with humans that is also cost efficient has brought zebrafish into focus for a large forward genetic screen. Zebrafish has functional homologs of about 70% of human disease associated genes (Santoriello & Zon 2012). It is small in size, with a length of 3 ~ 4 cm of an adult fish and 3.5 mm of a 3 dpf (days post fertilization) larvae, which makes it possible to keep high density laboratory stocks (Kimmel et al. 1995). Zebrafish embryos develop externally and embryos are transparent, which provided ease for direct visual inspection of phenotypes in vivo and for live imaging analysis (Dodd et al. 2000). For instance, the heart beat and blood circulation can be easily observed under a dissecting microscope. Simple means like touch and light can be used to assess the loco-motor behaviour and visual response. The availability of transgenic lines, in which fluorescent proteins are expressed in specific tissues or organs, also enables to screen specific phenotypes of interest in a large number of animals (Stewart et al. 2014).

The zebrafish was first proven to be suitable for producing homozygous diploid mutants in genetic analysis in 1981 by George Streisinger (Streisinger et al. 1981). Mullins et al (1994) further developed methods for ENU (N-ethyl-N-nitrosourea) induced genetic screen and performed a small pilot screen that successfully isolated mutants affecting embryogenesis. In 1992, the first two remarkable large scale forward genetic screens were initiated by two groups in Boston, USA and Tübingen, Germany. A total of 2383 mutants were discovered in the Boston screen (Driever et al. 1996) and 4264 mutants in Tübingen screen (Haffter et al. 1996). Genes isolated from the screens are involved in many aspects of embryonic development such as central nervous system, pigment formation, as well as in behaviour response (Nusslein-Volhard 2012; Lieschke & Currie 2007).

For the past decades, forward genetic screens in zebrafish have discovered many genes that are associated with human diseases. In human, muscle degeneration disease such as Duchenne muscular dystrophy was caused by the mutation of *dystrophy* gene (*dmd*) (Kawahara et al. 2011). A mutant *sapje* (*sap*) with *dmd* mutation presented similar muscle degeneration phenotype to that of the human was identified from a large genetic screen (Bassett & Currie 2003). It has been used as a model for human muscular dystrophy to understand the pathological mechanisms underlying this incurable disease (Bassett & Currie 2003). Once the disease model is established, the transparent embryos allow in vivo analysis and experimental manipulation in whole zebrafish embryos. The efficacy and efficiency of pharmaceutical agents and compounds can be tested in zebrafish disease models as the chorion of embryo is permeable to small molecules. Kawahara et al (2011) carried out a chemical screen in the *sap* mutant that models human muscle dystrophy and identified a compound called phosphodiesterase (PDE) inhibitor that was able to restore normal muscle structure and improve life spans of these dystrophin-null zebrafish. It has been shown that the phosphodiesterase 5 inhibitor (PDE5) reduced the muscle weakness in *dmd* mouse model (Percival et al. 2012), demonstrating the suitability of zebrafish in the study of human disease and the potential of zebrafish in forward genetic screen. Furthermore, non-directly human disease linked mutations could also be useful to reveal the new alleles, unknown functions of genes and uncover potential pathways. Van Eeden et al (1996) discovered mutants display both motor neuron defect and abnormal somite formation. The study found that a new allele named *deadly seven* (*des*) is important for encoding delta and notch proteins in zebrafish (van Eeden et al. 1996). Notch signalling pathway was proven to play a key role in the development of spinal cord (Appel et al. 2001) and motor neuron regeneration after injury (Dias et al. 2012). These evidences demonstrate the value of zebrafish in linking the developmental genetic studies to disease research.

Like any other animal models, there will be cases that the species and genome differences make the research complicate (Stewart et al. 2014). Zebrafish has 23 chromosomes, which is similar to 25 chromosomes in humans. However, many

genes in zebrafish are duplicated, which could result in a divergence in genes' expression and function.

In summary, the zebrafish is a valuable animal model as it enables the application of invertebrate-style forward genetic technology to vertebrate, and genes discovered will shed light to the studies of the development and diseases.

1.4.2 Zebrafish as a model for motor neuron regeneration

In contrast to mammals, fish and amphibians like salamanders have a great capacity to repair CNS injury. Salamanders (*Urodeles*) are able to regenerate spinal cord after an injury throughout their life and are the only tetrapod to regenerate a fully differentiated functional spinal cord as adults (Chernoff et al. 2003). In the lesioned spinal cord of salamander, ependymal cells rearrange, migrate to the lesion site and act as stem cells to produce neuronal cells. Regenerated and myelinated axons as well as functional synapses also contributed to successful spinal cord repair in salamander (Chernoff 1996). Anuran amphibians such as frogs and toads are also capable of regenerate injured spinal cord, however, this regenerative capacity fails after the metamorphosis stage (Beattie et al. 1986). Spinal cord regeneration occurs during embryonic development in birds. Shimizu et al (1990) transected the spinal cord of chick embryos at various ages from embryonic day 2 (E2) to E15 and found that chick embryos from E2 to E10 showed both anatomical and locomotor restoration. However the regenerative ability declined at later stages, for E15 transected chick embryos showed reduced number of motor neurons and insufficient recovery anatomically and functionally (Shimizu et al. 1990).

The zebrafish has a robust CNS regenerative ability after different types of insults. It has shown that following an injury in the telencephalon of adult zebrafish brain, the neuronal precursor cells in the injured telencephalon hemisphere reacted with increased proliferation, and differentiated into mature neurons around the injury site within a week post-injury (Kishimoto et al, 2012). In a recent study of my research group, adult zebrafish were found to be able to regenerate dopaminergic cells in the brain after a toxin-induced cell ablation (unpublished data of Dr Nick Davis). This is

in contrast to human, in which the loss of dopaminergic cells is permanent and causes Parkinson's disease.

After a spinal cord transection, neurons in the brain are able to extend axons beyond the transection site (Becker et al. 1997), and injured fish recover motor function within 6 weeks after the spinal lesion (Becker et al. 2004), indicating the regenerative capacity of the zebrafish spinal cord. Reimer et al (2008) revealed for the first time that the regeneration of motor neurons can be triggered by a mechanical lesion to the spinal cord. Like mammals, progenitor cells in the intact spinal cord of adult zebrafish are relatively quiescent. However, the pMN domain of adult zebrafish is highly plastic after an injury. In the injured spinal cord, proliferation of Olig2+ ependymo-radial glial progenitor cells is increased. These cells later gave rise to Hb9+ and Islet-1/2+ motor neurons. Unlike mammals, zebrafish with an injured spinal cord exhibited axon growth across the injury site (Reimer et al. 2008). Studies have shown that newly formed neurons and axons in adults recapitulate developmental mechanisms during recovery from spinal cord injury, indicating that many embryonic cues are essential for adult regeneration (Barreiro-Iglesias et al. 2015; Reimer et al. 2013). For instance, a recent study demonstrated that serotonin (5-HT) is able to facilitate spinal motor neuron generation in embryos and is reactivated during the process of motor neuron regeneration in adult zebrafish (Barreiro-Iglesias et al. 2015). Endogenous dopamine was found to promote embryonic motor neuron development (Reimer et al. 2013). Reduced dopamine signalling leads to decreased numbers of motor neurons and impaired motor behaviour in larvae. In the lesioned spinal cord of adult zebrafish, dopamine signalling promotes regeneration of new motor neurons. The same study, using human embryonic stem-cell-derived neural stem cells driven toward motor neuron differentiation, also showed that the application of a dopamine agonist stimulated the generation of Olig2+ progenitor cells as well as of motor neurons, hinting that molecules that affect the neurogenesis in zebrafish has similar effects in human stem cells (Reimer et al. 2013). Therefore, if we could understand the signals involved and the mechanisms behind larvae regeneration, we may be able to apply these findings to future therapeutic interventions and treatments. However, the regeneration of

motor neurons in the spinal cord of larval zebrafish had not been systematically studied.

Taken together, the accessibility of zebrafish embryos to developmental genetic studies, and the excellent regenerative ability of zebrafish, as well as the potential of applying findings from zebrafish to clinical research of human disease, make it a suitable model for forward genetic screening to look for essential developmental motor neuron genes, and the study of motor neuron regeneration after an injury.

1.5 Statement of aims

In this thesis, I aim to study genes that are essential for motor neuron development and axon differentiation. In parallel, I aim to investigate the utility of zebrafish larvae as a model to study motor neuron regeneration. To achieve these goals, I address the following aims:

(1) Forward genetic screen for gene identification.
– To establish and carry out a small-scale forward genetic screen. To identify mutants displaying altered motor neuron and/or motor axon development in order to find genes that influence motor neuron generation and axon differentiation.
– To initiate identification of the mutated genes.

To achieve the first aim, I conducted a forward genetic screen in 111 families and characterised 6 identified mutants that display motor neuron and/or motor axon phenotypes. 2 mutants with fewer numbers of motor neurons and absence of motor axons were selected for further analysis and DNA sequencing for causative mutation identification. I have started the analysis to identify candidate genes that may contribute to the observed phenotypes.

(2) Motor neuron regeneration in lesioned larval spinal cord.
– To investigate the plasticity of pMN in developing spinal cord after a lesion.
– To study whether the other progenitor domains and cell types, such as interneurons, are able to regenerate after an injury.

In this part, I validated that zebrafish larvae can be used as a model to study motor neuron regeneration in developing spinal cord. I demonstrated that pMN domain is able to switch from making oligodendrocytes to produce motor neurons. I also showed that progenitor domains have different potential in lesion-induced proliferation.

Chapter 2 Methods and Materials

Methods

2.1 Fish husbandry

All zebrafish lines were kept and raised in our animal facility with a 14 hour-light and 10 hour-dark cycle following the standard protocol of Westerfield (1995). Embryos were collected in conditioned aquarium water containing 0.00001% methylene blue and kept at 28.5 ºC; embryos used for mutagenesis genetic screen were raised in 25.5 ºC water bath at the first 48 hours. All embryos were staged by hour post fertilization (hpf) and day post fertilization (dpf) using standard procedures (Kimmel et al. 1995).

2.2 ENU-induced forward genetic screen

2.2.1. N-ethyl-N-nitrosourea (ENU) treatment

The design of this screen is based on the work of Mullins et al (1994), Driever et al (1996) and Haffter & Nusslein-Volhard (1996). A three-generation breeding scheme was adapted (Figure 2.1). ENU treatment was performed by Maria Rubio and Professor David Lyons. Wild-type (wik) males were incubated in ENU bath once a week for 3 weeks at a concentration of 3 mM. 3 males confirmed with successful mutagenesis were kept and mated with golden strain females to generate F1 generation. F1 families are heterozygous for induced genome modifications. The generation of F1 families were performed by Maria Rubio, and I carried out the generation of F2-F4 families.

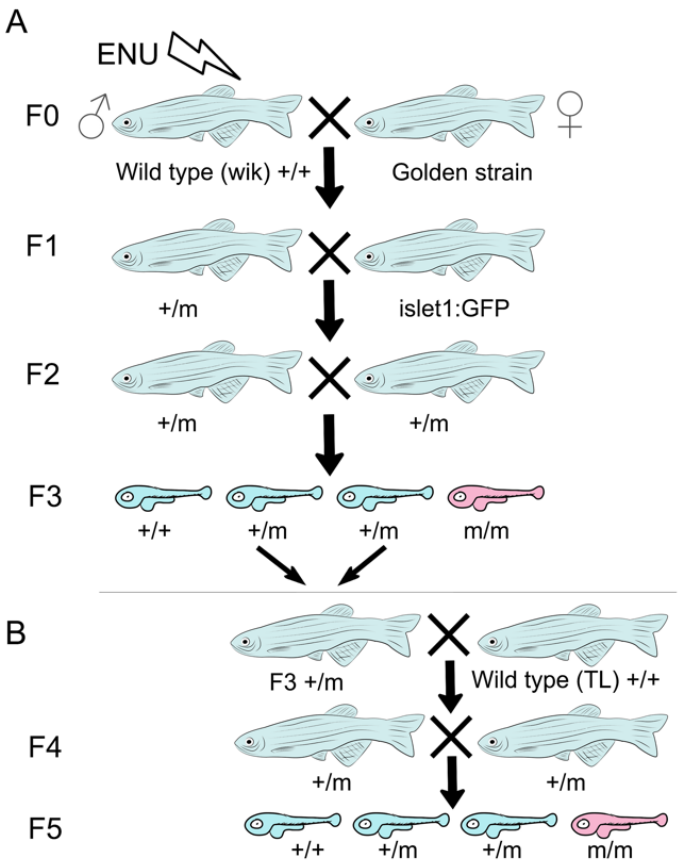

Fig 2.1 ENU-induced mutagenesis breeding procedure. (A) Mutations were induced by ENU-treatment in wik males. Mutagenised males were mated with golden strain females to generate F1 families. F1 families were then outcrossed with the islet-1:GPF transgenic line in order to obtain a F2 generation with GFP expressed secondary motor neurons and motor axons. Phenotypic analyses were performed in F3 embryos. 25% embryos in a F3 clutch would be homozygous for the induced mutation if both F2 parents were heterozygous for a mutated gene. **(B)** Mutant lines were outcrossed with another wild type line TL that is polymorphism to wik. F4 offspring were raised and in-crossed to confirm the phenotypes in subsequent generations.

2.2.2 Generation of F2-F4 off-springs

Individual F1 fish carrying random mutations was mated with an islet-1:GFP fish and kept separately from the original tank. Each successful F1 × islet-1:GFP pair mating represents an individual F2 family and was given a unique stock number.

Fifty percent of the fish in a F2 family are heterozygotes containing inherited mutagenized genomes. 4 to 6 pairs of F2 fish are mated randomly with their siblings and their F3 offspring were used for analysis. Mutants of interest were outcrossed with another wild-type line TL. Wik and TL are two different strains with different polymorphisms (Figure 2.1B). F4 embryos were raised and in-crossed to determine whether the subsequent generation replicates the phenotypes of interest.

2.2.3 Phenotypic screen in F3 generation

An average of 60 to 80 F2 pair mating tanks (around 10 to 12 families) were set up each week (Fig 2.2). Eggs were collected with embryo medium and kept at 25.5 ºC. We analysed 4 to 6 crosses from each F2 family, as it gives a 68% to 82% probability of finding a mutant in an F2 family (Driever et al. 1996). 12 to 20 F3 embryos from each F2 cross were screened, which gives a 96% to 99.6% chance of finding at least one mutant if both parents are heterozygous (Driever et al. 1996).

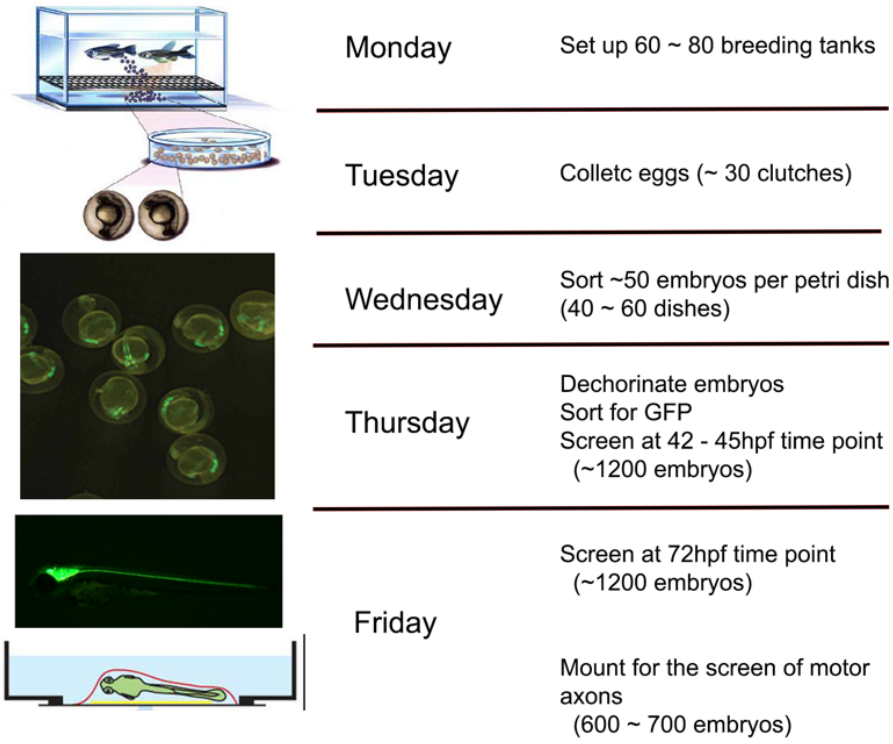

Fig 2.2 Weekly workflow for phenotypic screen of interest. Pictures in this figure were adapted and edited from Google image.

islet-1:GFP fish displays a full distribution of GFP positive motor neurons throughout the length of the spinal cord at 3 dpf (Fig 2.3 B). Based on my previous observation, the first appearance of the full islet-1:GFP+ motor neuron distribution (a full band) is at 48 ~ 49 hpf (hours post fertilization) at 28.5 ºC, by 72 hpf all wild-type embryos appear full positive GFP neuron distribution.

To screen islet-1:GFP+ motor neuron phenotype, 40 embryos were randomly selected from each clutch. Chorions were removed with 1mg/ml pronase (Sigma; P5147) and embryos were rinsed thoroughly in fresh E3 medium. Dechorionated embryos were anaesthetized and screened at two time points for motor neuron phenotype: (1) At 42 hpf to 45 hpf, when no control embryos display full distribution of GFP positive neurons in the spinal cord (0% full "band" in control siblings) (Fig 2.3 A). This allows the assessment of premature development of motor neurons. (2) At 72 hpf, when all control embryos display fluorescent motor neurons in the mid-trunk position (100% full "band" in control siblings). This enables to find genes that affect the development of motor neurons (Fig 2.3 B).

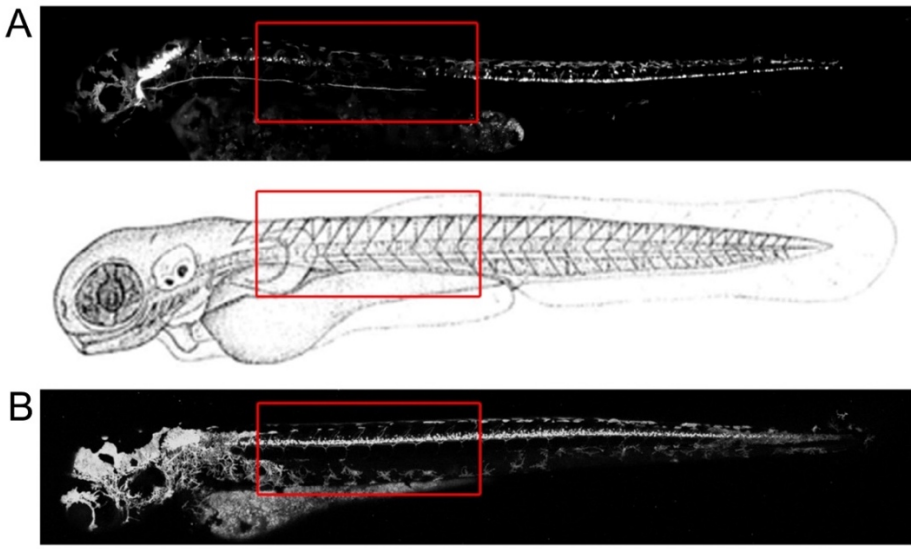

Fig 2.3 Illustrations of islet-1:GFP+ motor neuron distribution in the embryonic spinal cord. (A) An embryo displays a non-completed distribution of GFP+ motor neurons in the mid-trunk position. **(B)** An embryo displays a full distribution of GFP+ motor neurons throughout the length of the spinal cord.

To screen secondary motor axon phenotypes, 12 to 20 of 3 dpf embryos from each F2 cross were anaesthetized and mounted alive in a lateral position in 1.2% agarose gel under a dissection microscope (Nusslein-Volhard & Dahm 2002). islet-1:GFP+ motor axons (Fig 2.4) were assessed with a microscope at 10x and 20x objective. The parameters for islet-1:GFP+ motor axon phenotype assessment were: absent of dorsal axon projection, aberrant axon exits, abnormal branching, ectopic axon growth, and so forth. Heterozygous F2 parents that produced a specific mutant phenotype were re-crossed to determine the reproducibility of the observed phenotype. All screening results were recorded and mutant phenotypes found were described individually for their exhibited morphological phenotype, islet-1:GFP+ motor neuron phenotype and islet-1:GFP+ motor axon phenotype.

Fig 2.4 islet-1:GFP+ motor axons of a 3 dpf embryo. Scale bar = 100 μm.

2.3 Whole genome sequencing (WGS) and bioinformatics analysis

WGS sequencing was outsourced to Edinburgh Genomics (University of Edinburgh). Bioinformatics analysis for candidate genes was kindly performed by Dr. Richard Poole (University College London) using CloudMap (Minevich et al. 2012) from the Galaxy web platform.

2.4 Molecular biology

2.4.1 RNA extraction

RNeasy Mini Kit (QIAGEN; Cat. 74104) was used for RNA extraction. 30 embryos at desired developmental stage were dechorionated and terminally anesthetized with

MS 222. Lysis buffer (100 µl beta-mercaptoethanol (βME) in 1 ml RLT buffer) was added to each sample and then vortexed for 5 min, centrifuged briefly and vortexed again for 5 min; samples were centrifuged for 5 min at 13,000 rpm; supernatant of each sample was transferred to a clean tube, added in 600 µl 70% ethanol, and then transferred to a provided column from the kit to centrifuge for 15 s at 10,000 rpm; 500 µl RPE buffer was added and centrifuged for 15 s at 10,000 rpm; solution was centrifuged again for 3 min at 13,000 rpm to remove the residual RPE buffer. Finally, RNA was eluted by adding 30 µl water and centrifuge for 1 min at 10,000 rpm.

2.4.2 cDNA synthesis

The synthesis of first strand cDNA was based on the manufacturer's protocol (SuperScript III CellsDirect cDNA Synthesis System; Life Technologies; Cat. 18080-200). I used 3 ~ 4 ng RNA for reaction setup. cDNA was stored at -20 °C.

2.4.3 Primer design

Primers were designed by using a free online software Primer3 (http://bioinfo.ut.ee/primer3-0.4.0/) and outsourced to Source BioScience (http://www.sourcebioscience.com/) for manufacturing.

Primers

Primer name	Sequence	Purpose
Rbbp4-F (#0187)	5'-TTATTTGGATCCCCACCATGGCTGATA-3'	Sense RNA
Rbbp4-R (#0186)	5'-TTATTTCCCGGGGGAATGGCTGATAAA-3'	
Rbbp4-F (#0195)	5'-ATGGCTGATAAAGAAGCTGCATTTGAT-3'	Antisense RNA
Rbbp4-R (#0196)	5'-TTAGATGTCAGAGCCACAAGGGAAACA-3'	
Rbbp4-F (#0234)	5'-CCAGGCAGACCAGTAAAATAATG-3'	Genotyping

Rbbp4-R (#0235)	5'-GAGCCACAAGGGAAACACTC-3'	
Psmc2-F (#0227)	5'-TTATTTTTCGAACCACCATGCCTGATTATTTAGG-3'	Sense RNA
Psmc2-R #(0228)	5'-TTTATTCTCGAGTTAGTTGTAAGTCATGTAGCGAGGG-3'	
Psmc2-F (#0229)	5'-TTATTTCCCGGGGGAATGCCTGATTATTTA-3'	
Psmc2-F (#0230)	5'-AATCTCGCCCCTACAGTCAC-3'	Antisense RNA
Psmc2-R (#0231)	5'-TGACATCACAGAACGACAGGA-3'	
Psmc2-F (#0232)	5'-AATCTCGCCCCTACAGTCAC-3'	Genotyping
Psmc2-R (#0233)	5'-CTCCTACTCATGCCAACAAGC-3'	
Ankmy2b-F (#0260)	5'-ATTAAGCAGCCCAGAAACCA-3'	Genotyping
Ankmy2b-R (#0261)	5'-AGGTGTTTTGCACTGCCTCT-3'	

2.4.4 Polymerase chain reaction (PCR)

Expand High Fidelity PCR System (Roche; Cat. 11732641001) or Q5 High-fidelity DNA polymerase (NEB, M0491) were used for PCR. Where appropriate, gradients of annealing temperature were used.

Depending on the length of the product and the Tm of the primer, the cycler was set to the following values:

For Expand High Fidelity PCR System:

Initial denaturation: 94 °C 2 min
Denaturation: 94 °C 15 s
35x Annealing: 55-60 °C 30 s
Extension: 72 °C 25 s ~ 1 min
Final extension: 72 °C 7 min
Hold: 4 °C

For Q5 High-fidelity DNA polymerase:

Initial denaturation: 98 °C 30 s
Denaturation: 98 °C 10 s
7x Annealing: 59-61 °C 30 s
Extension: 72 °C 40 s ~ 1 min
Denaturation: 98 °C 10 s
35x Annealing: 69-71 °C 30 s
Extension: 72 °C 40 s ~ 1 min
Final extension: 72 °C 2 min
Hold: 4 °C

2.4.5 Gel electrophoresis and extraction

DNA and RNA fragments were analysed in a buffer filled electrical field in 1% Agarose gel (1.0 g agarose in 100 ml 1x TAE buffer). 5 µl ethidium bromide (EtBr; final concentration of 0.2 µl/ml) which binds to the DNA was added into the gel to allow the visualisation of the DNA under ultraviolet (UV) light. Gel extraction was performed by using QIAquick Gel Extraction Kit (QIAGEN; Cat. 28704) according to the manufacturer's instructions.

2.4.6 Ligations and cloning of PCR fragments

Where appropriate, PCR products were ligated and cloned into a vector by using either StrataClone PCR Cloning Kit (Agilent; Cat. 240205), or using T4 DNA ligase

(NEB, M0202) and cloned into a PCSP2+ vector (courtesy of Daniel Wehner for the vector).

2.4.7 Transforming the competent cells

To introduce a plasmid vector with foreign DNA insert, I used either StrataClone SoloPack Competent Cells (200185) or NEB 5-alpha Competent *E. coli* (C2987H), according to according to the protocols of the manufacturers.

2.4.8 Blue/White selection of ligated vectors

White colonies were picked for plasmid DNA analysis. The principle of the blue-white screening is to identify recombinant bacterial colonies based on the activity of β –galactosidase. β –galactosidase is an enzyme produced by *lacZ* gene in *E.coli* and is able to cleave lactose to glucose and galactose. A chemical X-gal that can also be cleaved by functional β-galactosidase is used to visualize the insert of the plasmid. A host *E. coli* strain containing a plasmid carrying an insert of PCR product is expected to form white colonies, while *E. coli* harbouring a plasmid without an insert will be blue.

2.4.9 Growth of bacterial culture

Single colony was picked and incubated in 6 ml LB medium with 12 µl ampicillin (50mg/ml, final working concentration 1:500) at 37 °C with agitation overnight.

2.4.10 Plasmid DNA isolation

FastPlasmid Mini Kit (5 Prime; 2300000) was used to isolate plasmid DNA according to the manufacturer's instructions.

2.4.11 Concentration measurement

Concentration (ng/µl) and purity of nucleic acid samples were measured with NanoDrop 1000 Spectrophotometer.

2.4.12 Sanger sequencing

Sanger sequencing was performed by Source Bioscience (http://www.sourcebioscience.com/). T3, T7 or sp6 promoters were selected based on appropriate plasmid map.

2.4.13 Restriction digestions

Appropriate NEB enzymes and buffers were selected for restriction digestions based on the instructions of the manufacturer. The success of the digestion was analysed by running agarose gel electrophoresis.

2.4.14 DNA purification

DNA purification was carried out using QIAquick PCR Purification Kit (QIAGEN, Cat. 28104) according to the manufacturer's instructions.

2.4.15 *in vitro* transcription of the RNA

The linearized DNA was precipitated overnight at -20 °C with 0.3 M Sodium Acetate, and two volumes of 100% ethanol. Antisense RNA was transcribed by using MAXIScript® Kit (Ambion), and sense RNA was transcribed by using mMESSAGE mMACHINE® Kit according to the manufacturers' instructions.

2.4.16 RNA clean-up

RNA clean-up was performed by using RNeasy Mini Kit (Invitrogen; AM1320) based on the protocol of the manufacturer.

2.4.17 Genomic DNA isolation

Genomic DNA was isolated using Gentra Puregene Tissue Kit (Qiagen; Protocol of Dr. Linde Kegel). 80 to 120 homozygous mutant embryos and their siblings were collected and frozen in liquid nitrogen. Before DNA isolation, sample tubes were thawed on ice and combined. 3 ml of Cell Lysis Solution and 15 µl Proteinase K (20 mg/ml) were added into each sample and inverted 25 times; sample were incubated at 55 °C overnight (O/N). On the next day, the lysates were cooled at room temperature (RT), 15 µl RNase A Solution was added and mixed by inverting

25times. Samples were incubated at 37 °C on a mixing table for 2~3 h, cooled on ice for 3 min and 1 ml Protein Precipitation Solution was added; the samples were then cooled on ice for another 5 min, vigorously vortexed for 20 s at high speed and cooled on ice for 5 min again. Tubes were centrifuged at 2,000 x g for 10 min at 4 °C and supernatant of each sample was transferred to a clean tube containing 3 ml 2-propanol, mixed by inverting 50x and then incubated at -20 °C O/N. Solution was centrifuged at 2000 x g for 30 min at 4°C, supernatant was removed and tubes were drained. 3 ml ice-cold 70% ethanol was added and tubes were inverted for several times to wash DNA pellet. Centrifuge again at 2,000 x g for 3 min at 4 °C, remove supernatant and air dry pellet. 150 µl of DNA Hydration Solution was added and incubated at 65 °C for a minimum of 30 min to 1h until DNA is dissolved. DNA solution was incubated O/N at RT while gently agitating at ~30 rpm. Isolated genomic DNA samples were stored at -80 °C.

2.4.18 Genotyping

Genotyping protocol was adapted from Dr. Marcos Cardozo. Whole embryos were incubated in 50 µl of 5 mM NaOH at 95 °C for 20 min, and then vortexed at the highest speed until dissolved completely. Tubes were put on ice, added with 1/10 of 1 M Tris PH 8.0, and then centrifuged for 2 min at maximum speed. 1 µl supernatant was used for PCR reaction setup.

2.5 Histology

2.5.1 Immunohistochemistry (IHC) on whole-mount embryos

Embryos and larvae were fixed in 4% PFA/1% DMSO and washed in 1x PBS. 33 ~ 72 hpf embryos were incubated with 2 mg/ml collagenase diluted in PBS; 3 to 5 dpf larvae were incubated in 10 mM citric acid (pH 6) at 110 °C for 10 min. Embryos and larvae were washed in 1x PBS and non-specific binding sites were blocked with whole mount IHC blocking buffer. Appropriate primary antibodies were diluted in IHC blocking buffer and incubated at 4 °C O/N. Embryos and larvae were washes in 1x PBStx (0.1% Triton X-100) and incubated in secondary antibodies diluted in 1x PBStx (0.1% Triton X-100) at 4 °C O/N protected from the light. After extensive

washing in 1x PBStx and 1x PBS, embryos were cleared in 70% Glycerol/1x PBS and mounted on slides.

2.5.2 IHC on cryostat sections

Larvae at desired developmental stage were terminally anesthetized with MS 222, fixed in 4% PFA/1% DMSO for 3 h at RT, and washed in 1x PBS. Fixed larvae were immersed in 30% sucrose/1x PBS and incubated overnight at 4 °C. Larvae were embedded in OCT embedding medium in a mould and flash frozen in liquid nitrogen- cooled methyl-2-butane for ~15 s. 14 µm non-consecutive sections were cut from the regions of interest on a cryostat (CM3050 S, Leica, Wetzlar, Germany), collected with Superfrost coated glass slides. Sections were dehydrated, delipidized and permeabilized in a pre-cooled methanol bath at -20 °C for 10 min. Section slides were washed in 1x PBS for 10 min and blocked in 200 µl IHC blocking solution for 1.5 h. Appropriate primary antibodies were added and incubated over night at 4 °C. After extensive washes in 1x PBStx (0.2% Triton X-100), sections were incubated in 200 µl secondary antibodies in IHC blocking buffer for 1 ~ 1.5 h at RT protected from the light. Sections were washed in 1x PBStx (0.2% Triton X 100) and 1x PBS, and then mounted in Fluoromount.

2.5.3 *In situ* hybridization on whole-mount embryos

This *in situ* hybridization protocol was based on Thisse & Thisse (2008). Embryos of desired developmental stages were dechorionated, terminally anaesthetized and fixed in 4% PFA/1x PBS RT at 4 °C. Embryos were dehydrated in 1 ml 100% methanol and left at -20 °C O/N. Through a 75%, 50%, 25% methanol/PBS rehydration series and extensive washes in 100% PBT, embryos were permeabilized in Proteinase K (10 µg Proteinase K / 1ml PBT) at RT. The digestion was terminated by incubating the embryos in 4% PFA for 20 min. Residual PFA was removed by washing in 1x PBT. Embryos were pre-hybridized with HM for 5 h in a 65 °C water bath to reduce the background staining. Embryos were incubated in 300 µl preheated HM containing RNA probe and left to hybridize O/N at 65 °C. To prevent nonspecific hybridization, embryos were washed with a series of pre-warmed HMW at 65 °C: 75%, 50%, 25% HMW diluted with 2x SSC; and then 100% 2x SSC; 0.2x SSC in

PBT. Embryos were washed again at room temperature through a series of 10 min washes: 75%, 50%, 25% 0.2x SSC in PBT; 1x PBT. Embryos were incubated for 4 h in blocking buffer at RT on a shaker, and then incubated in anti-DIG antibody solution (1/10,000 dilution in blocking buffer) O/N at 4 °C with gentle agitation. Embryos were washed in 1x PBT at room temperature for 6 x 15 min. To equilibrate the embryos for the staining, embryos were washed in Alkaline Tris buffer (pH 9.5). They were then incubated in NBT/BCIP staining solution at RT until the desired staining intensity was reached. The reaction was stopped by washing with stop solution at RT with gentle agitation. Wash in 1x PBS to remove and transfer embryos to 70% glycerol in PBS for mounting.

2.5.4 EdU detection

EdU labelling was detected by Click-iT EdU Alexa Fluor 647 Imaging Kit (Life Technologies; C10340). Larvae were terminally anesthetised and fixed in 4% PFA/1% DMSO for 3 h at RT, washed in 1x PBS and 1x PBStx (0.2% Triton X-100); emrbyos were digested for 40 min in collagenase (2 mg/ml in PBS), and washed again in 1x PBS and 1x PBStx (0.2% Triton X-100). Click-iT™ reaction cocktail was prepared by combining the following components in order: 4.3 µl 10x Click-it™ reaction buffer, 88.7 µl H_2O, 2 µl $CuSO_4$, 0.1 µl Alexa Fluor azide 647, 5 µl Reaction buffer additive. Samples were incubated in 500 µl reaction cocktail at 4 °C for 2.5 h protected from the light; and then washed in 1x PBS to remove the reaction cocktail. Finally, larvae were transferred to 70% Glycerol in PBS and mounted on slides.

2.5.5 Whole-mounted larvae TUNEL Assay

Zebrafish larvae at 5 dpf were anesthetized, fixed in 4% PFA/1% DMSO in PBS at RT for 3 h, washed in PBS and PBST (0.2% Tween® 20). Larvae were digested with collagenase (Sigma-Aldrich, Cat. No. C9891; 0.2 mg/ml in PBST) for 50 min. The TDT reaction cocktail was prepared according to the manufacture's description (Click-iT® TUNEL imaging assay, C10247). Larvae were washed in PBS and incubated in the reaction cocktail at RT for 3 h protected from the light. After

extensive washes in PBS, larvae were either processed for immunohistochemistry or transferred to 70% glycerol in PBS.

2.5.6 Acridine orange detection

Dechorionated embryos were incubated in 10ng/µl Acridine orange solution in the dark for 20 min. Embryos were washed in embryo medium 3 x 10min and analysed under a fluorescence microscope.

2.6 Spinal cord injury in zebrafish larvae

Spinal cord injury was performed on larvae from 3 dpf onwards (Protocol of Gianna Maurer). 1.2% low melting point agarose (0.12 g in 10ml PBS) was heated up in microwave and kept warm. Anesthetised larvae were mounted in agarose in a lateral position. Agarose was removed from desired areas to expose yolk and lesion site. Lesion was made using 30-gauge injection needle (Picture adapted from Gianna Maurer).

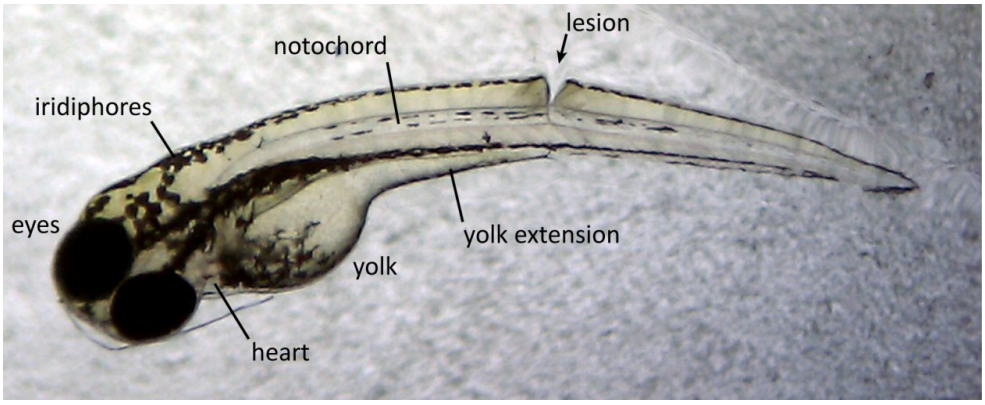

2.7 Microinjection

Injection needles were pulled from glass capillary by using a P-97 Flaming/Brown micropipette Puller. Messenger RNAs (mRNAs) were injected into one-cell stage embryos. mRNA was supplemented with 0.2% w/v phenol red (Sigma) to facilitate visualisation of the volume injected. For EdU injection, 5 nl of 5 mM EdU solution (2 µl EdU 10 mM, 1 µl 0.1 M KCl buffer, 1 µl PhenolRed Solution) was injected into the yolk of the larvae.

2.8 Quantification and statistical analysis

Zeiss stereomicroscope Lumar V.12 was used for the screen of motor neuron phenotypes, and Zeiss Imager.Z Apotome was used for the screen of motor axonal phenotypes. LSM 710 confocal microscope with a Zeiss Zen 2011 software was used for the acquisition of all fluorescent images. Acquired images were retrieved by image J/Fiji program (National institute of health, Bethesda, MD, USA).

For cell counts in whole embryos, confocal images were opened in Image J/Fiji (National Institute of Health, Bethesda, MD, USA). Numbers of cells in a defined area of interest were counted manually in a stereological fashion throughout the z-Confocal stack. For cell profile counts in sections, at least 4 sections were analysed per animal and values were expressed as profiles per 14 μm section. Stereological counts were manually performed in confocal image stacks of 4 randomly selected cryostat sections using Image J/Fiji software.

A Zeiss Scope.A1 microscope equipped with Axio Vision software was used for the acquisition of images stained with ISH. Figures were prepared using Adobe Photoshop CC 2014. The graphs and statistical analysis were obtained through GraphPad Prism 5.

Materials

2.9 Transgenic fish lines and mutants

Wild-type

Tg(islet-1:GFP), abbreviated as islet-1:GFP (Higashijima et al. 2000);

Tg(mnx1:GFP^{ml2}), abbreviated as Hb9:GFP (Flanagan-Steet et al. 2005);

Tg(olig2:DsRed2), abbreviated as olig2:DsRed (Kucenas et al., 2008);

Tg(pax2a:GFP), abbreviated as pax2a:GFP (Picker et al., 2002);

Tg(sox10(7.2):mRFP), abbreviated as sox10:mRFP (Kirby et al., 2006);

Tg(mbp:EGFP), abbreviated as mbp:GFP (Almeida et al., 2011);

Mutant family 55, abbreviated as #55;

Mutant family 151, abbreviated as #151;

Mutant family 160, abbreviated as #160;

Mutant family 171, abbreviated as #171;

Mutant family 249, abbreviated as #249;

Mutant family 151 x *Tg(olig2:DsRed)*, designated as #151 x olig2:Dsred.

2.10 Antibodies

Primary antibodies

Primary Antibodies	Host Species	Dilution	Supplier / Cat. No
Acetylated α-tubulin	Mouse	1:1000	Sigma-Aldrich / F7799
α-ChAT	Goat	1:500	Abcam / AB1449
α-Claudin K	Rabbit	1:1000	Eurogentec
α-GABA	Rabbit	1:1000	Sigma-Aldrich / A2052
α-GFP	Chicken	1:500	Abcam / AB13970
α-HB9	Mouse	1:400	DSHB
α-Islet1	Mouse	1:2000	DSHB
Alexa Fluor 546 phalloidin	Mouse	1:100	invitrogen
F59	Mouse	1:50	DSHB
Pax2	Mouse	1:500	Covance / PRB-276P
zn-8	Mouse	1:500	DSHB
zn-12	Mouse	1:1000	DSHB
3A10	Mouse	1:500	DSHB
4D9 engrailed	Mouse	1:50	DSHB
α-phospho-Histone H3(pH3)	Rabbit	1:1000	Millipore (06-570)

Secondary antibodies

Secondary Antibodies	Dilution	Supplier / Cat. No
Cy3 Donkey Anti-Chicken IgY (IgG)	1:200	Jackson ImmunoResearch Laboratories, Inc. 703-165-003
Cy3 Donkey Anti-Goat IgG	1:200	Jackson ImmunoResearch Laboratories, Inc. 705-165-147
Cy3 Donkey Anti-Mouse IgG	1:200	Jackson ImmunoResearch Laboratories, Inc.

		715-165-150
Cy3 Donkey Anti-Rabbit IgG	1:200	Jackson ImmunoResearch Laboratories, Inc. 711-165-152
Cy5 Donkey Anti-Rabbit IgG	1:200	Jackson ImmunoResearch Laboratories, Inc. 711-154-152
DyLight 649 Donkey anti Rabbit IgG	1:200	Jackson ImmunoResearch Laboratories, Inc. 711-495-152

2.11 Enzymes

Collagenase	Sigma-Aldrich (C9891)
Bam HI-HF	New England Biolabs Ltd (R3136T)
Hind III	New England Biolabs Ltd (R0104S)
Pronase E (Protease type XIV from Streptomyces griseus)	Sigma-Aldrich (P5147)
Proteinase K Solution	invitrogen AM2548
Proteinase K, recombinant, PCR grade	Roche (03115887001)

2.12 Buffers and solutions

Alkaline tris buffer	100 mM Tris HCl 1M pH 9.5 50 mM MgCl2 100 mM NaCl 0.1% Tween 20
IHC blocking buffer (whole-mount embryos)	1% Dimethyl sulfoxide (DMSO) 1% Normal donkey serum (NDS) 1% Albumin (BSA) 0.7% Triton X 100
IHC blocking buffer (sections)	2% Normal donkey serum or normal goat serum (NGS or NDS) 0.2% Triton X 100

In situ blocking buffer	1x PBT 2% Normal sheep serum 2 mg/ml BSA
Citric acid 10 mM pH 6	1.92 g Ctric acid In 1 L dH_2O Adjust to pH 6
EDTA 0.2 M pH 8	18.6 g EDTA 3 g NaOH pellets In 250 ml dH_2O Adjust to pH 8
Glycine 50 mM	0.0375 g Glycine In 10ml 0.2%Triton X 100/1x PBS
Hybridization mix (HM)	50% Formamide 5x SSC 0.1% Tween 20 50 µg/ml Heparin (50 mg/ml) 5 mg/ml tRNA from brewer's yeast In Nuclease-free dH_2O Adjust to pH 6.0
Hybridization mix for washes (HMW)	50 % Formamide 5x SSC 0.1% Tween 20 In Nuclease-free dH_2O
Paraformaldehyde (PFA) 4%	16 g Paraformaldehyde 40 ml 10x PBS In 400 ml dH2O
PBT	1x PBS pH 7.4 0.1% Tween 20
Phosphate buffered saline (PBS) 10x PH 5.5	10.8 g Na_2HPO_4 65 g NaH_2PO_4 80 g NaCl 2 g KCl In 1 L dH_2O Adjust to pH 5.5

Phosphate buffered saline (PBS) 10x PH 7.4	4 g KCl 28.3 g NaH_2PO_4 4.8 g KH_4PO_4 160 g NaCl In 2 L dH_2O Adjust to pH 7.4
Phosphate buffered saline (PBS) 20x pH 7.4	4 g KCl 4 g KH_2PO_4 23 g Na_2HPO_4 160 g NaCl In 1 L dH_2O Adjust to pH 7.4
SSC 20x pH 7	175.3 g NaCl 88.2 g Citric acid trisodium salt In 1L dH_2O Adjust to pH 7
In situ stop solution	1x PBS pH 5.5 1 mM EDTA 0.1% Tween 20
Tris HCl 1 M pH 9.5	121.1 g Trizma base In 1 L dH_2O Adjust to pH 9.5

2.13 Reagents and solvents

Name	**Supplier (Cat. No./Code)**
Agarose	Thermo Fisher Scientific (BP1356-100)
Anti-Digoxigenin-AP Fab fragments	Roche (11093274910)
Ampicillin sodium salt	Sigma-Aldrich (A9518)
2-mercaptoethanol (βME)	Fluka
Bovine Serum Albumin (BSA)	Sigma-Aldrich (A3912)

Dimethyl Sulfoxide (DMSO)	Sigma-Aldrich (D8418)
D(+)-Sucrose, ACS reagent	Acros Organics(424500010)
Ethylenediaminetetraacetic acid (EDTA)	Sigma-Aldrich (E5134)
Formamide	Sigma-Aldrich (47670)
Fluoromount-G	SouthernBiotech (0100-01)
Glycerol	Sigma-Aldrich (G5516)
Glycine for electrophoresis	Sigma-Aldrich (G8898)
Heparin sodium salt from porcine intestinal mucosa	Sigma-Aldrich (H3393)
LB-Medium	MP Biomedicals (3002-011)
Methanol	Thermo Fisher Scientific (M/4000/17)
2-Methylbutane	Sigma-Aldrich (320404)
Magnesium chloride ($MgCl_2$)	Sigma-Aldrich (M8266)
Magnesium chloride solution	Sigma-Aldrich (63069)
BCIP/NBT (5-bromo-4-chloro-3-indolyl phosphate/nitro blue tetrazolium) tablet	Sigma-Aldrich (B5655)
Normal donkey serum	EMD Millipore (S30)
Sheep serum	EMD Millipore (S22)
OCT Embedding Matrix	CellPath (KMA-0100-00A)
Potassium chloride (KCl)	Sigma-Aldrich (P5405)
Paraformaldehyde	Sigma-Aldrich (P6148)
2-propanol	Sigma-Aldrich (I9516)
RNaseOUT Recombinant Ribonuclease Inhibitor	invitrogen (10777-019)
Sodium phosphate dibasic dehydrate (Na_2HPO_4)	Sigma-Aldrich (71643)
tRNA (Ribonucleic acid from torula yeast, Type VI)	Sigma-Aldrich (R6625)
Triton X 100	Sigma-Aldrich (93426)
Tween 20	Sigma-Aldrich (P4348)
Trizma base	Sigma-Aldrich (93362)

2.14 Kits

Name	Supplier (Cat. No. /Product code)
Click-iT EdU Alexa Fluor 647 Imaging Kit	Life Technologies (C10340)
Expand High Fidelity PCR System	Roche (11732641001)
FastPlasmid Mini Kit	5 Prime (2300000)
Gentra Puregene Tissue Kit	QIAGEN (158667)
MAXIscript kit	Invitrogen (AM1320)
RNeasy Mini Kit	Invitrogen (AM1320)
QIAquick PCR Purification Kit	QIAGEN (28104)
QIAquick Gel Extraction Kit	QIAGEN (28704)
StrataClone SoloPack Competent Cells	Agilent Technologies (200185)
StratacClone PCR Cloning Kit	Agilent Technologies (240205)
SuperScript III CellsDirect cDNA Synthesis System	Life Technologies (18080-200)

Chapter 3 In vivo screen for motor neuron development and differentiation genes

3.1 Introduction

3.1.1 Development of motor neurons and axons in zebrafish spinal cord

In the developing zebrafish spinal cord, motor neurons group together in each spinal segment and extend axons in a stereotypical manner to innervate different muscle groups and facilitate locomotor movements (Myers et al. 1986; Eisen et al. 1986). Spinal motor neurons are classified into two types – primary and secondary motor neurons (Eisen et al. 1986; Eisen 1994; Pfaff & Kintner 1998). Primary motor neurons are born from 9 hpf onwards and can be subdivided into 3 groups: rostral primary (RoP), middle primary (MiP) and caudal primary (CaP) motor neurons (Myers et al. 1986) (Fig 3.1 A). Primary motor neurons initiate axon projections in a cell-type specific manner (Myers et al. 1986; Eisen et al. 1986; Zeller & Granato 1999). All three types of motor axons first extend their growth cones following a common path to reach the intermediate target – the horizontal myoseptum (HM) and pause for about two hours (Myers et al. 1986). After that, each type of motor axon diverges into their specific pathway to innervate ventral, dorsal and mediolateral muscles (McWhorter et al. 2003). The horizontal myoseptum is an important landmark and choice point for axon outgrowth. The CaP motor axon is the first to grow out of the spinal cord at around 18 hpf (Rodino-Klapac & Beattie 2004). At around 29 hpf, RoP, MiP and CaP axons have extended ventral-laterally, dorsally and ventrally into their target muscle groups (Rodino-Klapac & Beattie 2004). Secondary motor neurons are born from 16 hpf onwards (Eisen 1994). The first ventral secondary motor axon exits the spinal cord at around 28 hpf, while RoP-like and MiP-like axons extend from 48 hpf to 72 hpf (Myers et al. 1986; Ott et al., 2001). In human, α-motor neurons are the most abundant class of human motor neurons and control extrafusal muscle fibres, whereas γ-motor neurons innervate intrafusal muscle fibres (Patrick J Babin et al. 2014). Primary motor neurons have not been described in amniotes, and γ-motor neurons have not described in zebrafish, therefore secondary motor neurons are maybe more similar to human α-motor

neurons (Babin et al. 2014). A subtype of α-motor neurons – FF-subtype (fast-switch, fatigable) is found to be particularly vulnerable to degenerative disease such as spinal muscular atrophy (SMA) and amyotrophic lateral sclerosis (ALS), whereas γ-motor neurons are more resistant (Patrick J Babin et al. 2014; Conradi & Ronnevi 1993).

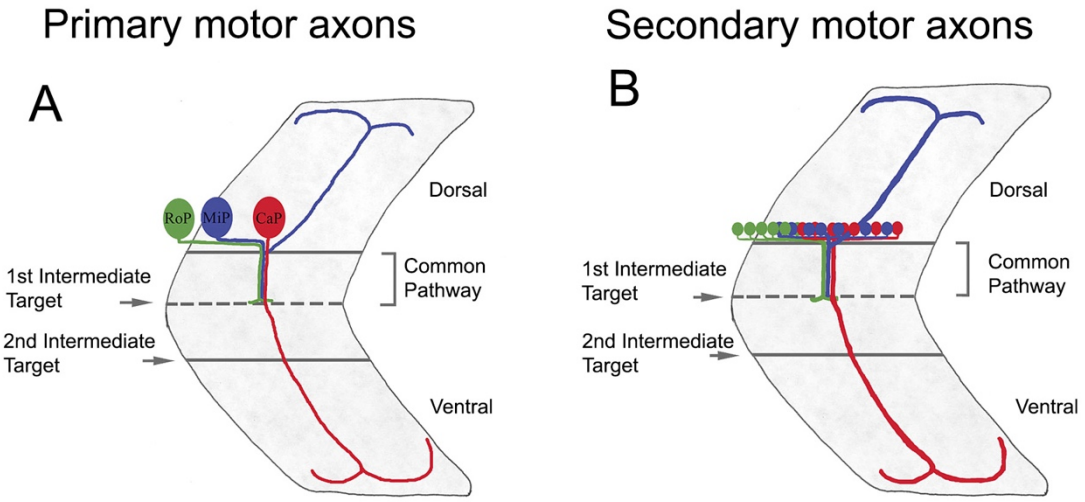

Fig 3.1 Projections of primary and secondary motor axons in embryonic spinal cord of zebrafish. This figure is adapted from McWhorter et al. (2003). **(A)** Schematic of three types of primary motor neurons: RoP, MiP and CaP. All three types of motor axons follow a common path to reach the first immediate target HM, and then diverge after reach the second intermediate target – the ventral edge of the notochord, to grow ventral-laterally, dorsally and ventrally. **(B)** Schematic of secondary motor neurons extending axons for ventral and dorsal muscle innervation.

Primary motor axons pioneer the paths of secondary motor axon (Pike et al. 1992). However, primary motor axons may not be required for the path-finding of secondary motor axons. Pike et al (1992) ablated primary motor neurons and showed secondary motor neurons are able to form normal ventral nerves without the guidance of primary motor axons. Panzer et al (2005) described a "*where's waldo*" (*wdo*) mutant, in which secondary motor axons grow aberrantly and ectopically, whereas primary motor axons remain unaffected, indicating additional cues are involved in the growth of secondary motor axons (Panzer et al. 2005).

So far, many genes have been identified to play a role in primary motor axon exits in zebrafish. For example, the *diwanka* gene is important for motor axon migration (Zeller & Granato 1999). In the *diwanka* mutant, motor neuron differentiation and survival are unaffected, however, primary motor axons failed to grow beyond the horizontal myoseptum to the somites. The *topped* gene specifically impact the extension of CaP axons (Rodino-Klapac & Beattie 2004). In *topped* mutants, ventral primary CaP axon stalled in the horizontal myoseptum, whereas the dorsal MiP axons project normally. *PlexinA3* is an essential guidance receptor for primary motor axon path-finding (Feldner et al. 2007; Palaisa & Granato 2007; Plazas et al. 2013). Knock down or knock out of *plexinA3* results in aberrant primary motor axon branching and ectopic exiting from the spinal cord. Work of Zhong et al (2012) elucidated the role of *chondrolectin (chodl)* gene in motor axon development by knock-down of *chodl* in zebrafish embryos, which caused a stalling of primary motor axon development in the horizontal myoseptum. However, there is little know about the essential genes that take part in secondary motor neurogenesis and their axon differentiation and growth. As mentioned above, secondary motor neurons are maybe more similar to human motor neurons (Babin et al. 2014). Therefore, if we understand how these motor neurons are generated and how their axons find their targets, we might be able to promote the regeneration of motor neurons that are not replaced in human motor neuron diseases and spinal cord injury in the future. Therefore, I was interested in searching for genes that influence the development of secondary motor neurons and their axon path-finding.

Owing to the generation of a transgenic reporter line, *Tg(islet-1:GFP)* (GFP; green fluorescent protein), in which the expression of GFP is driven by *islet-1* promoter (Uemura et al. 2005), I was able to examine the secondary motor neurons and axon morphologies in living animals. In *Tg(islet-1:GFP)* transgenic line (referred to as islet-1:GFP form here onward), GFP is expressed in trigeminal ganglion neurons, Rohon-Beard sensory neurons and some commissural interneurons (Uemura et al. 2005). In the spinal cord, at 72 hpf, islet-1:GFP+ neurons are the dorsal subset of the secondary motor neurons, although some ventral projection can be observed, they project axons mainly dorsally to innervate the dorsal trunk muscles (Uemura et al.

2005; Menelaou & Svoboda 2009) (Fig 3.2). For studies of ventrally projecting secondary motor neurons, another transgenic line *Tg(gata2:GFP)*, in which GFP is expressed in ventral sub-population of secondary motor neurons that innervate ventral group of muscles, is commonly used (Menelaou & Svoboda 2009). In my study, I used islet-1:GFP line that is available in my research group as a readout in our genetic screen.

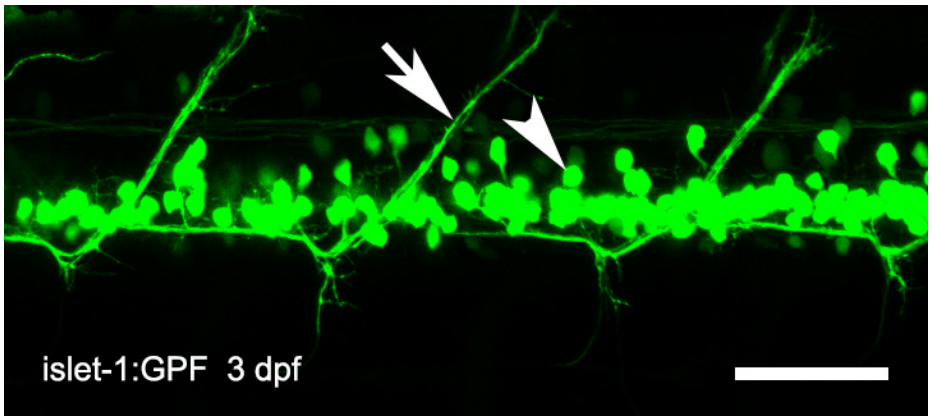

Fig 3.2 In the spinal cord of islet-1:GFP transgenic line, GFP positive neurons are the dorsal subset of the secondary motor neurons (arrowhead) that project to innervate dorsal muscle group at 72 hpf. Arrow indicates islet-1:GPF motor axon. Scale bar = 50 μm.

3.1.2 ENU-induced forward genetic screen

In order to identify genes important for secondary motor neuron development and axon differentiation in an unbiased manner, I conducted a N-ethyl-N-nitrosourea (ENU) induced mutagenesis screen. It is a chemical mutagenesis method by incubating adult male fish with a potent mutagen ENU in order to generate progenies carrying heritable genetic lesions (Mullins et al. 1994).

ENU is a chemical mutagen used to create point mutations that affects single genes in large scale mutagenesis screen. It is an alkylating agent that acts by transferring its ethyl group to oxygen or nitrogen site of DNA bases and causes mis-pairing and base-pair substitutions (Argmann et al., 2006). ENU has proven to be the most

efficient chemical mutagen with a rate of ~10^{-5} (about 1/1000 of the offspring) to generate point mutation in a given gene (Argmann et al., 2006). ENU has a lot of advantages compared with other mutagenesis methods. For instance, ethylmethanesulfonate (EMS) is commonly used in *Drosophila* and *C.elegans,* however, it gives a lower rate of recoverable mutations in zebrafish. Radiation mutagenesis such as X-rays and gamma rays show 10 folds lower rates of recoverable point mutation than ENU (Mullins et al. 1994; Solnica-Krezel et al. 1994). Point mutations allow the study of gene mutation in either complete or partial loss-of-function, as well as gain of function (Detrich et al. 1999).

In order to obtain progeny with non-mosaic DNA modifications (Solnica-Krezel et al. 1994), a pre-meiotic mutagenesis was performed (Professor David Lyons, Maria Rubio). ENU targets all cell stages in the male germ line, however, only mutations in pre-meiotic spermatogonial stem cells create non-mosaic mutation (Knapik 2000). This is because lesions are induced in a single strand of DNA and are fixed in both strands during DNA replication and cell proliferation before differentiation to mature sperm cells (Nair & Pelegri 2011; Mullins et al. 1994). The genome modifications created by ENU are heritable and mutations can be recovered in their F2 offspring (Solnica-Krezel et al. 1994). In this case, 50% of a F2 family are heterozygous and 25% F3 progeny are homozygosis for recessive mutations following the Mendelian ratios (Nusslein-Volhard 2012). This is in contrast to the mutagenesis in mature spermatozoa and female germ cells, in which the mutagenic effect is mosaic and recoverable mutation rate is low, as modifications are not fixed until after fertilization (Balling 2001). In post-meiotic germ cell mutagenesis, less than 25% progeny in F2 family carries new mutations due to the mosaic character of F1 generation, and subsequently give rise to less than 10% F3 progeny exhibiting a mutant phenotype (Driever et al. 1996).

In our genetic screen, individual F1 fish were mated with individual islet1:GFP animal to produce a F2 generation with GFP expressed motor neurons and motor axons. Phenotypic analysis is carried out in the F3 generation, and embryos are assessed for their islet-1:GFP motor neuron appearance and/or islet-1:GFP motor

axon projections for identifying genes impacting secondary motor neuron generation and/or axon development.

3.1.3 Whole genomes sequencing for gene identification

The ultimate goal of the ENU screen is to search for a causative gene that is responsible for a particular mutant phenotype. Briefly, genetic mapping involves the localization of a critical interval on a chromosome containing the mutation, followed by a targeted examination for candidate genes within this region, and subsequent validation by genotyping individual phenotypically wild-type siblings and phenotypic mutants.

A traditional method for the identification of a phenotype causing gene is positional cloning. Positional cloning is to use genetic markers (DNA segments) to localize candidate genes to a specific linkage group, and then increasingly narrow it down to a critical interval on chromosome (Detrich et al. 1999). For fine mapping and candidate gene search, bulked segregant analysis (BSA) was used to identify closely linked markers by comparing the amplification difference of genomic DNA pools between mutant and their phenotypically wild-type siblings (Quarrie et al. 1999; Puliti et al. 2007). Linked markers are defined when PCR (Polymerase chain reaction) amplified fragments only present in wild-type pool but absent in mutant pool. The process of positional cloning is cumbersome, tedious and time-consuming. For a low coverage, mapping has to be carried out in pools of embryos to test the linkage of hundreds of markers, which are to be verified with individual embryos to confirm the linkage of the mutation to a specific chromosome, and to further isolate markers tightly linked to the mutation. These steps usually involve hundreds even thousands of PCR amplifications and gel electrophoresis.

Next Generation Sequencing (NGS) technology, it has become widely used as a high-throughput method for linkage analysis and to identify mutated genes that correspond to an observed phenotype in both zebrafish (Voz et al. 2012) and other species. The principal of NGS is to identify a single nucleotide polymorphism (SNP) allele that is linked to a mutation, by comparing SNP variants between mutant

sequence and their phenotypically wild-type siblings (Henke et al. 2013). It requires the generation of homozygous mutants from a mutant founder to a separate polymorphic mapping strain, in order to provide a high level of polymorphic variation for genetic mapping as well as to distinguish strain specific alleles from the phenotype-causing mutation (Henke et al. 2013). For sequencing, embryos are collected from heterozygous carriers and sorted into mutant and phenotypically wild type embryos. Genomic DNA pooled from the mutants and their siblings are fragmented to short fragments using routine preparation of DNA libraries and processed with an Illumina sequencing technology equipped with manufactured primers. For genetic linkage analysis, the short sequences generated are assembled and aligned to the wild type reference genome. Chromosome regions containing the mutation are established from comparing the differences between the reference sequence and the mutant sequence. Through the public available genomic database, SNP within the linked region can be identified as potential candidate gene that is causing the phenotype (Voz et al. 2012; Schneeberger 2014).

WGS is a powerful replacement for traditional positional cloning due to its efficiency, easy applicable and time-effective features. With the recent advancement of the technology the cost is becoming more and more affordable, making it an excellent tool for genetic mapping of mutate genes. In my research, I took advantage of the WGS technique to identify genes that are responsible for phenotypes observed in mutants of interest.

3.2 Results

3.2.1 A screen for mutants that affect secondary motor neuron and their axon differentiation

To discover new genes that are essential for the differentiation of spinal motor neurons and axons, I conducted a forward genetic screen for recessive alleles affecting secondary motor neuron generation and their axon path-finding in zebrafish mutagenized with ENU. I used a transgenic reporter line that selectively labels dorsal subtypes of secondary motor neurons as a readout for the assessment of motor neuron and motor axon defects. I was particularly interested in (1) finding mutants in

which the timing of islet-1:GFP motor neuron development or the number of cells were altered, in order to find genes that are important for motor neuron development; (2) mutants that display errors in islet-1:GFP motor axon projections, such as ectopic spinal exits, abnormal branching, mis-projection or stalling, in order to identify genes that are essential for motor axon path-finding.

I started ENU screening by generating F2 heterozygotes that are carrying random mutations. Nearly one thousand pairs of individual F1 animals and individual islet-1:GFP fish were mated. 301 F2 families from 666 successful pair mating were raised, representing a total of 602 mutagenized genomes. Of these 301 F2 families, 111 with reasonable numbers (> 8) of fish and relatively balanced gender were used for the screen, representing 222 mutagenized genomes. With the help of my colleagues Dr. Karolina Mysiak and Dr. Antón Barreiro-Iglesias, 60-80 pairs from the F2 families were set up each week, an average of 1200 embryos were screened for any motor neuron phenotype, and islet-1:GFP+ dorsal projections were examined in 700-800 flat-mounted living embryos at 3 dpf under a microscope. The mating and screening process lasted for 44 weeks and a total of 52,800 embryos were screened for phenotypes of interest. On average 4-6 crosses per family were evaluated from a total of 111 F2 families. This correspond to approximately 1.6 mutagenized genome screened per F2 family. I calculate that we effectively screened 178 mutagenized genomes of the 222 genomes represented in the 111 F2 families.

We found 6 families in which embryos display gross morphological defects. In all 6 families, embryos showed different morphological phenotypes including small eyes, heart oedema, curved body axis and signs of necrosis which eventually lead to complete degeneration (Fig 3.3). To avoid any indirect effects on motor neuron or axon development due to the overt physical impairment, these mutants were discarded.

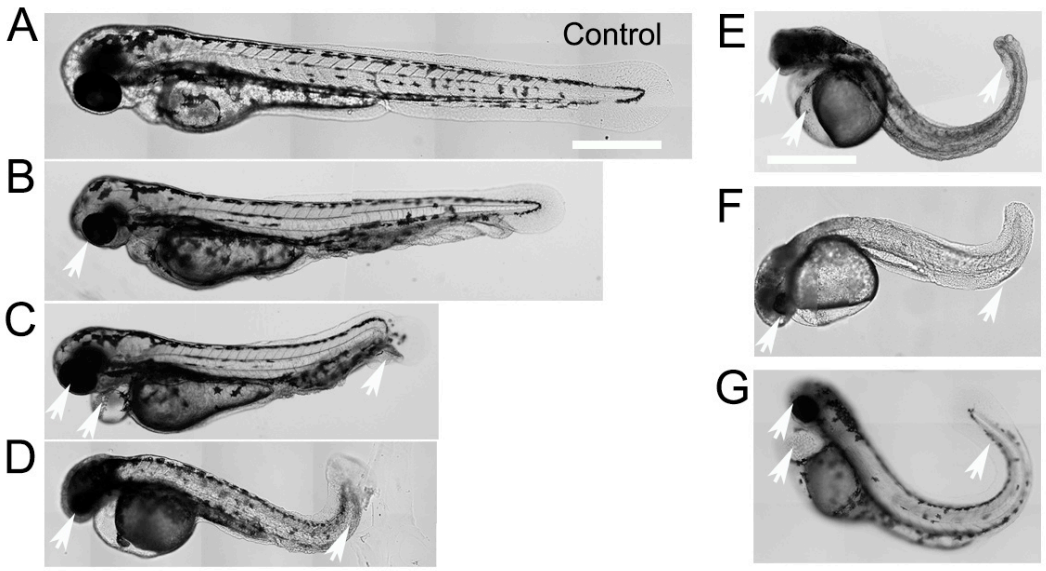

Fig 3.3 Identified mutant lines with general morphological defects. (A) Phenotypically wild-type control sibling at 3 dpf. **(B-G)** 6 mutants with general developmental defects showing small heads, small eyes, heart oedema and curved body axis are shown (indicated with arrows). Lateral views of embryos are shown, rostral is left, dorsal is up. Scale bar: 500 μm in A for B-D; 500 μm in E for F,G.

From the screen, another 6 mutant lines were discovered with altered motor neuron numbers and/or motor axon outgrowth. Among these 6 mutant lines, 4 were identified with fewer islet-1:GFP motor neurons at 3 dpf (Fig 3.4 B'-E'). These 4 mutant lines were designated #151, #160, #171, #217 on the basis of their F2 family names. In addition to their motor neuron defects, mutants also displayed morphological phenotypes such as small eyes and more rounded yolk sac (Fig 3.4 B-E).

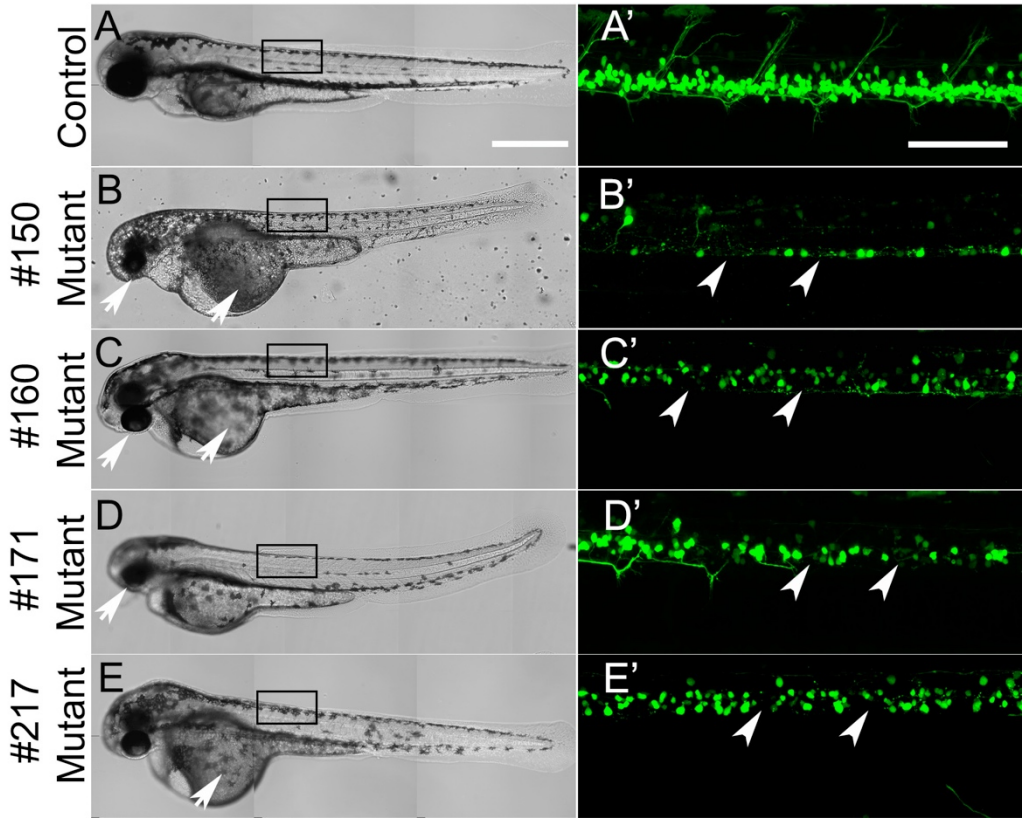

Fig 3.4 Four mutant lines identified with fewer islet-1:GFP+ motor neurons at 3 dpf. (A) Bright field image of a control sibling at 3 dpf. **(B-E)** Bright field images of the morphologies of 4 mutants designated #151, #160, #171, #217 are shown. Mutants displayed morphological phenotypes such as small eyes and rounded yolk sac (arrows). **(A'-E')** Higher magnification of the areas boxed in A-E, respectively, are shown. The number of islet-1:GFP+ motor neurons (arrowheads) is reduced in all 4 mutants (B'-E'), compared with the control sibling (A'). Lateral views of embryos are shown, rostral is left, dorsal is up. Maximum intensity projection. Scale bars: 500 μm in A for B-E; 100 μm in A′ for B′-E′.

The remaining 2 mutant lines showed defects in islet-1:GFP+ motor axon outgrowth (Fig 3.5). At 3 dpf, mutants from designated #55 were shorter in size and appeared curved compared to non-homozygous siblings. Islet-1:GPF+ motor axons were disorganized in ventral position while dorsal projections were missing. The mutant line designated #249 showed an absence of dorsal projections and short ventral axons.

#249 mutants have smaller eyes and a more rounded yolk sac compared with their control siblings.

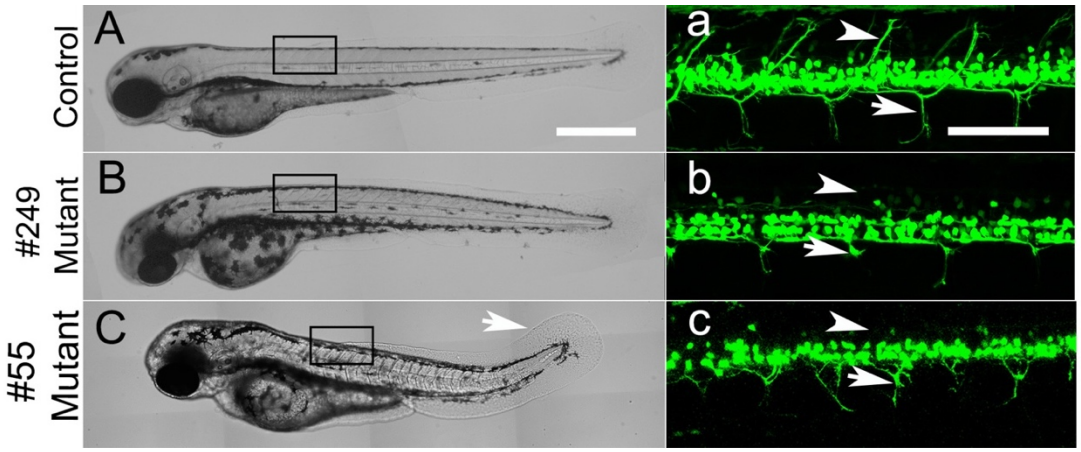

Fig 3.5 Two families identified with islet-1:GFP+ motor axon defects. (A-C) Bright field images of a control sibling, a #249 mutant and a #55 mutant at 3 dpf. #55 showed short body size and curved body axis (arrow in C). **(a-c)** Higher magnification of the areas boxed in A-C, respectively, are shown. In #249 mutant (b), dorsal motor axons were absent (arrowhead) and ventral axons were relatively short (arrow), whereas in #55 (c), dorsal islet-1:GFP+ axons (arrowhead) were missing and ventral projections (arrow) were disorganised, in comparison with control sibling (a). Lateral views of embryos are shown, rostral is left, dorsal is up. Maximum intensity projection. Scale bars: 500 μm in A for B, C; 100 μm in a for b, c.

In order to confirm the mutation is inherited from their founder parents (germline transmission), mutant lines were outcrossed with another wild type line (eg. TL) that is polymorphic to the founder fish (wik). Off-springs raised were used for in-crosses and assessed for their phenotypic replications in the subsequent generations. Successive outcrosses also reduce the probability that more than one mutation leads to the observed phenotypes. Moreover, genetic mapping to identify phenotype-causative genes relies on detecting the DNA polymorphism difference between two strains (Detrich et al. 1999), therefore this is a time-consuming but necessary step in obtaining mutants as well as creating a mapping strain for genetic linkage analysis (Nusslein-Volhard 2012; Voz et al. 2012; Zhou & Zon 2011). Reproducibility of

phenotypes were confirmed in the F4 generation of 4 mutant lines: #151 and #171 with fewer numbers of islet-1:GFP+ motor neurons; #55 and #249 with islet-1:GFP+ motor axon defects.

3.2.2 Mutant characterization at early developmental stage

3.2.2.1 Sonic hedgehog signalling pathway is not affected

I first analysed the molecular pathways that could possibly be affected in these mutants. Sonic hedgehog signalling (Shh) is a pivotal morphogen in spinal cord differentiation and regulates the generation of motor neurons from the motor neuron progenitor domain (pMN) in the ventral spinal cord (Francius & Clotman 2014). For example, in the mutant *smoothened (smo)*, primary motor axons are disorganized and secondary motor neurons are missing (Chen et al. 2001). Reimer et al (2013) shown that endogenous dopamine acting on the Shh pathway enhances motor neuron generation in the ventral spinal cord. Morpholino oligonucleotides (MOs) knock-down of dopamine receptor drd4a delayed the production of dorsal subtype of islet-1:GPF+ motor neurons in zebrafish embryos (Reimer et al., 2013).

In Shh pathway, transmembrane protein Patched 2 (Ptc2) binds to another protein Smoothened (Smo), which inhibits glioma-associated oncogene homolog 3 (Gli3) and result in repressed gene expression. When Shh binds to Ptc2, Smo is de-repressed, which in turn activates the downstream pathway. This indicates that Ptc2 acts as a negative regulator in a Shh feedback loop (Fig 3.6). To test the possible involvement of Shh, I used an antisense RNA probe to detect *ptc2* and performed in situ hybridization at 24 hpf. As mutants cannot be clearly distinguished from their phenotypically wild-type siblings at 24 hpf, I used a pool of mixed embryos (+/+, +/m, m/m) for each mutant line (n = 20-30, N = 3). If Shh was affected in a mutant line, the expression of *ptc2* would be altered in 25% of embryos. I observed no apparent change in *ptc2* expression in embryos examined in 4 mutant lines (15-22 out of 60-90 embryos for each line were expected to show a change in *ptc2* expression) (Fig 3.7), suggesting that a different pathway may be affected in these four mutant lines.

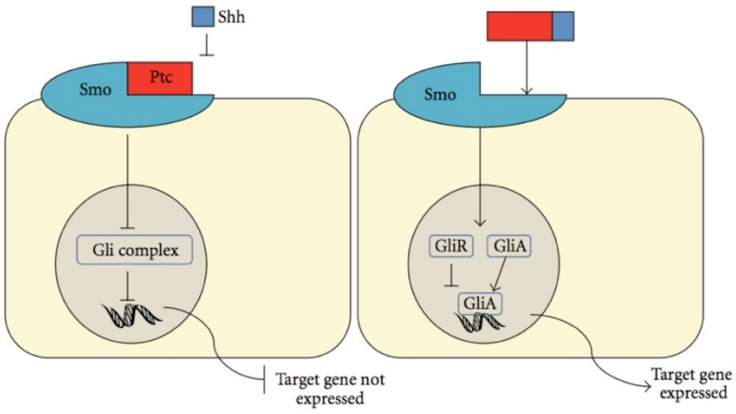

Fig 3.6 Illustration of Shh pathway. This figure is adapted from Evans et al. (2012). The left figure shows when Shh cannot bind to Ptc, Ptc protein binds to Smo, which lead to inactivated downstream pathway. The right figure shows when Shh binds Ptc, the Ptc-Smo complex is disassociated, which lead to functional Gli activator (GliA) and activate gene expression.

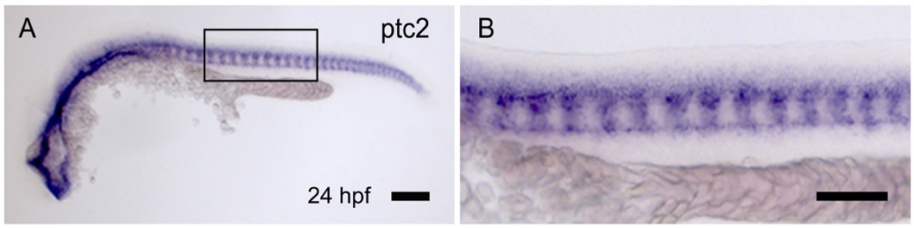

Fig 3.7 Illustration of *ptc2* expression at 24 hpf. (A) Lateral view is shown, dorsal is up, anterior is to the left. **(B)** High-magnification image of the area boxed in A. Scale bars: A = 50 μm, B = 100 μm.

3.2.2.2 Immunohistochemistry (IHC) to verify the specificity of mutant phenotypes

To verify whether the motor neuron and axon phenotypes observed were the consequences of early abnormalities, I surveyed the degree of defects in all 4 mutants at early developmental stage (Table 3.1). I used several molecular markers to examine early born neurons and axons at 33 hpf. Similar to *ptc2* in situ hybridisation, antibody labelling at this time point was applied to a pool of embryos (+/+, +/m, m/m) for each mutant line and qualitative analysis was performed. If a mutant line has

early developmental abnormalities, I expected to detect ~25% of embryos with altered patterns for the markers tested.

I applied acetylated α-tubulin to label brain commissure tracts, cell bodies and early projecting motor axons (Fig 3.8 A-B). A zn-12 antibody is also applied to label motor axon projections (Feldner et al. 2007). HB9 antibody was used to detect the appearance of early born motor neurons (Fig 3.8 F) (Barreiro-Iglesias et al. 2015). To analyse the appearance of interneurons, I used anti-3A10, which labels Mauthner cells in the hindbrain and commissural ascending primary (CoPA) interneurons in the spinal cord (Feldner et al. 2007) (Fig 3.8 D,E). A 4D9-engrailed antibody that marks muscle pioneer cells at the horizontal myoseptum (Feldner et al. 2007) was also included (Fig 3.8 G). I found that in mutant lines #151, #171 and #249, embryos showed no apparent abnormalities for all markers used. This indicates that early development of cell types, recognised by the above antibodies was not altered. However, mutant line #55 displayed abnormal formations of primary motor axons (Fig 3.9 C-C'), Mauthner axons as well as CoPA interneuron axons (Fig 3.9 A-B'), suggesting the motor axon phenotype is likely to be the secondary effect of an early general developmental defect. This also demonstrates that I was able to detect early deficits in a mutant line from a pool of mixed embryos. As I was looking for genes more specifically involved in motor neuron development, the analysis was not further pursued and mutant line #55 was discarded.

Table 3.1 Mutant lines and structures analysed at 33 hpf by IHC

Mutant line (n with a phenotype / Total n analysed)		**#55**	**#151**	**#171**	**#249**
3A10	Mauthner cells & axons	7/29 (24%)	0/41	0/55	0/26
	CoPA interneurons & axons	7/29 (24%)	0/41	0/55	0/26
acetylated α-tubulin	CaP axons	6/22 (27%)	2/53 (3.7%)	0/37	0/22
	RB neurons		0/53	0/37	0/22
	Brian commissural tracts		0/53	0/37	0/22
Zn-12	CaP axons		0/62	1/46 (2.1%)	0/34
Hb9	Motor neurons	0/21	0/24	0/33	0/25
4D9 engrailed	Muscle pioneer cells	0/19	0/20	0/18	0/15

Note: (1) As mutants cannot be clearly distinguished from their control siblings, the works presented here are qualitative analysis. **(2)** N with a phenotype/Total n analysed stands for numbers of embryos display an abnormal phenotype in the marker tested among the total number of embryos examined. **(3)** Occasionally, I observed one or two extra motor axon exits from the spinal cord in #151 and #171 in α acetylated tubulin and zn-12 labelled CaP axons. However, the number of embryos exhibit extra motor exits is significantly lower than 25% of the total embryos examined.

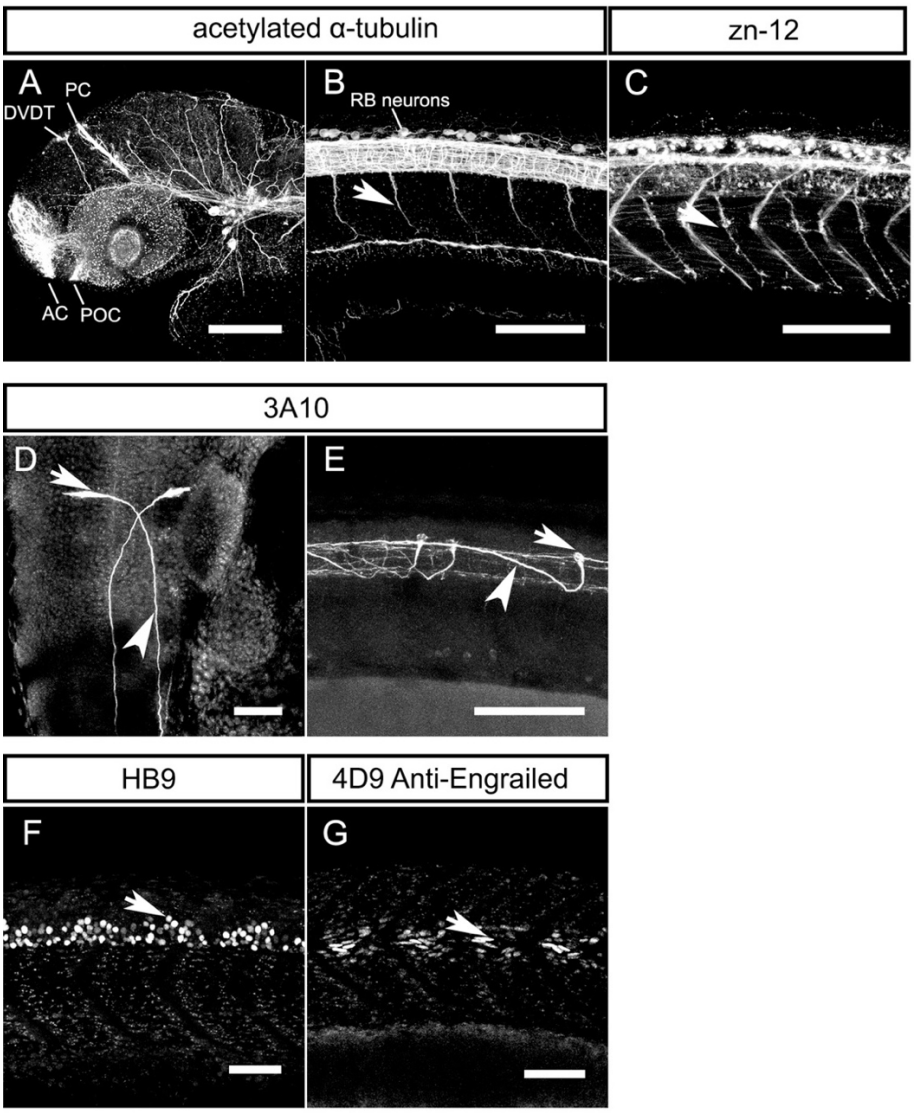

Fig 3.8 Illustrations of antibody staining at 33 hpf non-mutant embryos. (A) Acetylated α-tubulin labelled commissural tracts in the brain. DVDT stands for dorsal-ventral diencephalic tract; PC indicates posterior commissure; POC indicates post-optic commissure; AC indicates anterior commissure (Chitnis & Kuwada 1990; Hjorth & Key 2002). **(B)** Acetylated α-tubulin labelled ventral nerve tracts (arrow) and Rohon-Beard (RB) sensory neurons. **(C)** zn-12 antibody labelled ventral axons (arrow). **(D)** 3A10 labelled Mauthner cells (arrow) and axons (arrowhead) in the brain, as well as **(E)** CoPA interneurons (arrow) and axons (arrowhead). **(F)** Appearance of HB9 immuno-labelled early born motor neurons (arrow) in embryonic spinal cord. **(G)** 4D9 engrailed antibody labels muscle pioneer cells (arrow) in the spinal cord. Lateral views of embryos are shown, rostral is left, dorsal is up; expect for (D) Coronal view of the embryo is shown; anterior is up. Maximum intensity projection. Scale bars: 100 μm in A, B, C; 50 μm in D; 100 μm in E; 50 μm in F, G.

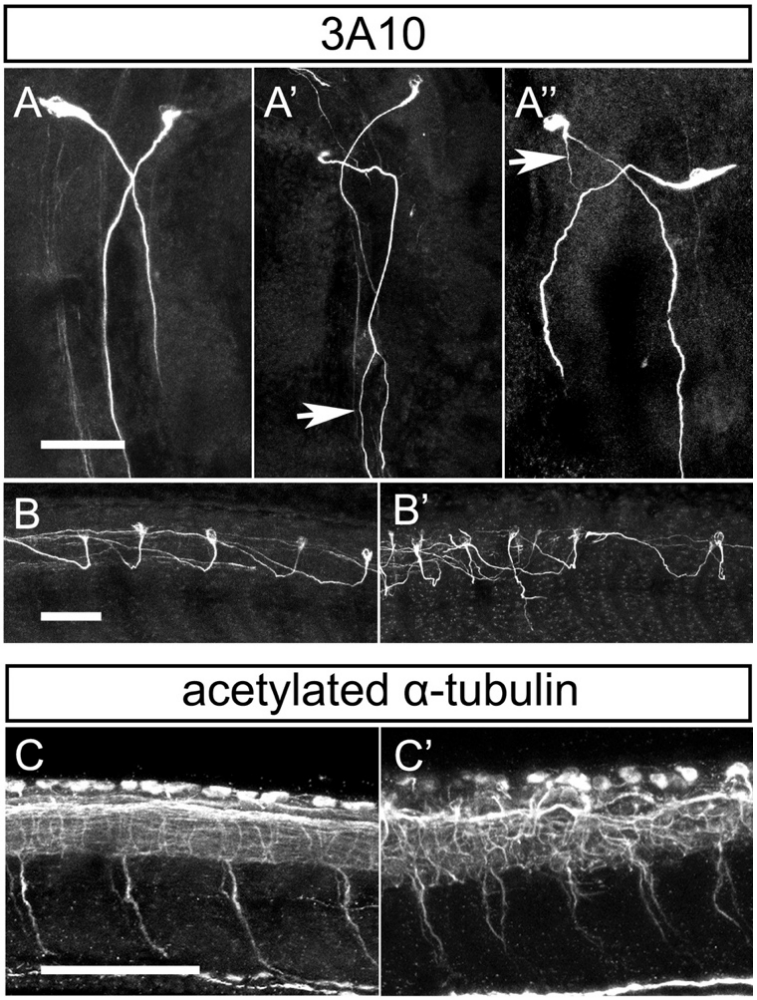

Fig 3.9 Mutant line #55 showed motor axon and interneuron axon abnormalities at 33 hpf. (A-A'') Coronal view of embryos are shown; anterior is up. Compared with the control sibling (A), 3A10 antibody labelled Mauthner axons in mutants (A',A'') displayed abnormal branches (indicated by arrows). **(B,B')** Lateral views of embryos are shown, rostral is left, dorsal is up. In the spinal cord, CoPA interneurons and axons are disorganized in the mutant (B'). **(C,C')** Mutant embryo (C') showed a deformation of acetylated α-tubulin stained motor neuron cell bodies and axons. Maximum intensity projection. Scale bars: 100 μm in A for A', A''; 50 μm in B for B'; 50 μm in C for C'.

In Summary, we conducted a small scale ENU screen in 111 F2 families in search for genes that influence motor neuron and motor axon differentiation – specifically for dorsal project motor neurons. In the initial screen, together with my colleagues, we identified 6 families with fewer islet-1:GFP+ motor neurons and/or deficient dorsal motor axons. From these 6 mutant lines, phenotypes of 4 mutant families (#55, #151, #171, #249) were confirmed and analysed at early stage to verify the phenotypic specificity. Except for #55, which showed aberrant islet-1:GFP axons, I found embryos from the remaining 3 mutant lines showed no early developmental abnormalities with the markers tested.

In my research, I focused on two mutant lines for more detailed examinations at later stages: #151, in which mutant embryos displayed the most prominent islet-1:GPF motor neuron defects; and #249 with missing islet-1:GPF motor axons.

3.2.3 Verification of mutant line #249

3.2.3.1 Dorsal secondary motor axons failed to grow out and the late born motor neuron generation is compromised in #249 mutant

At 3 dpf, #249 mutants showed a failure in islet-1:GFP+ motor axon outgrowth, whereas in their control siblings, axons have extended dorsally (Fig 3.10). As mentioned earlier, although GFP is mainly expressed in those dorsally projecting secondary motor neurons (Uemura et al. 2005), some ventral projection can also be observed in islet-1:GPF transgenic line (Menelaou & Svoboda 2009). Mutants also showed altered ventral extension compared with control siblings.

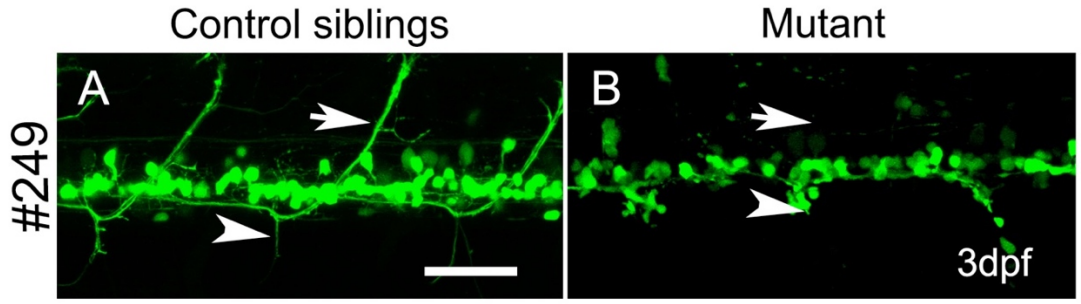

Fig 3.10 islet-1:GFP+ motor axons are absent in #249 at 3 dpf. (A) A control sibling has dorsally extended islet-1:GFP motor axons (arrow) and some ventral

projection (arrowhead). **(B)** Mutant failed to grow dorsal axons (indicated with arrow), and showed altered ventral projections (arrowhead) compared with control. Lateral views of embryos are shown, rostral is left, dorsal is up. Scale bar = 50 μm.

To test if the axon defect is specific to secondary motor axons, I used acetylated α-tubulin that labels both primary and secondary axons at 3 dpf, and a cell-type-specific marker zn-8 for secondary motor axons. Antibody zn-8 recognizes the cell recognition molecule neurolin/DM-GRASP, which is present only on secondary motor neurons and their axons (Ott et al., 2001; Menelaou & Svoboda 2009). Results showed in both control siblings and mutants that an antibody to acetylated α-tubulin labelled dorsal and ventral motor axons are present (Fig 3.11 A'',B''), whereas dorsally projecting secondary motor axons are missing in zn-8 staining (Fig 3.11 A',B'), indicating that the development of primary motor axons was normal. Interestingly, the mutant also showed axons accumulated in the pathway above the HM, suggests that the secondary motor axons that project ventro-medially in RoP pathway may also be affected (Fig 3.11 B'). These data indicate that the failure of motor axon outgrowth is specific to the dorsal secondary motor axons in #249 mutants.

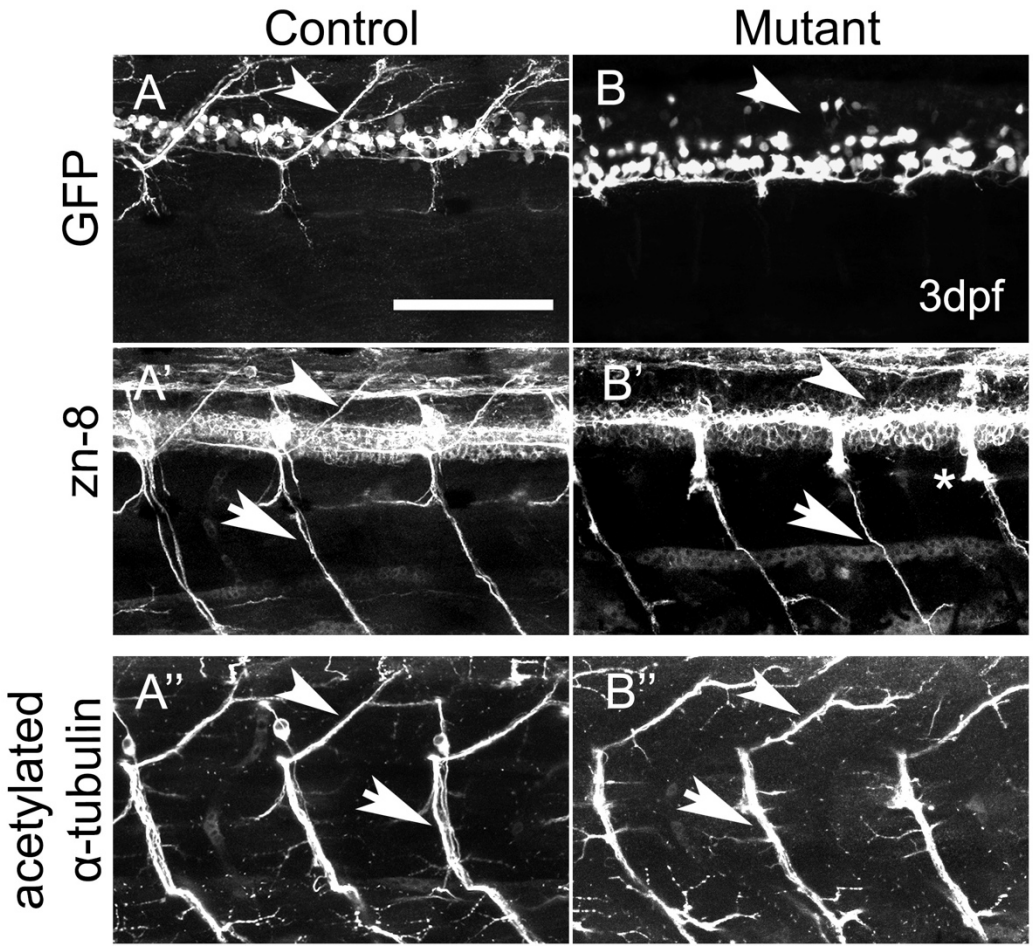

Fig 3.11 #249 mutant embryos show a lack of secondary dorsal motor axons. (A,B) At 72 hpf, islet-1:GFP control sibling has grown dorsal projection (arrowhead), whereas dorsal axons are missing in the mutant (indicated by arrowhead). **(A',B')** zn-8 antibody staining revealed both dorsal (arrowhead) and ventral secondary axons (arrow) in the control sibling (A'). However, zn-8 labelled dorsal projection is absent in the mutant (indicated by arrowhead), and showed accumulated axons in the pathway above the HM (indicated by asterisk). zn-8 labelled ventral projection is present in the mutant (arrow). **(A'',B'')** Acetylated α-tubulin labelling in control sibling (A'') and mutant (B'') showed dorsal and ventral projection. Lateral views of embryos are shown, rostral is left, dorsal is up. Scale bar = 100 μm.

In order to investigate whether the generation of motor neurons in the mutants is altered, I used two antibodies to examine the numbers of motor neurons. I used anti-Islet-1 to label late-born motor neuron somata (Feldner et al. 2007). Islet-1 is a transcription factor that belongs to LIM family. *islet-1* mRNA can be detected in Rohon-Beard sensory neurons and interneurons such as DoLA (dorsal longitudinal ascending neuron) (Inoue et al. 1994). In motor neurons, endogenous *islet-1* mRNA is also expressed by secondary motor neurons after 20 hpf (Inoue et al. 1994). This is unlike the islet-1:GPF transgenic line, in which GFP is expressed mainly in the dorsal subtype of secondary motor neurons. Reimer et al (2008) showed that 89% of the GFP-expressing neurons in the islet-1:GFP animals are double-labelled by the Islet-1 antibody, indicating the transgene expression is specific (Reimer et al. 2008). I also used choline acetyltransferase (ChAT) to label mature motor neurons in the spinal cord.

I first compared the number of GFP+ cells in spinal cord sections of the mutants and control siblings. At 3 dpf, the number of GFP+ cells in mutant group was 6.75 ± 0.91, 34% less than the control group 10.22 ± 0.56 (**p=0.0050; 14 μm spinal cord section, 4 sections per embryo; n = 9-9; Mean ± SEM; Unpaired t test, two-tailed) (Fig 3.12 C). Using anti-ChAT to label fully differentiated motor neurons, mutant embryos showed 30% fewer numbers ChAT immune-labelled cells in comparison with control siblings (Control group: 14.81 ± 0.65, mutant group 10.39 ± 0.61; Mean ± SEM; ***p=0.0001; 14 μm spinal cord section, 4 sections per embryo; n = 9-9; Unpaired t test, two-tailed) (Fig 3.12 D). I observed 14% lower numbers of Islet-1 immunoreactive motor neurons in the mutant group, compared with control group (Control: 116.2 ± 3.23, Mutant: 100.2 ± 3.97; 60 μm spinal cord; Mean ± SEM; **p=0.0044; n = 13-12; Unpaired t test, two-tailed) (Fig 3.12 G). These results indicate that the generation of the late-born motor neurons is decreased in the mutants

Taken together, these data suggest that the mutation affects not only the dorsal and rostral secondary motor axon outgrowth, but also the number of a small population (about 14-34%) of the late born motor neurons.

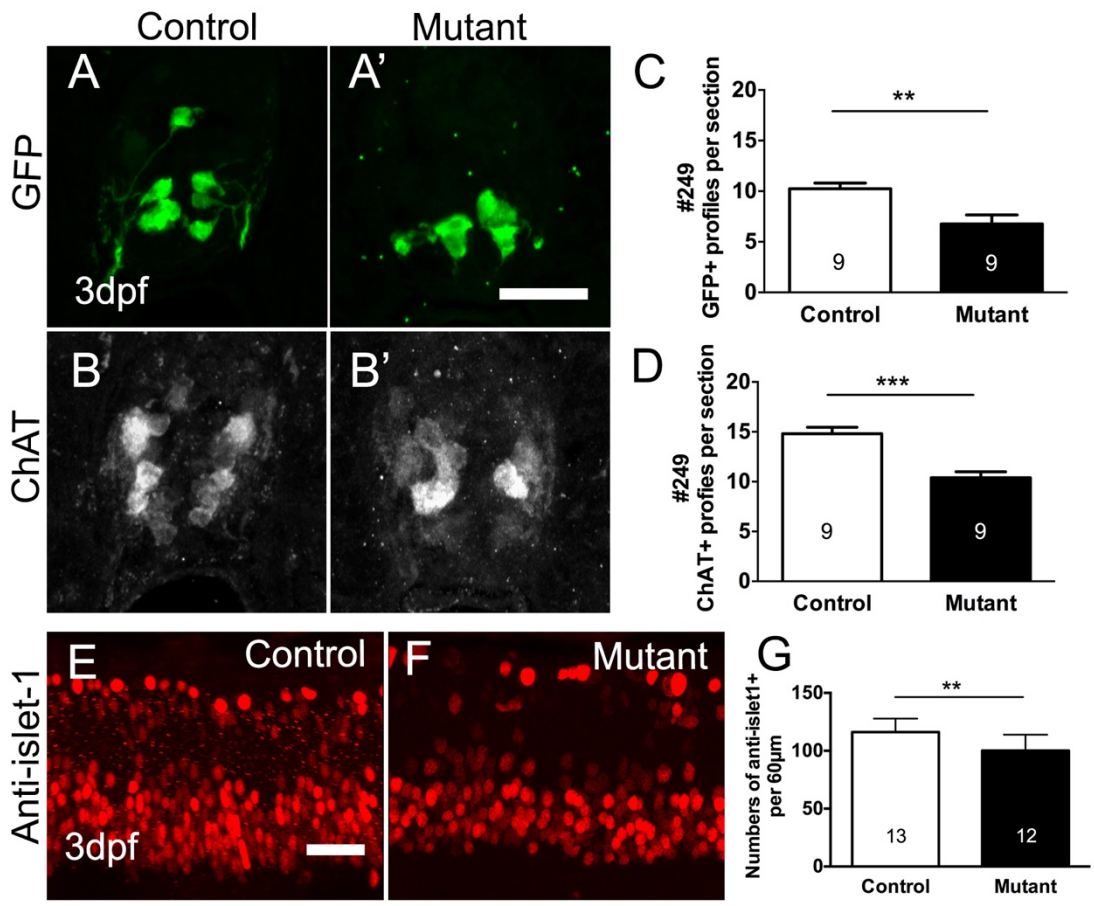

Fig 3.12 #249 mutants have fewer motor neurons at 3 dpf. (A-B') Cross sections of the spinal cord; dorsal is up. **(C)** Quantification shows few numbers of GPF+ motor neurons are generated in the mutants (**p=0.0050; Unpaired t test). **(D)** Control siblings show higher numbers of fully differentiated spinal motor neurons at 3 dpf, compared with the mutants (***p=0.0001; Unpaired t test). **(E,F)** Lateral views of embryos are shown; rostral is left; dorsal is up. Rohon-Beard sensory neurons are indicated with RB, Islet-1 immuno-labelled motor neuron are indicated with arrows. **(G)** Fewer numbers of anti-Islet-1 labelled motor neurons in the mutants, compared with control siblings (**p=0.0044; Unpaired t test). Scale bars: A'' = 25 µm for A-B''; E = 25 µm for F.

To test whether fewer motor neurons are due to decreased motor neuron progenitor cell proliferation, I crossed #249 heterozygotes with a olig2:DsRed transgenic line. In the olig2:DsRed line, DsRed protein is expressed in motor neurons and oligodendrocytes lineage cells (OPCs) under the regulatory sequences of the *olig2* gene. #249/olig2:DesRed heterozygous parents were identified from further in-crosses and mutant embryos express DsRed protein were used for progenitor cell proliferation detection. I investigated the proliferation of olig2:DsRed+ cells in the mutant pMN zone at 51 hpf, when mutants can be distinguished from their phenotypically wild-type siblings, and at 72 hpf. To do so, I used the proliferation marker anti-phospho-Histone H3 (PH3) to label cells in M phase of the cell cycle. In this case, proliferating progenitor cells in the pMN were PH3 positive and DsRed positive cells. Quantification analysis of the number of olig2:DsRed+/PH3+ double labelled cells showed no significant difference between control and mutant group at 51 hpf (Control: 6.14 ± 0.70, Mutant: 9.42 ± 1.36; Mean ± SEM; P=0.0950; 300 μm spinal cord; n = 7-7; Mann Whitney test, two-tailed) (Fig 3.13 A-C). At 72 hpf, I observed 0.50 ± 0.22 olig2:DsRed+/PH3+ cells in control siblings, whereas no double labelled cells were detected in the mutants (Fig 3.13 D-F) (P=0.1818; 300 μm spinal cord; n = 6-5; Mean ± SEM; Mann Whitney test, two-tailed). I observed some PH3 positive cells outside of the pMN domain, demonstrating that I am able to detect such cells. However, to confirm that the proliferation of motor neuron progenitor cells in the mutants is indeed not reduced, bigger sample size is required to increase the statistical power of the findings. For example, at 51hpf PH3 labelling, 13 samples in each group is needed in order to achieve statistical power of over 80%.

Furthermore, as the earliest time point that the mutants can be phenotypically distinguished from their control siblings was at 51 hpf, it is necessary to examine the proliferation at earlier time points once the phenotype causative gene is confirmed. Future experiments also need to address that reduced number of motor neurons is not due to the cell death.

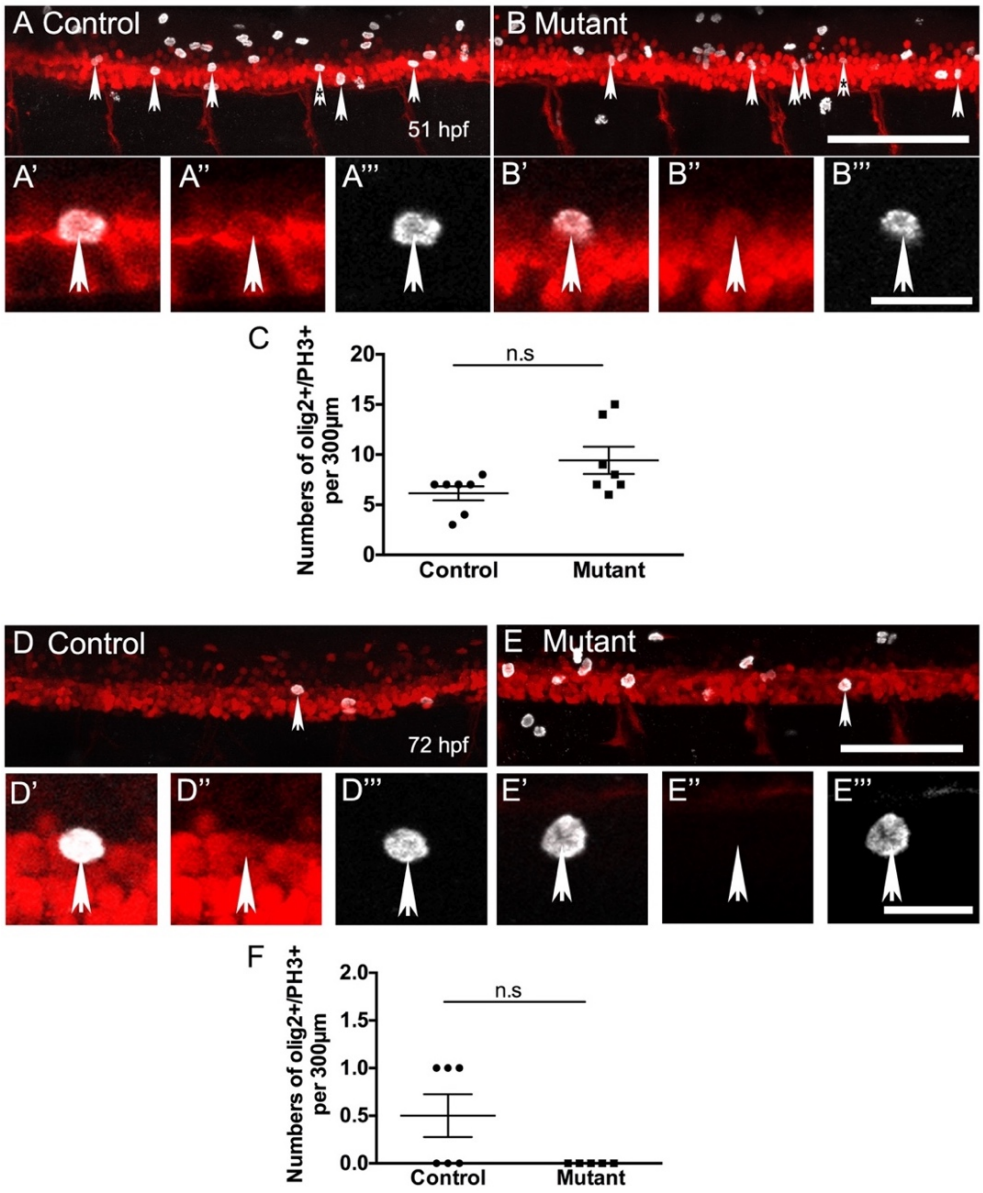

Fig 3.13 Proliferation of motor neuron progenitor cells is not reduced in #249 mutants. (A,B) Lateral views of 51 hpf embryos are shown; rostral is left, dorsal is up. PH3 positive and DsRed positive cells are indicated by arrows. **(A'-B''')** Single optical sections at higher magnification show a DsRed+/PH3+ double labelled cell (indicated by asterisks in A, B). **(C)** Quantification showed no significant difference in numbers of olig2:DsRed+/PH3+ cells in the pMN zone between control group and mutant group at 51 hpf (P=0.0950, Mann Whitney test). **(D,E)** Lateral views of 72 hpf embryos are shown; rostral is left, dorsal is up. **(D'-D''')** Single optical sections at higher magnification show a DsRed+/PH3+ double labelled cell (indicated by arrow in D). **(E-E''')** Single optical sections at higher magnification show a PH3 positive

cell outside of the areas of interest (indicated by arrow in E). **(F)** No significant difference in numbers of olig2:DsRed+/PH3+ cells in the pMN zone between control group and mutant group at 72 hpf (P=0.1818, Mann Whitney test). Scale bars: B = 100 μm for A; B''' = 15 μm for A'-B''; E = 100 μm for D; E''' = 15 μm for D'-E''.

3.2.3.2 Mutant embryos failed to form myelin

In embryonic spinal cord, *olig2*-expressing pMN domain specifies motor neurons as well as oligodendrocytes (Kazakova et al. 2006). Oligodendrocyte progenitors (OLPs) produced from pMN first proliferate, then migrate laterally and dorsally before differentiating into mature oligodendrocytes. In the central nervous system, single or multiple axons are enwrapped by multiple layers of myelin sheaths formed by oligodendrocytes (Kazakova et al. 2006). Myelination of motor axons reduces energy consumption for neuronal communication and facilitates rapid saltatory conduction of action potentials along axons. In the CNS system, neurons and oligodendrocytes interact reciprocally to coordinate myelination. Neurons are capable of regulating the development of myelin-forming oligodendrocytes (Simons & Trajkovic 2006). Neuronal signals such as plate-derived growth factors (PDGF) were found to mediate myelination by controlling OPC proliferation and survival (Simons & Trajkovic 2006). Vartanian et al (1999) suggested that neuregulins derived from motor neurons in the ventral ventricular zone of the spinal cord are likely to be required for oligodendrocytes lineage development. Spinal cord cultures from neuregulin knock-out mice showed specific loss of myelin-forming oligodendrocytes, whereas the addition of recombinant neuregulin rescued oligodendrocytes development (Vartanian et al. 1999). Axonal factors are also found to be able to stimulate the development of oligodendrocytes and myelination (Barres & Raff 1999; Gabrièle Piaton et al. 2010). It has shown that oligodendrocytes and myelin specific proteins also play a role in motor axon development. For example, a myelin protein called proteolipid protein (PLP) was identified as an essential mediator for myelinated axon stability and integrity (Gabrièle Piaton et al. 2010). PLP-deficient mice showed axonal swelling and degeneration in the optic nerve and spinal cord (Griffiths et al. 1998). Moreover, mature oligodendrocytes provide long-term support for axon

survival. Defects in oligodendrocytes could cause demyelination which leads to subsequent axon degeneration (Nave 2010).

To investigate if the myelin formation was compromised in the mutants, I examined myelination in mutant embryos with an antibody against the myelin protein Claudin k (Münzel et al. 2014). I did not detect myelin sheath in the mutants at both 72 hpf and 80 hpf (Fig 3.14), suggesting the gene may also influence oligodendrocyte formation and/or myelination.

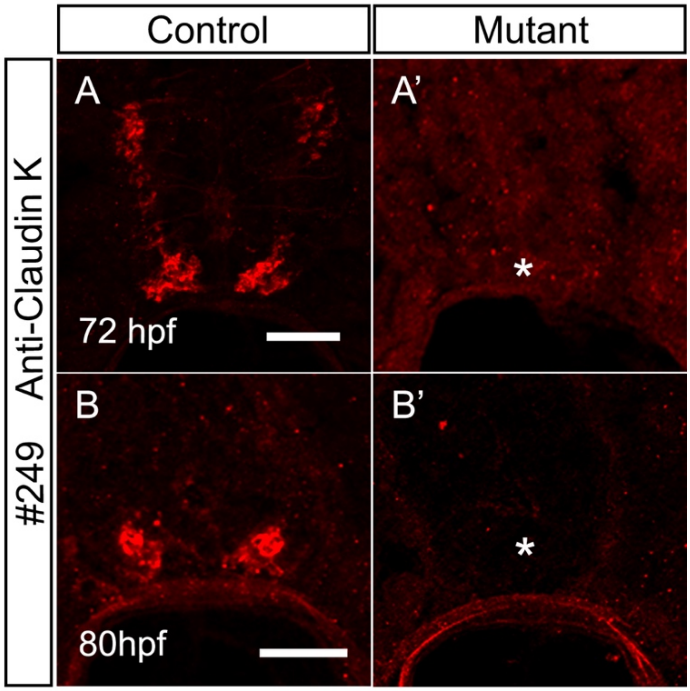

Fig 3.14 Mutants failed to form myelin at 3 dpf. (A,A') Mutants show an absence of myelin (indicated by asterisk) at 72 hpf, compared with control siblings. **(B,B')** Anti-Claudin K labelling confirms the failure of myelination in the mutants (asterisk) at 80 hpf. Dorsal is up, ventral is down. (Cross sections, 14 µm spinal cord per section, 4 sections per embryo; n = 6-6). Scale bars: 20 µm in A for A'; 20 µm in B for B'.

3.2.3.3 Muscle development is impaired in the mutants

Muscle precursor cells located adjacent to the notochord in the horizontal myoseptum (HM) region and can differentiate into specific types of muscle fibres (Devoto et al. 1996). In zebrafish, spinal motor neurons in each somatic hemisegment first project their axons in a common path to reach the HM, then choose their individual pathway to reach their target muscle groups. Primary motor axons mainly innervate fast muscle fibres whereas secondary motor axons are responsible for both types of fast and slow muscles (Patrick J Babin et al. 2014). A zebrafish mutant *spadetail* provided evidence that muscle fibres play a role in axonal pathway selection (Eisen & Pike 1991). In the *spadetail* mutant, fewer primary motor neurons were produced and primary motor axons display severe pathfinding defects in muscle deficient myotomes. A reduction in the number of muscle cells in wild-type embryos leads to a similar motor neuron and axon phenotype to that of the *spadetail* mutant embryos, suggesting that deficiency in muscle development may create an unsupportive environment for the navigation of axon growth. Other studies have also shown that genes functioning in muscle cells can be crucial for motor axon outgrowth. For instance, a zebrafish mutant *topped* discovered from a genetic screen manifests a defect in CaP axon pathfinding (Rodino-Klapac & Beattie 2004). Cell transplantation of wild-type cells into the mutant embryos revealed the non cell-autonomous function of *topped* for motor neurons. By examining the cell types that provide *topped* activity, studies in chimeric embryos showed that the correct CaP axon pathfinding can only be restored by ventromedial fast muscle cells. This indicates a role of *topped* gene in promoting motor axon outgrowth by acting in fast muscle cells. Another two motor axon mutant genes, *diwanka*, which plays a role in establishing the common projection for primary motor axons, and *unplugged*, which is important for the correct pathfinding for CaP and RoP axons, have also been identified to act through a non cell-autonomous mechanism and functioning in slow muscles (Zeller & Granato 1999; Zhang et al. 2004). In the *unplugged* mutant, transplant experiments showed that the *unplugged* gene, which encodes a homolog of muscle specific kinase (MuSK), is not required in CaP and RoP motor neurons, but activates in the surrounding environment to guide axon pathway choices (Zhang & Granato 2000; Zhang et al. 2004). A subset of adaxial cells were found to provide the

unplugged gene activity and were capable of rescue the motor axon defects. Adaxial cells are a type of muscle pioneer cells that develop into slow muscle fibres of the adult fish (Devoto et al. 1996). In chick, motor nerve formation was affected by the removal of somatic muscle precursors (Eisen 1994). Taken above, muscle development can be crucial for the proper axon outgrowth of motor neurons.

To test if muscle morphology is impaired in the mutants, I used phalloidin to label fast muscle fibres, and F59, which recognises slow muscle fibres. In general, mutants display reduced labelling intensity in both antibodies labelled muscle types in the trunk, and showed disrupted muscle fibres in the tail at 3 dpf (Fig 3.15), indicates muscle fibres are affected in the mutants.

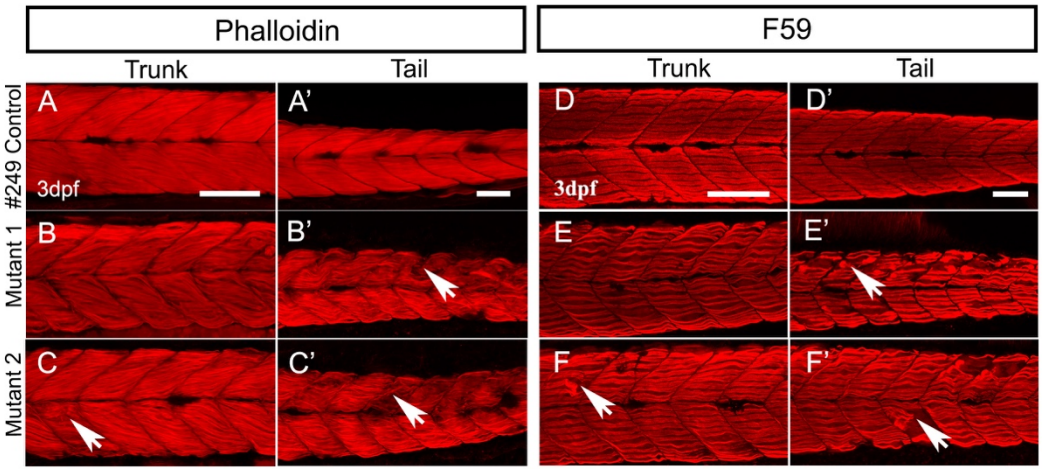

Fig 3.15 Muscle development is impaired in the mutants. (A-C') Mutants showed less density in Phalloidin labelled fast muscles and disconnected muscle fibres (arrows) in trunk region and tail at 3 dpf, compared with control siblings. **(D-F')** F59 labelled slow muscles revealed less density in mutants and disconnected muscle fibres (arrows). Lateral views of embryos are shown; rostral is left; dorsal is up. Scale bars: 100 μm in A for B,C; 50 μm in A' for B',C'; D = 100 μm for E,F; D' = 50 μm E',F'.

3.2.3.4 Generation of Pax2 interneurons is not changed

To detect the impact of the gene on the other neuron populations such as interneurons, I quantified and compared the numbers of Pax2 immuno-labelled interneurons by immunohistochemistry antibody labelling. In control siblings, numbers of Pax2+ cells reached 56.77 ± 2.58, comparable to the numbers in mutant embryos 57.67 ± 3.50 (P=0.8367; 60 µm spinal cord; n = 13-12; unpaired t test, two-tailed) (Fig 3.16). This result indicates the generation of Pax2 interneurons in #249 mutants is not affected.

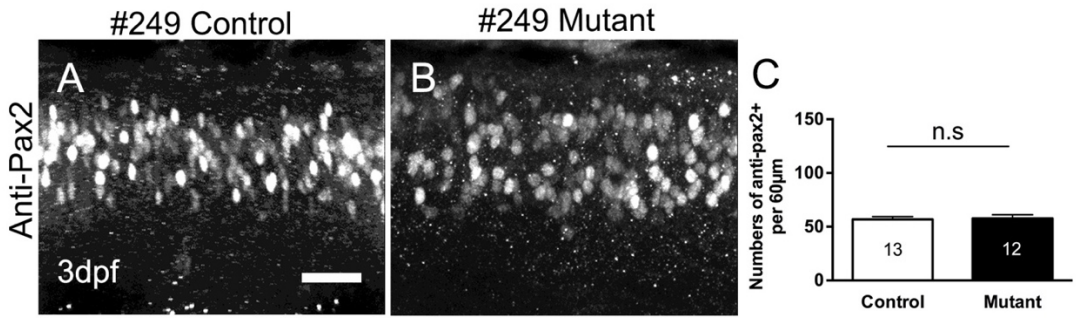

Fig 3.16 Numbers of Pax2 positive immunoreactive interneurons in mutants are comparable to control embryos. (A,B) Lateral views of embryos are shown, rostral is left, dorsal is up. **(C)** Quantification shows no statistical difference in numbers of Pax2+ interneurons between control siblings and mutant embryos (Unpaired t test, P=0.8367). Scale bar = 25 µm.

3.2.4 #249 candidate gene identification

To identify mutated gene that is responsible for the motor axon phenotype observed in #249, I isolated genomic DNA pools from 141 control siblings and 90 mutants at 3dpf. NGS was outsourced to Edinburg Genomics. Bioinformatics analysis of raw reads generated from NGS and gene annotation was kindly performed by Dr Richard Poole (University College London), using a CloudMap (Minevich et al. 2012) tool that is available on Galaxy web platform. Assembled sequence was aligned to zebrafish reference genome Zv9/danRer7 and was viewed via UCSC genome browser. The mutation was mapped between 10-15 Mb on chromosome 4 containing 7 predicted protein-coding genes. A critical approach for the identification of

causative mutation in #249 is to priorities a suitable candidate gene that may possibly play a role in the process of motor axon growth. From these candidates, only one was a nonsense mutation at Chr4:1399241952.8 in the transcript ENSDART00000019647, coding for a Psmc2 (proteasome 26S subunit, ATPase 2) protein. The remaining candidate genes cause missense mutations (Appendix 1). A nonsense mutation is a point mutation in DNA sequence that give rise to a pre-mature stop codon. A missense mutation causes a change in amino acid and lead to the change in protein sequence. In the nonsense mutation, a premature stop codon occurred in the coding sequence often give rise to unfinished or inactivate protein product, thus it is likely to have considerable impact on protein function and lead to a phenotypic effect that is severer than the missense mutation. Furthermore, *psmc2* encodes a sub-unit of 26S proteasome, which is a major component of the ubiquitin proteasome system (UPS) (Yi & Ehlers 2007). Studies have shown that ubiquitin proteasome system (UPS) plays a role in axon guidance (Imai et al. 2010; Lewcock et al. 2007; Mehta et al. 2004). Taken above, *psmc2* is a reasonable choice and was selected as a candidate gene potentially responsible for the #249 mutant phenotype for further validation.

3.2.4.1 PCR based candidate gene genotyping

In the #249 mutant genome, a C-to-T substitution occurred at the first exon of candidate gene *psmc2* give rise to a nonsense mutation. This C-to-T conversion caused a pre-mature stop codon in the coding region, resulting a truncated protein translation of *psmc2* (Fig 3.17). To confirm the presence of the C/T transition in genomic DNA (gDNA) in #249 mutants, I amplified and sequenced a fraction of gDNA (~340 bp) flanking the mutation site for both mutants and their siblings. Results from sequencing individual control embryo (n = 10) and mutant embryo (n = 9) confirmed that this G-to-T replacement exits in the DNA sequence of *psmc2* candidate gene. This piece of information is important as it confirmed the change of amino acid in the resulting protein sequence, and hinted a possible functional impact on motor axon growth.

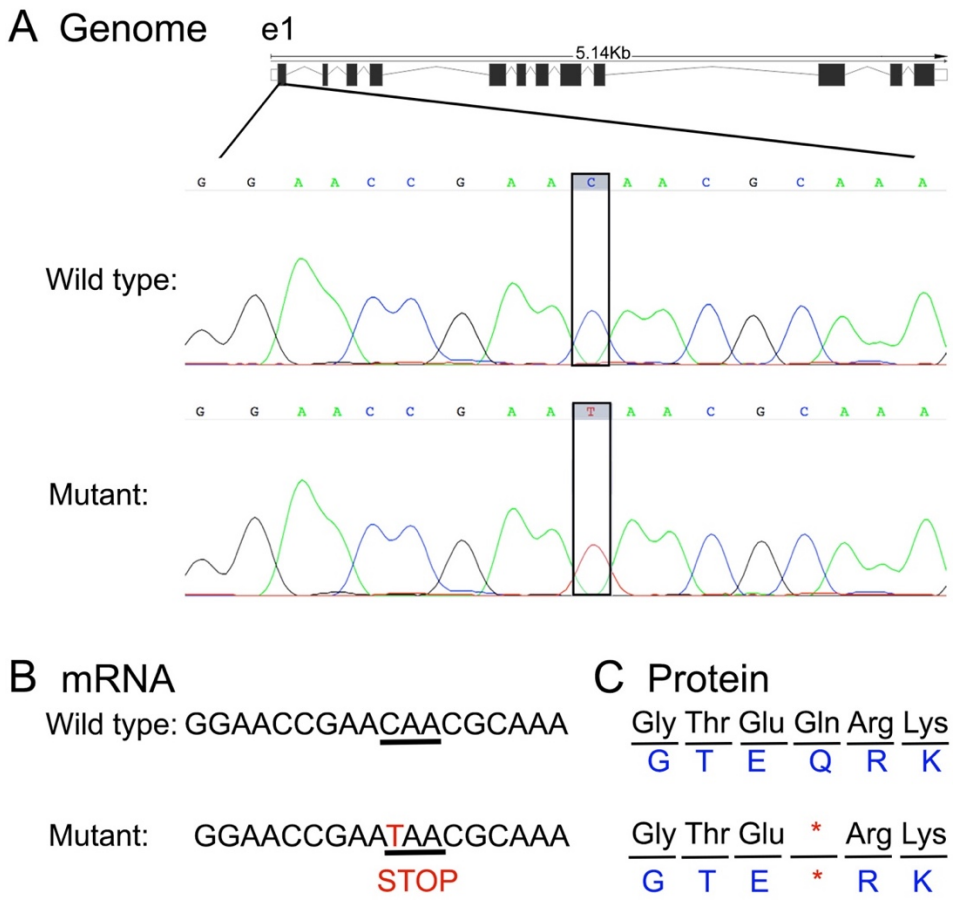

Fig 3.17 #249 mutant has a pre-mature stop codon in candidate gene *psmc2*. **(A)** Illustration of *psmc2* genome. Sequence electropherograms of a wild-type embryo and a #249 mutant from individually genotyped control siblings (n = 10) and *#249* mutants (n = 9) indicating the nucleotide substitution from C to T in the exon 1 (boxed area). **(B,C)** Schematics show the C to T mutation caused a one-base change that results in a pre-mature stop codon in the *psmc2* mRNA and protein translation.

3.2.4.2 *psmc2* gene is widely expressed during embryonic development

Full length cDNA of zebrafish *psmc2* encodes a protein of 433 amino acids. Comparison of the amino acid sequence of zebrafish across species revealed a high degree of overall conservation: 98.8% identity with human, 99% identity with mouse and 98% with rat, 98.8% identity with Xenopus (Fig 3.18 A).

To study whether the *psmc2* gene is expressed during embryonic development, I generated an anti-sense RNA probe for *psmc2* and examined the expression pattern. I first performed *psmc2 in situ* hybridization at 24 hpf in whole-mounted wild-type wik embryos. I observed a widely expressed *psmc2* in the whole embryo and prominent expression in somites (Fig 3.18 B-C''). This broad expression pattern is expected, as *psmc2* encoded 26S proteasome sub-unit belongs to the ubiquitin proteasome system, in which ubiquitin is named after its universal presence (Yi & Ehlers 2007). This data suggests *psmc2* is expressed at early stage of embryonic development. To further investigate the *psmc2* gene regulation (the amount and the timing of the appearance), in situ can be performed at earlier as well as later stages of development.

To test whether the mRNA expression of *psmc2* is affected in #249 mutants. I applied RNA in situ hybridization using a *psmc2* anti-sense probe in a pool of embryos (+/+; +/m; m/m) collected from #249 heterozygotes. I expected to detect that 25% of the embryos display an altered expression if *psmc2* mRNA is disrupted in the mutants. I observed a similar expression pattern to that of the wik embryos (n=20), and no apparent change in the expression of *psmc2* at 24 hpf in #249 embryos tested (10/40 were expected to show a change if *psmc2* mRNA is affected) (Fig 3.18 C-C'). A possibility could be that the mutation only affects protein synthesis. Another possibility is that mRNA in the mutants did not undergo nonsense-mediated RNA decay (NMD). Nonsense-mediated RNA decay is a mechanism that prevents truncated protein synthesis by eliminating mRNA transcripts containing pre-mature stop codons (Brogna & Wen 2009). NMD in the mutant mRNA would lead to low level of mRNA expression.

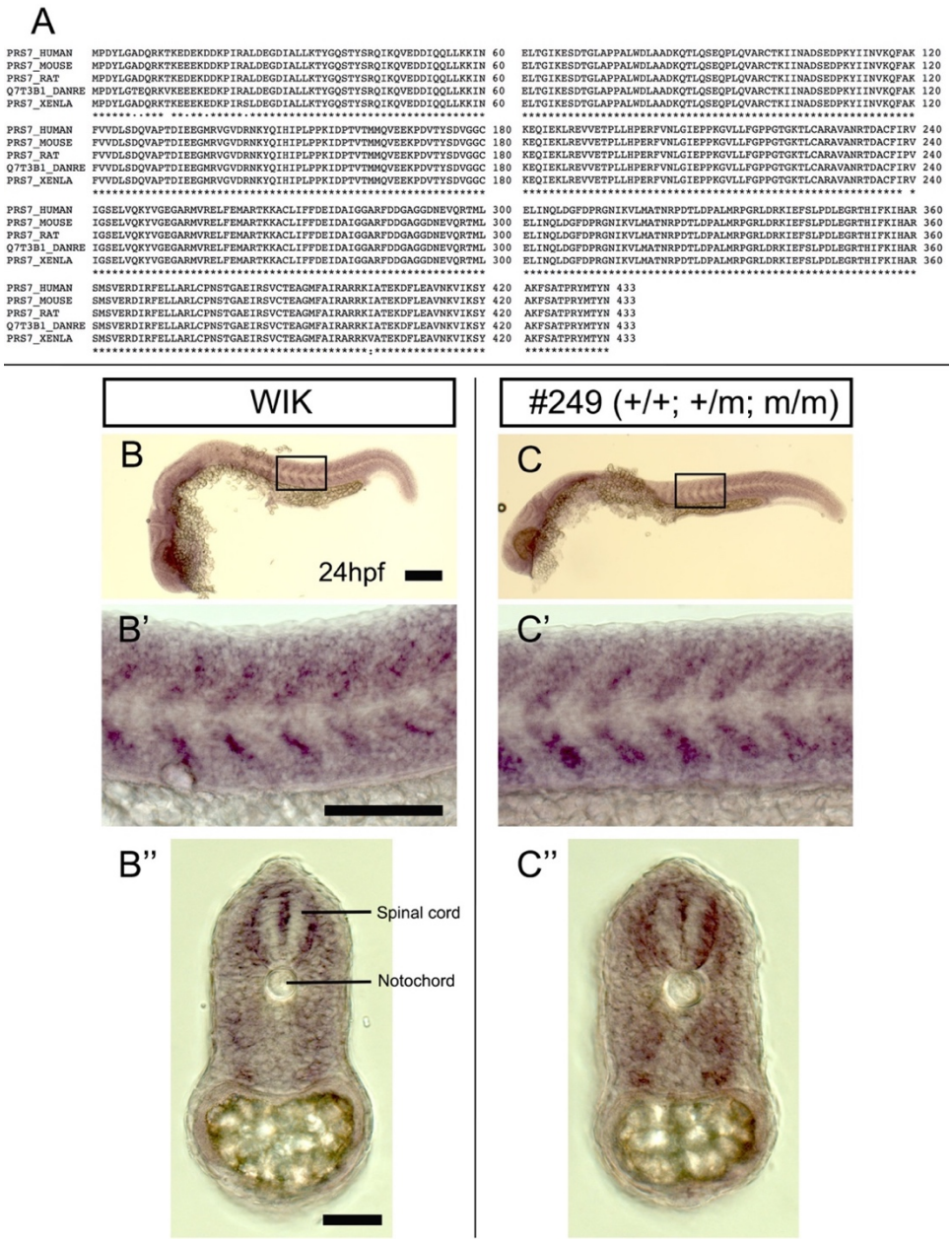

Fig 3.18 Expression of *psmc2* gene is during embryonic development. (A) The amino acid sequence of *psmc2* shows high conservation with *psmc2* of other species (DANRE – zebrafish; XENLA – Xenopus laevis). **(B)** Examples of *psmc2* expression in 24 hpf wik embryos. Lateral views of embryos are shown, rostral is left, dorsal is up. (n = 20; N = 2). **(C)** Examples of *psmc2* in situ in #249 embryo pools. Embryos tested showed similar expression pattern to that of the wik embryos and no obvious changes in *psmc2* expression. **(B',C')** Higher magnification of areas boxed in (B,C) indicates prominent expression in somites. **(B'',C'')** Cross sections are shown, spinal cord and notochord are indicated by lines; dorsal is up. Scale bars: B = 50 µm for C; B' = 100 µm for C'; B'' = 50 µm for C''.

3.2.4.3 Overexpression of *psmc2* mRNA leads to ectopic dorsal axon outgrowth and improved morphology in #249 mutants

Functional analysis such as a gain-of-function and loss-of-function approaches are often used to further confirm whether the phenotype of interest is caused by the candidate gene. A gain-of-function study is an attempt to rescue the mutant phenotype by over-expressing wild type mRNA. Theoretically, a phenotype caused by a disrupted allele can be functionally complemented and genetically rescued by expressing a wild-type endogenous allele of the mutated gene (Schneeberger 2014). Another common approach is a loss-of-function study to knock-down/out target gene for the purpose of mimicking the phenotype observed in the mutant, and therefore confirm the function of the gene (Puliti et al. 2007).

To determine whether *psmc2* is the affected gene causing motor axon outgrowth defects in #249 mutants, I first carried out a rescue experiment by overexpressing *psmc2* mRNA. I amplified full-length *psmc2* cDNA from wild-type whole-embryo RNA and inserted the product into a pCSP2 vector for in vitro transcription of mRNA. *psmc2* mRNA was injected into wild-type embryos to test the toxicity at a range of concentrations of 50 ng/µl, 100 ng/µl and 150 ng/µl. Injected embryos showed no developmental abnormalities in the concentrations tested. To overexpress *psmc2*, embryos collected from single pairs of heterozygous #249 mutants were divided into an un-injected control group and an injected group. Approximately 1.67nL in volume of mRNA (150 ng/µl) were injected into one-cell stage embryos and phenotypic examination was conducted at 3 dpf. In the un-injected control group, islet-1:GFP axons had extended dorsally in the phenotypically wild-type embryos at 3 dpf (Fig 3.19 A,A'), and un-injected control mutants showed a failure in islet-1:GFP axon outgrowth (Fig 3.19 C'). However, in the *psmc2* mRNA-injected group, mutants showed ectopic GFP positive dorsal projections, and an improvement in gross morphology such as eye sizes and more absorbed yolk sac (Fig 3.19 B,B'). Follow-up to 4 dpf, most un-injected mutants (13/18) have died, and the remaining (5/18) showed curved body axis and signs of degeneration (Fig 3.19 F). All mRNA-injected mutants (n=16) survived at 4 dpf (Fig 3.19 E). Control embryos (n=20) have developed inflated swimming bladder at this time (Fig 3.19 D). These

evidences suggest overexpressing *psmc2* mRNA can partially rescue the axonal and morphology phenotypes in #249 mutant. This supports *psmc2* as a causative gene for #249 mutant phenotype. To examine if there is complete rescue in some embryos, future experiment needs to be done by genotyping injected embryos.

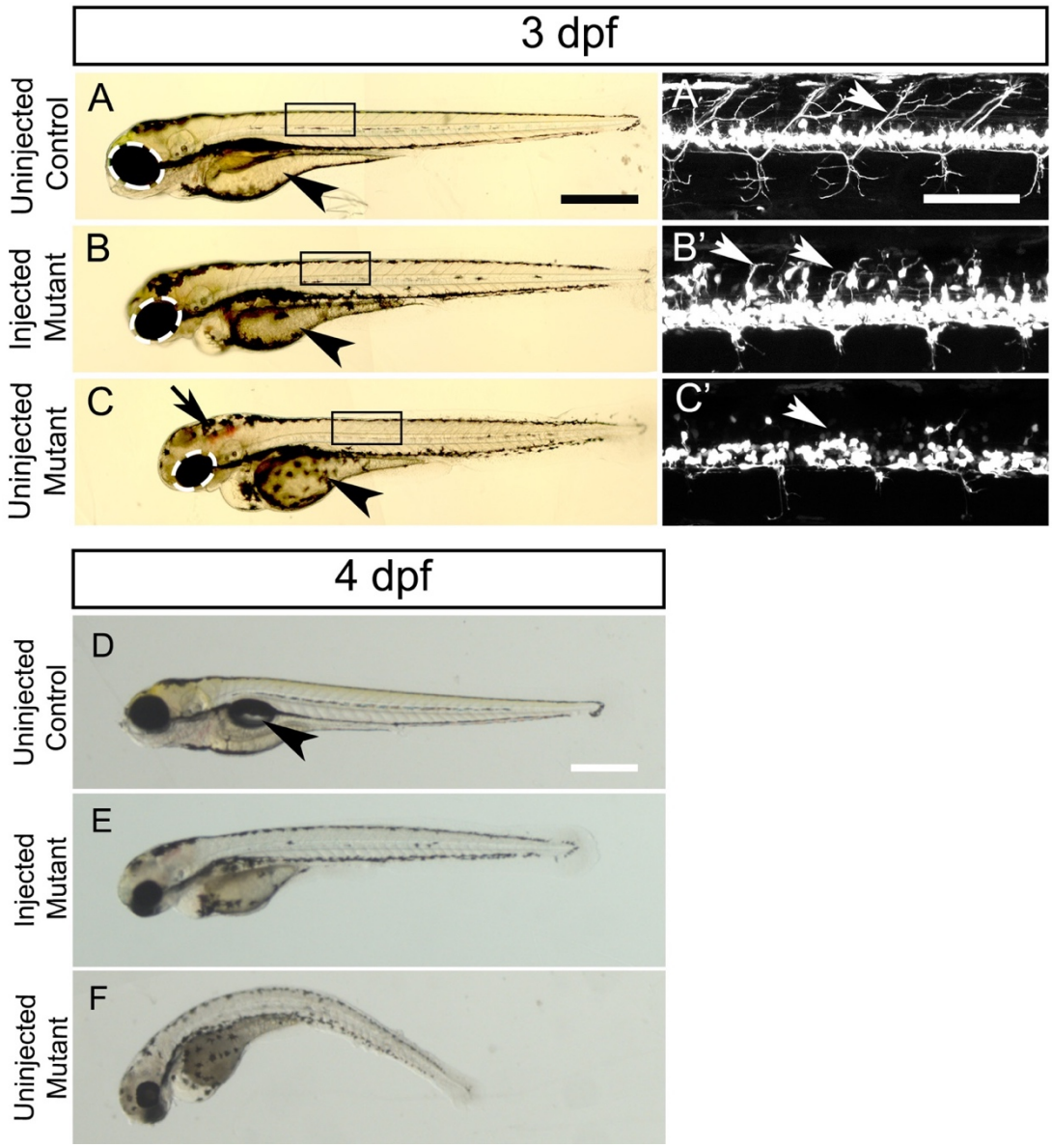

Fig 3.19 *psmc2* mRNA overexpression results in ectopic dorsal axon growth and morphological improvement. Lateral views of embryos are shown, rostral is left, dorsal is up. **(A-C)** Examples of an un-injected control sibling, a *psmc2* mRNA-injected mutant and an un-injected mutant at 3 dpf. Mutant displayed small sized eyes (dashed circle line), more rounded yolk sac (arrowhead) and haemorrhage

(arrow) in the brain (B), compared with un-injected control (A). The mRNA-injected mutant showed an improvement in eye size (dashed circle line), more absorbed yolk sac (arrowhead), and no sign of haemorrhage (C), compared with un-injected mutant (B). **(A'-C')** Higher magnification of the areas boxed in (A-C), are shown. (A') Un-injected phenotypically wild-type control has developed islet-1:GFP+ dorsal projections at 3 dpf (arrow). Injection of *psmc2* mRNA in the mutant induces ectopic projection of GFP expressing dorsal axons (arrows, B'). Un-injected mutant showed a failure in islet-1:GFP+ motor axon outgrowth. **(D-F)** Follow-up embryos at 4 dpf. Inflated swimming bladder (arrow) can be observed in 4 dpf control embryo (D). Maximum intensity projections are shown. Scale bars: 500 μm in A for B,C; 100 μm in A' for B',C'; 500 μm in D for E,F.

3.2.5 Characterization of mutant line #151

3.2.5.1 Mutation affects motor neuron generation and motor axon outgrowth

To verify the isle-t:GFP motor neuron phenotype in #151 mutant, I analysed the number of motor neurons including primary and secondary motor neurons in the mutants (Fig 3.20). To do this, I used three different markers: HB9, Islet-1 and ChAT to detect numbers of motor neurons in the spinal cord. Endogenous *islet-1* is expressed in RoP, MiP primary motor neurons as well as secondary motor neurons (Appel et al. 1995; Inoue et al. 1994), whereas in islet-1:GPF transgenic animals, GFP is expressed in the secondary dorsal subtype of motor neurons (Higashijima et al. 2000). *hb9* (also known as *Mnx1*) is a member of *mnx* family genes that is expressed in early developing primary motor neurons as well as in a sub-population of VeLD interneurons (ventral longitudinal interneuron) (Seredick et al. 2012). It is known that anti-HB9 labels early born primary motor neurons and a small percentage of vsx1:GFP+ V2 interneurons that derived from P2 progenitor zone (Mysiak 2015). ChAT expression in cholinergic motor neurons is used as a marker for terminally differentiated motor neurons (Reimer et al. 2008).

At 3 dpf, there were 8.21 ± 0.70 of GFP+ cells in spinal cord sections of control sibling group, which is 97% more cells than in the mutant group 0.25 ± 0.31 (14 μm

spinal cord per section, 4 sections per embryo; n = 6-5; **p=0.0043; Mean ± SEM; Mann Whitney test, two-tailed) (Fig 3.20 B). This data suggest that numbers of islet-1:GFP+ motor neurons are significantly reduced in the mutants. #151 mutants showed 34% fewer numbers of mature motor neurons labelled by choline acetyltransferase (ChAT) compared with control group (Control: 19.45 ± 1.18, Mutant: 6.89 ± 1.54; Mean ± SEM; ****p<0.0001; 14 μm spinal cord section, 4 sections per embryo; n = 15-13; Unpaired t test, two-tailed) (Fig 3.20 D). I also used anti-HB9 to examine the numbers of early-born motor neurons and anti-Islet-1 to investigate the late-born motor neurons. I found that mutants have 19% fewer HB9 immuno-labelled cells and 17% fewer Islet-1 immuno-labelled cells than the control group (Fig 3.20 F,H). (Anti-HB9 cells: Control = 14.67 ± 1.79, Mutant = 11.95 ± 0.82; 14 μm spinal cord per section, 4 sections per embryo; **p=0.0087; Mean ± SEM; n = 6-5; Mann Whitney test, two-tailed) (Anti-Islet-1 cells: Control = 115.3 ± 3.88, Mutant = 96.31 ± 1.33; 60 μm spinal cord; n = 12-13; ****p<0.0001; Mean ± SEM; Unpaired t test, two-tailed). These data suggest that the production of motor neurons was decreased in the mutants. Particularly, the generation of late-born islet-1:GPF motor neurons were significantly reduced by 97% compared with control embryos.

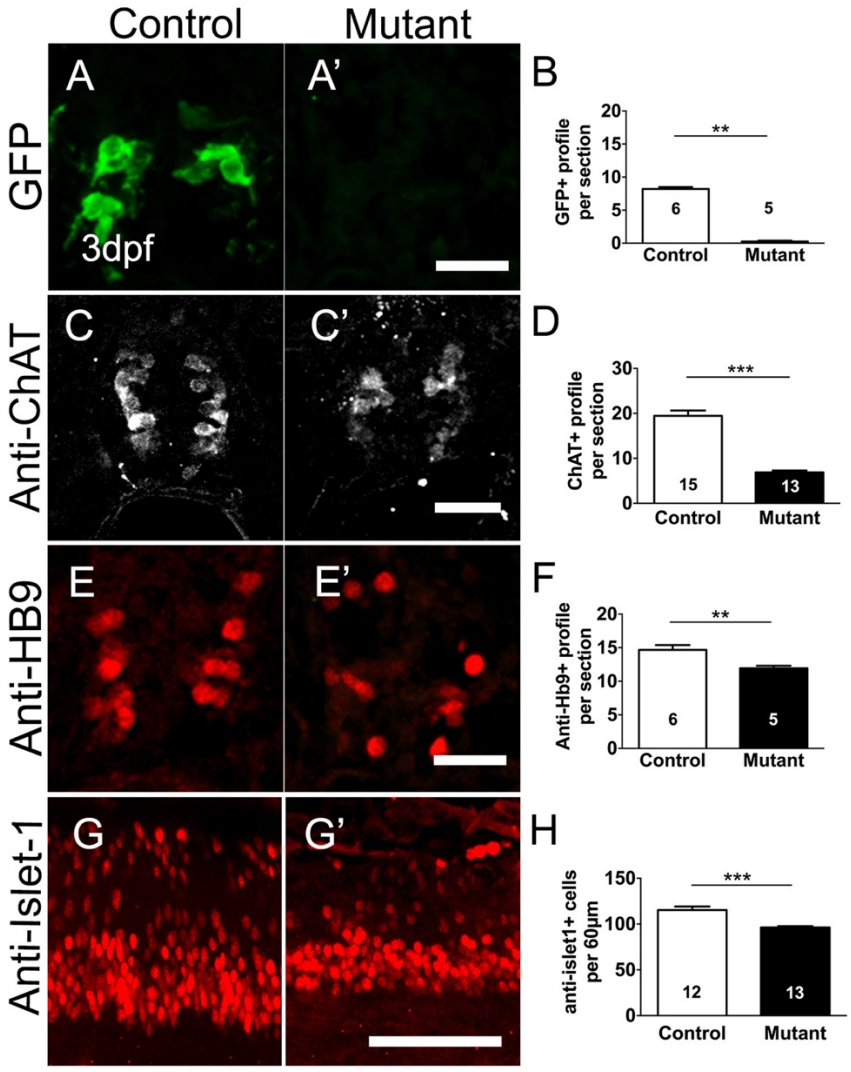

Fig 3.20 Motor neuron number is reduced in the #151 mutants. (A,A') Cross sections of the spinal cord show islet-1:GFP+ cells. **(B)** Quantifications show fewer numbers of islet-1:GFP+ cells in the mutants compared with control group (**p=0.0043; Mann Whitney test). **(C,C')** Cross sections of the spinal cord show anti-ChAT labelling. **(D)** Mutants have fewer ChAT positive cells compared with control group (****p<0.0001; Unpaired t test). **(E,E;)** Cross sections of the spinal cord show motor neuron marker HB9 labelled cells. **(F)** Mutants show significantly fewer numbers of HB9 immuno-labelled cells in control group (**p=0.0087; Mann Whitney test). **(G,G')** Lateral views of embryos are shown; rostral is left; dorsal is up. Islet-1 immuno-labelling in the control sibling and mutant. **(H)** Fewer numbers of anti-Islet-1 labelled motor neurons in the mutants, compared with control siblings (****p<0.0001; Unpaired t test). Scale bars: A' = 20 µm for A; C' = 25 µm for C; E' = 20 µm for E; G' = 60 µm for G.

I analysed the presence of motor axons in different pathways in the #151 mutant. At 3 dpf, islet-1:GFP+ motor neurons and their dorsal extensions are present in the control embryos, whereas in #151 mutants no GFP+ motor neuron axon projections were present (Fig 3.21 A,B). I used an antibody that binds acetylated α-tubulin to label both primary and secondary motor axons, and antibody zn-8, which is specific to secondary motor axons. In the acetylated α-tubulin staining, both dorsal and ventral axons were present in the mutants (Fig 3.21 B''). However, I did not observe RoP primary motor axons in acetylated α-tubulin labelled mutant embryos (Control n=10; Mutant n=12). zn-8 staining confirmed absence of dorsal secondary motor axons in the mutant (Fig 3.21 B') already seen in the islet-1:GFP transgenic fish. The secondary axons projecting ventro-laterally in the RoP pathway were also missing in the mutant group (Control n=8; Mutant n=8). These data suggest that in addition to the generation of motor neurons, rostral primary motor axons, as well as secondary motor axons that project in rostral and dorsal pathways are affected in the #151 mutants (Fig 3.21 C).

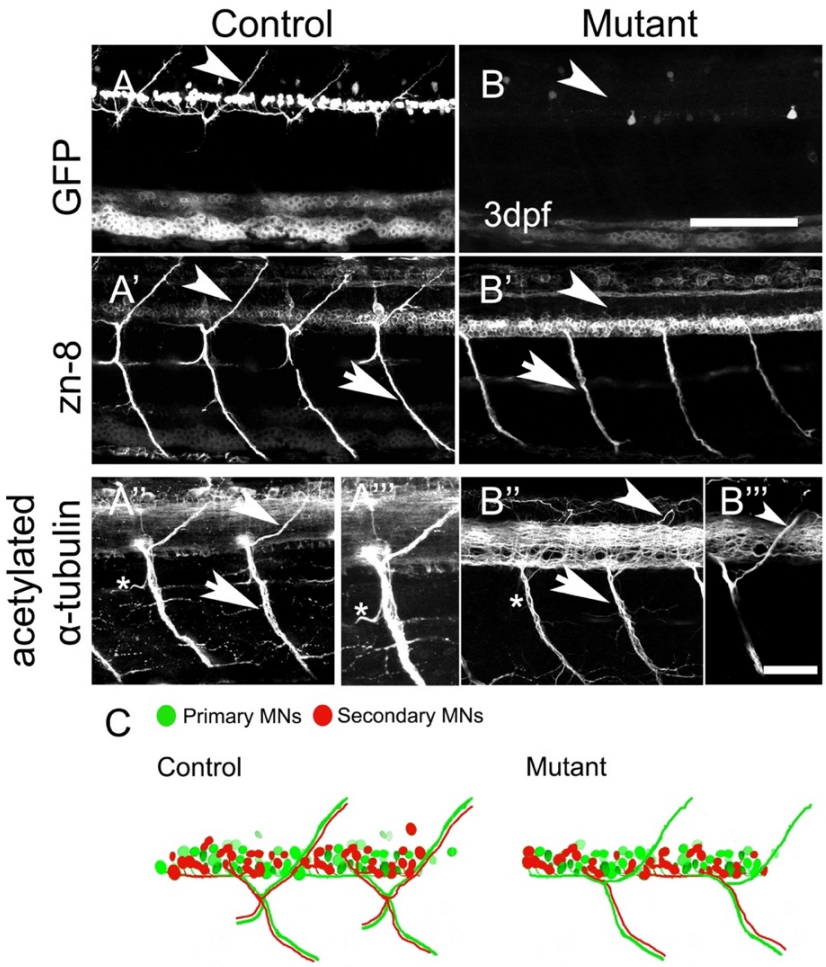

Fig 3.21 #151 mutant showed secondary motor axons defects. (A-A'') islet-1:GFP+ motor neurons and their dorsal extensions (arrowhead) in the control embryo at 3 dpf (A). zn-8 and Acetylated α-tubulin staining revealed dorsal (arrowhead in A',A'') and ventral axon (arrow in A',A'') projections in control siblings. Selectively stacked sections of a rostral projection (asterisk) is shown in (A''') to clearly reveal the rostrally projecting motor axon. **(B-B''')** #151 mutant showed fewer islet-1:GFP+ motor neurons (indicated with arrowhead) at the same stage (B). (B') Mutant also showed an absence of zn-8+ dorsal (arrowheads) projections. (B'') Acetylated α-tubulin labelling showed that both dorsal (arrowhead) and ventral (arrow) axons are present in the mutant, indicating that primary motor axons remain unaffected. RoP primary motor axons is absent in mutant embryo (asterisk in B''). A single optical section of a dorsal projection (arrowhead) is shown in (B''') to clearly reveal the dorsally projecting motor axon. **(C)** A schematic of primary motor axon (green) and secondary motor axons (red) in control animal and mutant. Lateral views of embryos are shown; rostral is left, dorsal is up. Scale bars: B = 100 μm for A-B''; B''' = 50 μm for A'''.

3.2.5.2 Survival of motor neuron progenitor cells is not affected

There are several possibilities that could result in fewer islet-1:GFP motor neurons in #151 mutant. For instance, progenitor cells undergoing cell death could result in fewer motor neurons been produced. This can be examined by applying cell death detection with a progenitor marker such as *olig2*. Alternatively, reduced neurogenesis from progenitor cells could also affect the number of motor neurons. This hypothesis can be tested using proliferation marker to label pMN progenitor cells. The third possibility is that the survival and proliferation of progenitor cells are not affected, but the survival of motor neurons is compromised. To test this, cell death detection can be used in combination with motor neuron markers.

To investigate whether the apoptotic cell death in motor neuron progenitor cells give rise to lower numbers of islet-1:GFP+ spinal motor neurons, I crossed #151 heterozygotes with olig2:DsRed transgenic line and investigated the cell death of olig2:DsRed+ cells in the pMN zone of the mutants. I applied cell apoptosis detection at 38 hpf, when over 60% of islet-1:GFP+ motor neurons and 30% of hb9:GFP+ primary motor neurons are still to be born after this time; and at 48 hpf, when almost all motor neurons are born (Reimer et al. 2013).

To test if the motor neuron progenitor domain undergoes selective cell death, I used a Terminal deoxynucleotidyl transferase (TdT) dUTP nick end labelling (TUNEL) assay (Kyrylkova et al. 2012). The TUNEL assay has been widely used in cell death analysis by detecting DNA under degradation. The hallmark of late cell apoptosis is the DNA double-strand breaks generated by DNA fragmentation. Blunt-ends DNA is detected by labelling its 3'-hydroxyl ends with modified dUTP and subsequently visualized by immunohistochemistry (Kyrylkova et al. 2012). The TUNEL assay also detects necrotic cell deaths, which is often caused by the deprivation of oxygen or toxin (Grasl-Kraupp et al. 1995).

I observed no significant increase in the number of TUNEL positive cells in the mutants at either time points examined. At 38 hpf, mutants can be identified from their morphologies such as small eyes and small head. I observed 0.13 ± 0.35 of

TUNEL+/DsRed+ double labelled cells in control group, which is comparable with the mutants 0.13 ± 0.35 cells (P>0.9999; 100 μm spinal cord; n = 8-8; Mean ± SEM; Mann Whitney test, two-tailed) (Fig 3.22 A-C). Both control group and mutants showed no detectable TUNEL+/DsRed+ cell death at 48 hpf (P>0.9999; 100 μm spinal cord; n = 6-6; Mean ± SEM; Mann Whitney test, two-tailed) (Fig 3.22 D-F). However, apoptotic cells engulfed by macrophages disappear quickly in a few hours (Abrams et al. 1993). TUNEL-stained cells in fixed tissues allow only a snapshot of cell death at a time point. Also, to exclude that no detectable TUNEL+ cells at 48 hpf is not due to poor antibody penetration, I performed an in vivo cell death detection to further confirm the survival of olig2:Dsred cells.

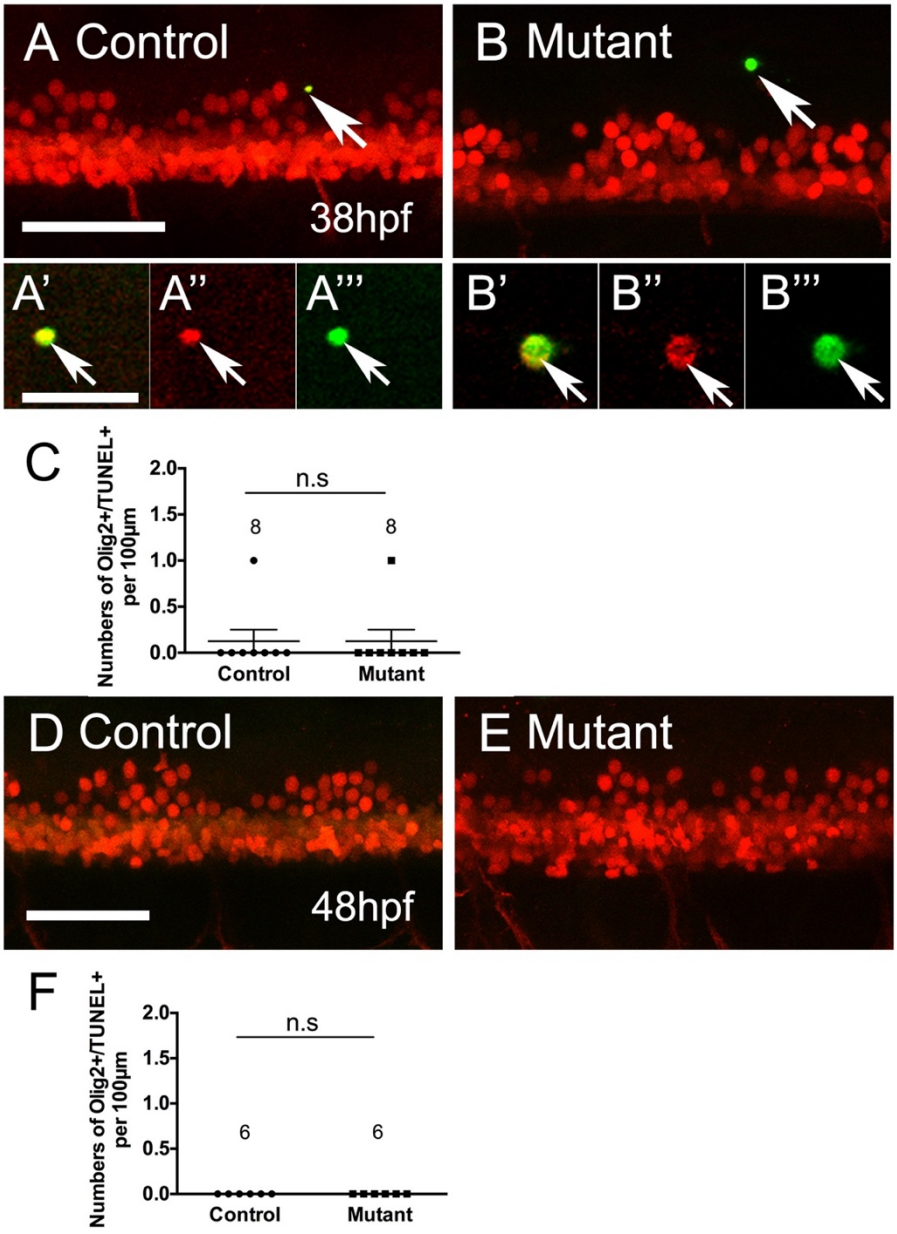

Fig 3.22 No increased TUNEL positive olig2:DsRed cells in mutants. (A,B) Lateral views are shown; rostral is left, dorsal is up. TUNEL+/ DsRed+ double labelled cells are indicated by arrowheads. **(A'-B''')** Single optical sections at higher magnification show a TUNEL+ and DsRed+ cell (arrowheads in A, B). **(C)** No significant increase in number of TUNEL+ cells at 38 hpf (P>0.9999, Mann Whitney test). **(D,E)** TUNEL+ cells were not detected in control sibling and #151 mutant at 48 hpf. **(F)** Quantification shows no increase in numbers of cell death in #151 mutants at 48 hpf, compared with control (P>0.9999, Mann Whitney test). Scale bars: 50 µm in A for B; 15 µm in A' for A''-B'''; 50 µm in D for E.

The study of *in vivo* apoptotic cell death detection was elucidated by Abrams et al (1993) by using a vital dye acridine orange (AO) in live *Drosophila* embryos and demonstrated that AO staining is specific for apoptotic cells. AO is cell permeable and statins individual cells that undergo phagocytes engulfment (Abrams et al. 1993). In my study, I incubated 38 hpf and 48 hpf embryos in 10ng/µl AO solution in the dark for 20 min, followed by washes in E3 embryonic medium (courtesy of Kelda Chia, protocol modified based on the methods of Barrallo-Gimeno et al. (2004)). The staining was visualized and documented using a confocal microscopy. At 38 hpf, no apparent increase of AO+/DsRed+ double stained cells was observed in the mutant group (Control: 0.43 ± 0.17, Mutant: 0.50 ± 0.17; Mean ± SEM; P=0.7730; 100 µm spinal cord; n = 14-14; Unpaired t test, two-tailed) (Fig 3.23 A-C). Similarly, statistical analysis revealed that no significant difference in numbers of DsRed+ cells stained with AO between control group and mutant group (Control: 0.11 ± 0.11, Mutant: 0.33 ± 0.23; Mean ± SEM; P=0.7353; 100 µm spinal cord; n = 9-9; Mann Whitney test, two-tailed) (Fig 3.23 D-F). As the olig2:DsRed line labels both progenitor cells and motor neurons, both TUNEL staining and AO staining suggest that the pMN progenitor cells did not undergo increased apoptotic cell death, and there is no increased motor neuron death in #151 mutants.

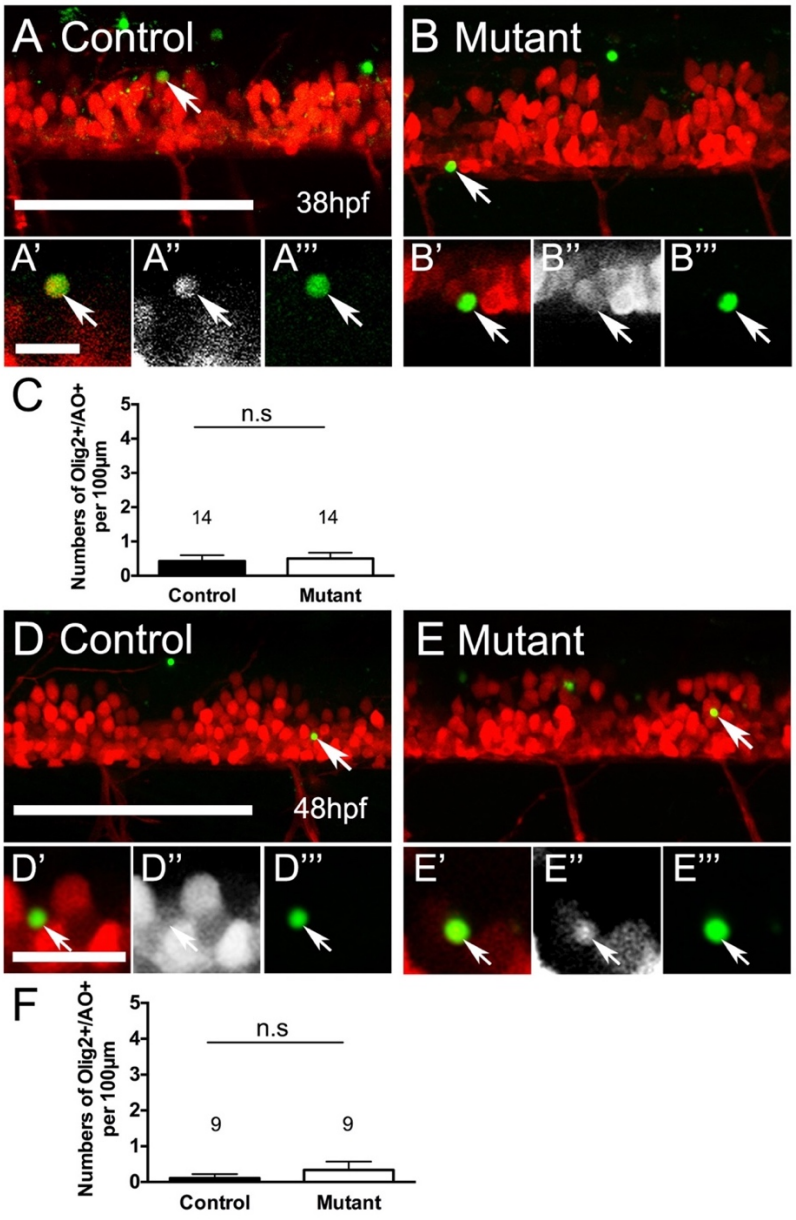

Fig 3.23 No increase in apoptotic pMN cells and motor neurons detected *in vivo*. (A,B) Lateral views of live embryos are shown; rostral is left, dorsal is up. AO+ and DsRed+ cells are indicated by arrows. **(A'-B''')** Single optical sections at higher magnification show a DsRed+/AO+ double labelled cell (arrows in A, B). **(C)** The number of olig2:DsRed+ cells that take up AO is not increased in mutants compared to control siblings at 38 hpf (P=0.7730, Unpaired t test). **(D,E)** AO detected cell death in control sibling and #151 mutant at 48 hpf. **(F)** The number of olig2:DsRed+ cells that take up AO is not increased in mutants compared to control siblings at 48 hpf (P=0.7353, Mann Whitney test). Scale bars: 100 µm in A for B; 15 µm in A' for A''-B'''; 100 µm in D for E; 15 µm in D' for D''-E'''.

3.2.5.3 Fewer numbers of olig2:DsRed+ cells are produced in #151 mutants

As no apparent increase of cell death was observed in olig2:DsRed+ cells, I investigate the possibility that whether fewer motor neurons are due to fewer progenitor cells produced. I counted the number of olig2:DsRed+ cells in the AO treated samples presented and described above. At both 38 and 48 hpf, mutants showed fewer olig2:DsRed+ cells than the control group (Fig 3.24). At 38 hpf, there were 69.57 ± 1.61 olig2:DsRed+ cells in the control group, compared with 61.57 ± 2.65 in the mutant group (Mean ± SEM; *P=0.0160; 100 μm spinal cord; n = 14-14; Unpaired t test, two-tailed). At 48 hpf, there were 103.7 ± 3.66 olig2:DsRed+ cells in control group, whereas mutant group has 85.22 ± 2.11 olig2:DsRed+ cells (Mean ± SEM; ***P=0.0005; 100 μm spinal cord; n = 9-9; Unpaired t test, two-tailed). This suggests that decreased production of progenitor cells give rise to fewer numbers of motor neurons.

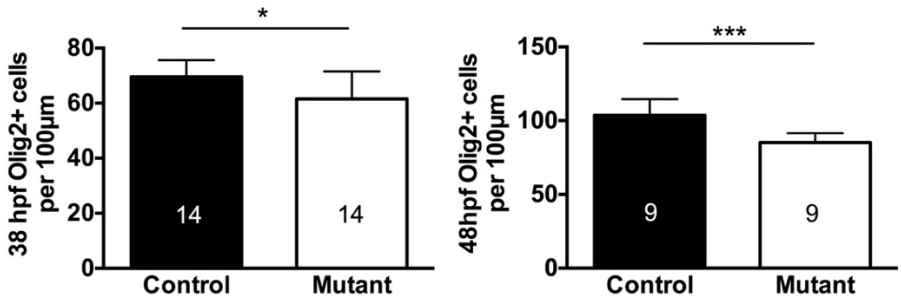

Fig 3.24 Reduced number of olig2:DsRed+ cells in #151 mutant. In the left panel, quantification shows fewer numbers of olig2:DsRed+ cells in the mutants compared with control siblings at 38 hpf (*P=0.0160, Unpaired t test). The right panel shows that at 48 hpf, the number of olig2:DsRed+ cells in the mutant group is significantly fewer then the control group (***P=0.0005, Unpaired t test).

I examined the proliferation of olig2:DsRed+ progenitor cells in the mutant pMN at 38 hpf using a proliferation marker PH3 to label cells in M phase of their cell cycle. I observed lower numbers of olig2:DsRed+/PH3+ double labelled proliferating progenitor cells in the mutant group compared with control group (Control: 7.33 ± 0.92 cells, Mutant: 4.29 ± 0.75; Mean ± SEM; *P=0.0414; 300 μm spinal cord; n =

6-7; Mann Whitney test, two-tailed) (Fig 3.25). This is probably due to fewer pMN cells proliferating, which reduces the likelihood to see a division.

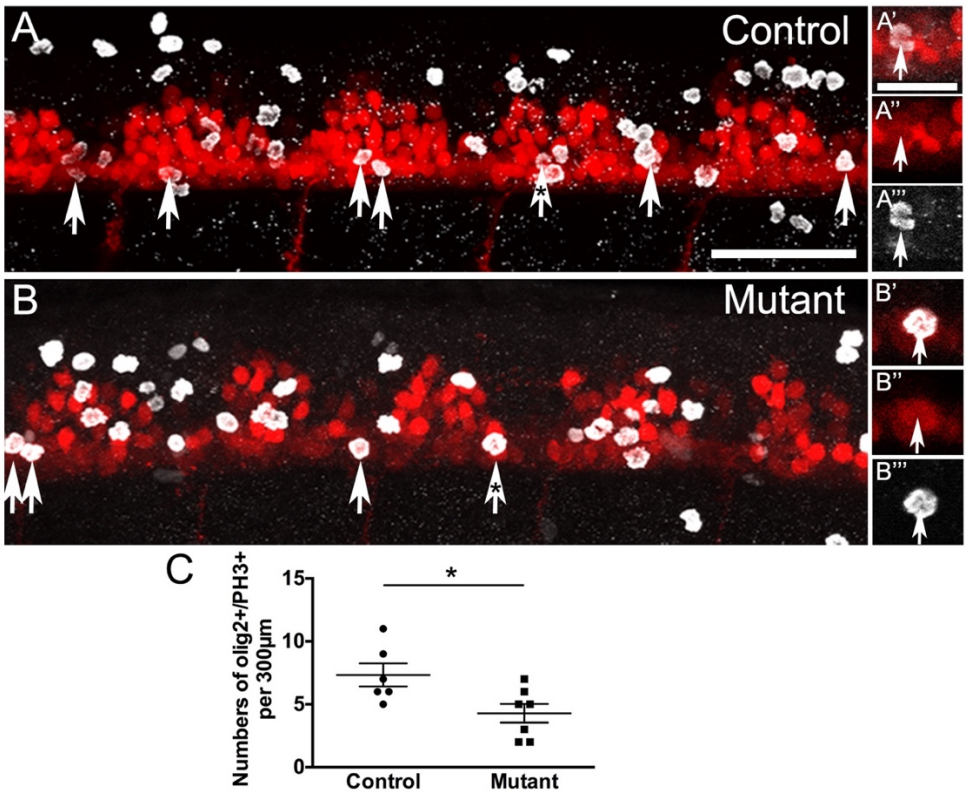

Fig 3.25 #151 mutants show fewer proliferating pMN cells. (A,B) Lateral views are shown; rostral is left, dorsal is up. PH3+ and DsRed+ cells are indicated by arrows. **(A'-B''')** Single optical sections at higher magnification show a DsRed+/AO+ double labelled pMN progenitor cell (indicated by asterisks in A, B). **(C)** Quantification showed lower numbers of olig2:DsRed+/PH3+ cells in the pMN zone of the mutants compared with control siblings at 38 hpf (*P=0.0414, Mann Whitney test). Scale bars: 50 µm in A for B; 20 µm in A' for A''-B'''.

3.2.5.4 #151 mutants display defects in other systems

To investigate the impact of the gene mutation in the #151 mutant, I adopted similar approaches to that used in the analysis of the #249 mutant to examine myelin formation, muscle morphologies as well as interneuron generation in #151 mutants. Using Claudin k antibody against the myelin protein (Münzel et al. 2014) revealed a

failure in forming myelin sheath in the mutants (Fig 3.26) indicating the gene may also influence generation of oligodendrocytes and/or myelination.

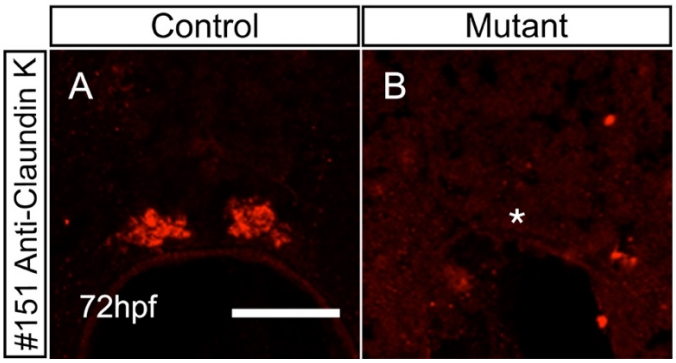

Fig 3.26 #151 Mutants failed to form myelin at 3 dpf. (A) Anti-Claudin K labelled myelin sheath in the control sibling. **(B)** #151 mutant showed an absence of myelin sheath (indicated with asterisk) at 72 hpf. Cross sections of the spinal cord, dorsal is up (14 μm per section, 4 sections per embryo, n = 5-5). Scale bar: A = 25 μm for B.

To examine the muscle morphology in #151 mutants, I performed IHC labelling in fast muscle fibres and slow muscle fibres at various time points. Mutants display disorganized muscle fibres in both muscle types at 28 hpf, 48 hpf and 72hpf (Fig 3.27). Therefore, muscle development is affected in the mutants.

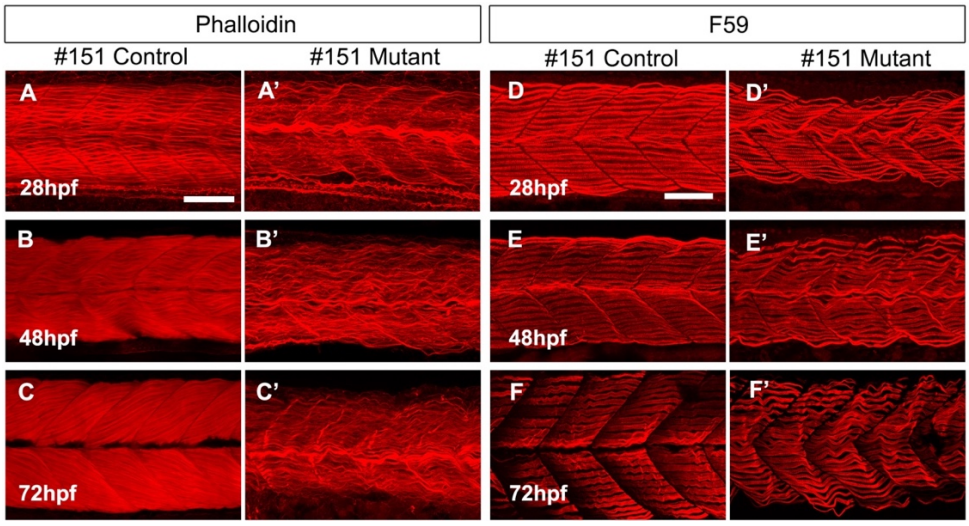

Fig 3.27 Muscle morphology is abnormal in #151 mutants at different time points. (A-C') Phalloidin labelled fast muscles at 28 hpf, 48 hpf and 72 hpf. Mutants showed disorganized (A'-C') fast muscle fibres, compared with control siblings (A-C). **(D-F')** F59 labelled slow muscles revealed abnormal slow muscle development in mutants (D'-F'). Lateral views of embryos are shown; rostral is left; dorsal is up. Scale bars: A = 50 μm for A-C'; D = 50 μm D-F'.

Next, I investigated the interneuron generation using anti-Pax2 to label a sub-class of interneurons followed by IHC. In the mutant group, I observed 41.23 ± 2.52 of Pax2+ cells at 3 dpf, which showed 27% fewer cells than the control sibling group 56.75 ± 4.33 (Fig 3.28) (**P=0.0044; 60 μm spinal cord; n = 12-13; Mean ± SEM; Unpaired t test, two-tailed). The result suggests the Pax2+ interneuron generation is decreased in #151 mutants.

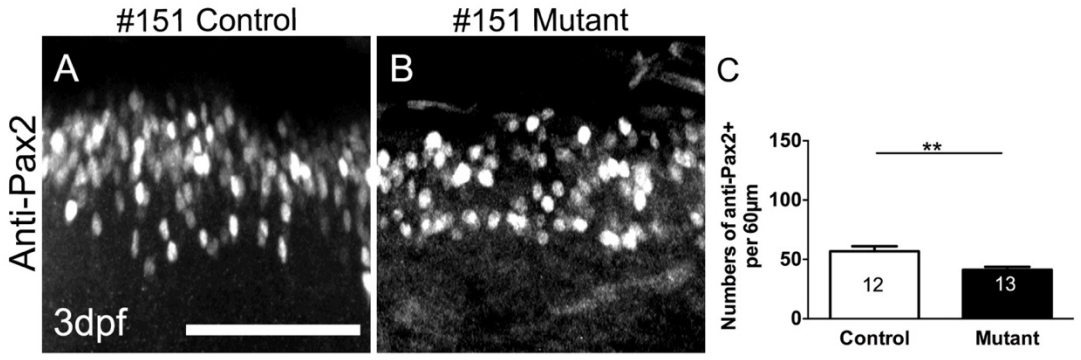

Fig 3.28 Generation of Pax2+ interneurons are affected. (A,B) Lateral views of embryos are shown, rostral is left, dorsal is up. **(C)** Quantification shows fewer numbers of Pax2 immuno-labelled interneurons in the mutants compared with control siblings (Unpaired t test, **P=0.0044). Scale bar = 60 μm.

3.2.5 #151 candidate gene identification

From Next Generation Sequencing (Edinburgh Genomic) and bioinformatics analysis of the sequencing data (courtesy of Dr. Richard Poole), 14 protein-coding genes on chromosome 19 were identified as potential candidate genes that may be responsible for the #151 mutant phenotype (Appendix 2). To prioritize a suitable

gene for further confirmation, I first selected candidates that causing a nonsense mutation, as a premature stop codon in protein coding sequence could lead to truncated or non-functional protein product. I then looked at the function of the gene through the literature: whether it is known to be involved in pathways that might explain the phenotype. I then designed a genotyping assay to check if only the mutants have the mutation. A SNP causing a nonsense mutation at 32244010 on chromosome 19 in the transcript ENSDART00000130326, coding for Rbbp4 (retinoblastoma-binding protein 4) protein was identified as a potential phenotypic causing mutation for #151 mutant. Rbbp4 is a component of the Nucleosome Remodeling and Deacetylase (NuRD) complex (Pfefferli et al. 2014). It has found that *rbbp4* is involved in fin regeneration in adult and zebrafish embryos (Pfefferli et al. 2014). Knock-down of *rbbp4* leads to reduced proliferation of blastema progenitor cells and re-differentiation of their daughter cells, which are the cells required during regenerative outgrowth and patterning of the fin (Pfefferli et al. 2014). The study also showed that *rbbp4* knock-down impairs blastemal proliferation without inducing cell deaths (Pfefferli et al. 2014). Therefore, *rbbp4* is a reasonable choice for further analysis.

In order to verify the possible involvement of *rbbp4*, I first validated whether the mutation appears in the gDNA of #151 mutants. In the *rbbp4* gene, a G-to-T substitute result in a pre-mature termination codon in exon 13 of *rbbp4-201* transcript (Ensembl). The nucleotide change leads to a loss of restriction enzyme site BtsCI in the mutants. Therefore, I designed primers to amplify a fraction of gDNA (100 bp) flanking the mutation site, and analysed PCR products with restriction enzyme digestion using BtsCI enzyme for both individual control siblings (n = 12) and mutants (n = 11). The digestion results were visualised in analytical gel. In this case, both gDNA strand of a wild-type embryo will be cleaved by BtsCI (Fig 3.29 B, +/+), whereas the mutant gDNA fragment without the BtsCI site would appear as "uncut" on the gel (Fig 3.29 B, m/m). In heterozygous embryos, only one strand will be cleaved by BtsCI and therefore appear as two bands on an analytical gel (Fig 3.29 B, +/m). Genotyping results confirmed the existence of G/T conversion in the mutants.

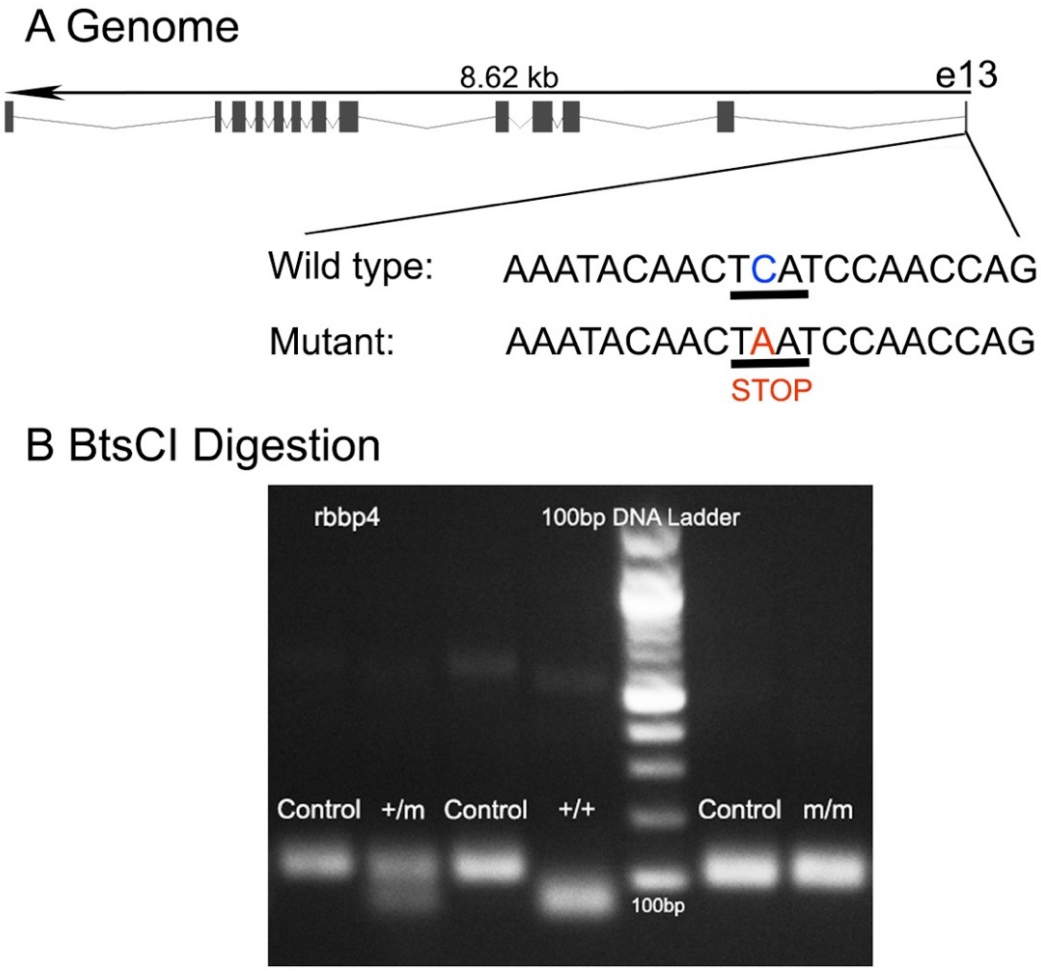

Fig 3.29 #151 mutant has a pre-mature stop codon in candidate gene transcript *rbbp4-201*. (A) Illustration of the reversed strand of *rbbp4-201* transcript. G to T (C/A in the reversed strand) mutation caused a one-base change in the *rbbp4-201* mRNA and protein sequence that results in a pre-mature stop codon (underline). **(B)** 12 phenotypically wild-type siblings and 11 mutants were genotyped individually using restriction enzyme digestion. Control refers to un-digested sample of +/m, +/+ and m/m.

Full length cDNA of zebrafish *rbbp4-201* transcript encodes a protein of 444 amino acids. I*n situ* hybridization using RNA probe for *rbbp4-201* displayed a broad expression of *rbbp4-201* in whole-mounted wik embryos at 24 hpf (Fig 3.30). I examined *rbbp4-201* RNA expression in a pool of embryos (+/+; +/m; m/m) from #151 heterozygotes, and observed similar expression pattern to that of the wik embryos. I also did not find apparent changes in *rbbp4-201* RNA expression in #151 embryos tested (data not shown), indicates RNA expression is not disrupted in the mutants.

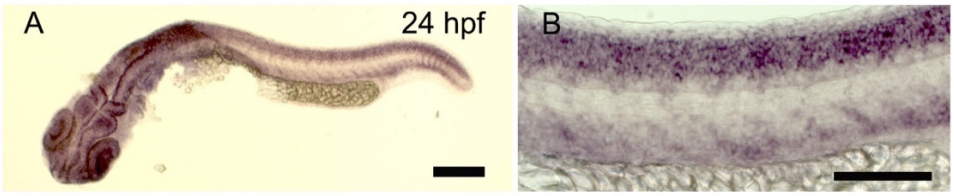

Fig 3.30 *rbbp4* is widely expressed in developing embryos. (A) *rbbp4 in situ* showed a broad expression in 24 hpf embryos. **(B)** Higher magnification of trunk area. Lateral views of embryos are shown, rostral is left, dorsal is up. (n = 20; N = 2). Scale bars: A = 50 µm; B = 100 µm.

To test whether overexpress *rbbp4-201* mRNA could possibly rescue the observed islet-1:GFP motor neuron deficit in #151 mutants, I amplified full-length *rbbp4-201* cDNA from wild-type whole-embryo RNA, the product was cloned into a pCSP2 vector and transcribed to mRNA. *rbbp4-201* mRNA was injected into wild-type embryos to test the toxicity and showed developmental abnormalities at 500 ng/µl. Therefore, to overexpress *rbbp4-201*, I injected less than 500 ng/µl to avoid false results. I injected 1 nl of mRNA ranged from 50 ng/µl to 400 ng/µl into #151 embryos at the one-cell stage and examined larvae at 3 dpf. I did not observe a rescue of the islet-1:GPF motor neuron defect in #151 mutants (data not shown), suggesting the attempted recue was unsuccessful. However, at this stage I cannot exclude the possibility that the injected mRNA was not expressed. Thus, it is necessary to measure mRNA expression in the injected animals in further experiment.

3.3 Discussion

In our genetic screen, I performed phenotypic characterizations in two mutant lines showing defects in motor neuron generation and motor axon development, and I started initial investigations for causative gene defects. In this part, I will discuss what has been achieved during the ENU screen and I will make suggestions for further work.

In #249, phenotypical analysis showed no apparent abnormalities at early stages of development, including the development of primary ventral motor axons (See Table 3.1). In 3 dpf #249 mutants, secondary ventral motor axons (CaP pathway) as well as primary motor axons project normally (Table 3.2). However, most islet-1:GFP motor neurons were present but failed to grow their dorsal projections (MiP pathway). The mutants also showed accumulated secondary axons ventro-medially, suggesting a subset of secondary motor axons projecting in RoP pathway could also be affected. In the islet-1:GPF transgenic line, GFP is expressed in the dorsal subtype of secondary motor neurons, whereas endogenous *islet-1* mRNA is expressed in the RoP and MiP primary motor neurons and secondary motor neurons (Appel et al. 1995; Inoue et al. 1994). By using Islet-1 marker, I found a small percentage of reduction in the numbers of Islet-1 immuno-labelled motor neurons (14-34%) in the mutants at 3 dpf. Interestingly, the generation of Pax2 interneurons are not affected in the mutants, hinting that motor neurons are probably more vulnerable to the mutation. Phenotypic examination of #249 mutants also displayed defects in myelination, reduced labelling intensity and disrupted muscle fibres in both fast and slow muscle types. These observations suggest that the impact of the gene is not specific to motor neurons and secondary dorsal motor axons. However, the critical question remains whether the gene acts in differentiation of islet-1:GFP transgenic neurons cell-autonomously, or whether the altered environment, such as defective muscles prevented axons from growing out of the spinal cord. Answering this question requires confirmation of the causative mutation, and to use cell transplantation to assess whether the mutant phenotype of interest is caused by the defects of the gene on motor neurons or the surrounding environment. For instance, if mutant cells transplanted into wild-type animals failed to grow islet-1:GFP axons,

or wild-type cell transplanted into mutant embryos are not influenced by the surrounding mutant cells and develop properly to extend dorsal projections, the gene is considered to be required only by the cells of interest. However, if wild-type cells fail to grow dorsal projections in the mutant environment regardless of their genotype, or mutant cells are able to develop properly by the influence of wild-type environment, means the gene acts non-cell autonomously.

Additionally, I examined numbers of proliferating cells in the pMN domain of #249 mutants in order to test whether the failure of the dorsal axon outgrowth was linked to the reduced proliferation of progenitor cells. I did not detect a significant decrease of proliferating progenitor cells. However, an increased sample size is required to increase the statistical power of the results, and to answer the question whether the olig2:GFP proliferation is reduced in #249 mutants. Also, it is not clear whether the reduced number of differentiating secondary motor neurons is due to the selective cell death.

Table 3.2 Characterizations of #249 mutants

Motor axons	Primary motor axons	CaP	Present
		MiP	Present
		RoP	Present
	Secondary motor axons	CaP pathway	Present
		MiP pathway	Absent
		RoP pathway	Accumulated axons above the HM
Motor neurons	islet-1:GFP+ neurons		34% Reduction
	Anti-Islet-1 labelled neurons		14% Reduction
	Anti-ChAT labelled neurons		30% Reduction
Interneurons	Anti-Pax2 labelled neurons		Normal
Progenitor cells	olig2:Dsred cell proliferation (51 & 72 hpf)		No significant reduction (Statistical power 51%; Bigger sample size required)
Myelination	Anti-Claudin K labelled myelin sheaths		No myelin detected
Muscle fibres	Fast muscle fibres		Affected
	Slow muscle fibres		Affected

The approach of candidate gene identification involves the prioritisation of a suitable candidate gene that may be relevant to motor neuron or motor axon development, the determination of the existence of the mutation that may results in altered protein function, and the functional tests of the candidate gene in motor neuron development and motor axon outgrowth.

I have initiated candidate gene verification for mutant #249 by first investigating the possible involvement of the gene *psmc2*. The one-base nucleotide substitute in *psmc2* resulted in a premature stop codon, which could lead to a non-functional protein product that causes a phenotypic effect. The amino acid sequence of Psmc2 shows

high similarity across species, suggesting the gene's function maybe conserved. Psmc2 is a 26S proteasome sub-unit that belongs to the ubiquitin proteasome system (UPS). It is also known as 26S proteasome AAA-ATPase subunit (Rpt1) in mammals. A major role of UPS is to control intracellular protein degeneration (Korhonen & Lindholm 2004). UPS degenerates proteins through two major processes: Enzymes-mediated process to target mis-folded protein, and 26S proteasome complex regulated degeneration (Korhonen & Lindholm 2004). In UPS, E1 (ubiquitin activation enzyme) activates a small protein ubiquitin (Ub) in an ATP-dependent manner and transfer it to E2 (ubiquitin conjugation), E2 transfers activated Ub to E3 (ubiquitin protein ligases), which ligates Ub into lysine residues on target protein and then degenerated by 26S proteasome (Hamilton & Zito 2013) (Figure 3.31 A). The 26S proteasome consists one 20S core and two 19S regulatory particles. The 19S regulatory particle is composed of a base subcomplex (PSMC1 – PSMC6) and a lid subcomplex (PSMD1 – PSMD14) (Figure 3.31 B) (Bedford et al. 2008). It is essential for unfolding the protein and opening the gate of 20S core particle to facilitate the translocation of protein substrates for degradation. PSMC2 belongs to the base subunit of the 19S regulatory particles and its expression is important for the formation and function of 26S proteasome (Nijhawan et al. 2012).

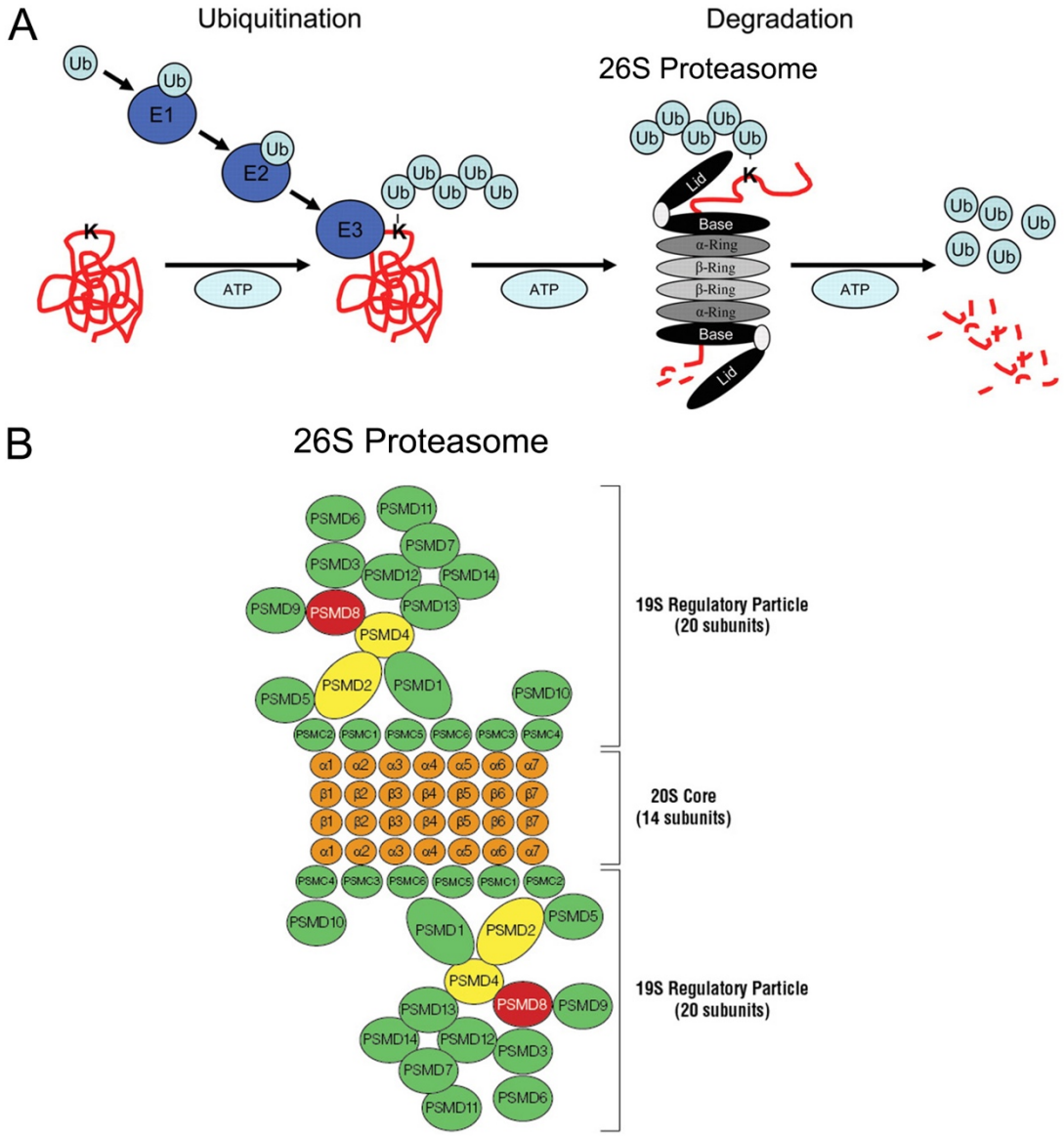

Fig 3.31. (A) Schematic representation of UPS regulated protein degradation. In the ATPase dependent ubiquitin-proteasome pathway, ubiquitin (Ub) is activated by E1 (ubiquitin activation enzyme) and transferred to E2 (ubiquitin conjugation). E2 transfers activated Ub to E3 (ubiquitin protein ligases), which ligates Ub on target protein. In the 26S proteasome, ATPases within the 19S regulatory particle (lid and base) unfold the target protein substrate and translocate it into the 20S catalytic core (α and β rings), which cleaves protein substrate to small peptides. **(B) A diagram of the structure of 26S proteasome complex.** The 26S proteasome complex is made up of one 20S core and two 19S regulatory particles. The 19S regulatory particle consists of a base subunit (PSMC1 – PSMC6) and a lid subunit (PSMD1 – PSMD14). Adapted and modified from (Carrier et al. 2010; Hook & Schagat 2011)

UPS has shown to be involved in neurodegenerative diseases such as Amyotrophic lateral sclerosis (ALS) – knock-out a proteasome subunit specifically in motor neurons caused locomotor dysfunction and loss of motor neurons in mice; Parkinson's disease (PD), in which a mutation in *parkin* encoded E3 ligase causes early on-set PD; and Huntington disease (Jansen et al. 2014). Bedford et al (2008) showed that conditional knock-out of a 19S complex subunit, PSMC1 (Rpt2), results in 26S proteasome depletion and leads to neurodegeneration in mice brain. Furthermore, UPS is linked to axon outgrowth and degeneration (Hamilton & Zito 2013; Yi & Ehlers 2007). (Korhonen & Lindholm 2004) suggested that UPS is essential for protein turnover and synapse maintenance in nerve endings. The dysfunction of the UPS could cause an aggregation of mutant proteins, which affect the axonal transport and neuronal connectivity, and eventually lead to axon degeneration. In *C.elegans,* a genetic screen identified an *ot1* mutant encodes Lin-23, which belongs to E3 ubiquitin ligase complex of UPS (Mehta et al. 2004). *Ot1* mutants displayed deficit in motor axon outgrowth in two sub-classes of motor neurons (Mehta et al. 2004). Lewcock et al (2007) conducted a ENU mutagenesis screen in mice in searching for genes affect spinal motor axon path-finding. The study found a mutant *Magellan* with mis-projection and ectopic branching of motor axons (Lewcock et al. 2007). Genetic mapping indicated a premature stop codon in the *phr1* gene, which encodes E3 ubiquitin ligase (Lewcock et al. 2007). The 26S proteasome complex also plays a role in motor neuron survival and axon outgrowth. For example, PSMC4 (Rpt3) is a subunit of 19S regulatory particle that belongs to 26S proteasome complex (Tashiro et al. 2012). Conditional knock-out PSMC4 (Rpt3) in mice spinal motor neurons caused disrupted 26S proteasome activity, which leads to motor neuron loss and ALS phenotypes. Cheroni et al (2005) observed a decrease level of both 20S core subunit and 19S regulatory particle in spinal cord motor neurons in ALS mouse model SOD1G93A. In *Drosophila*, two mutations in 19S regulatory particle subunits, *Mov34* and *Rpn6*, lead to decreased neuroblasts number and defected axon projection and dendrites pruning during development (Watts et al. 2003). Moreover, Imai et al (2010) found MO knock-down *psmc2,* zebrafish embryos showed defects in lens fibre differentiation (Imai et al. 2010). These evidences support the role of 26S proteasome in motor neurons and axon growth

across species. Although UPS is expressed in various tissues, it is possible that mutations in the ubiquitously expressed housekeeping gene can cause specific phenotype. For instance, *retinal inosine monophosphate dehydrogenase 1 (IMPDH1)* is widely expressed in various tissues in human (Bowne et al. 2008). However, due to the unique requirement of photoreceptors for IMPDH1, it only causes degeneration in retina-specific photoreceptor. As PSMC2 is an essential part that forms the 19S regulatory particles and is important for the 26S proteasome activity (Nijhawan et al. 2012), it is possible that the mutation in *psmc2* may lead to 26S proteasome dysfunction and cause motor neurons and motor axon defects. Taken together, *psmc2* is a suitable candidate gene for further validation.

In the first exon of the *psmc2* gene, a one-base nucleotide substitute C to T resulted in a pre-mature termination codon. *In situ* hybridization using *psmc2* RNA at 24 hpf wild-type embryos showed a wild expression in whole embryos, with prominent expression in somites. This broad expression of *psmc2* showed a correlation with the multiple defects identified in #249 mutants. However, it is not clear if *psmc2* mRNA is expressed in differentiating motor neurons. This can be verified by *in situ* hybridization in islet-1:GPF transgenic embryos, followed by IHC labelling of GFP cells with horseradish peroxidase (HRP). I examined the *psmc2* mRNA expression in a pool of #249 embryos containing mutants, heterozygotes and wild-types, and observed no apparent change in *psmc2* expression pattern. This suggests that mRNA did not undergo nonsense-mediated RNA decay in the mutants, otherwise I would detect low level of RNA expression in the mutant embryos. It is also possible that mutation only affects protein synthesis. Further investigation of changes in protein level can be done by using western blot.

As part of the gene functional analysis, I performed a rescue experiment and overexpressed *psmc2* mRNA in the mutants. I found *psmc2* mRNA-injected mutants showed ectopic dorsal projections and improved morphological phenotype. This indicates that overexpression of *psmc2* mRNA can partially recue the #249 mutant phenotype. To assess if a full phenotypic rescue is present, injected embryos need to be genotyped and sequenced in the future experiment. Furthermore, as an essential

step of gene function validation, a knock-down or knock-out experiment has to be carried out to study if the lack of *psmc2* in wild-type embryos leads to a similar islet-1:GPF motor axon phenotype as that observed in #249 mutant. If *psmc2* is not the phenotype causing gene in #249 mutant, the next candidate gene can be chosen for further analysis is *nell2b* (neural epidermal growth factor-like 2) (Appendix 1). The one-base change in *nell2b* caused a missense mutation. The hydrophobic amino acid Isoleucine (I) is substitute by polar amino acid Asparagine (N), which could potentially have an effect on protein (Barnes & Gray 2003). The amino acid sequence of Nell2b is conserved across species (data not shown). *nell2b* has found to be specifically expressed in motor neuron and sensory neuron differentiation in chick (Nelson et al. 2004)

In the #151 mutant line, mutants showed a 97% reduction in the number of islet-1:GFP+ motor neurons at 3 dpf compared to control siblings (Table 3.3). Examination of the numbers of Islet-1 and HB9 immuno-reactive motor neurons revealed a 17-19% decrease in motor neuron numbers. These results indicate that the majority of motor neurons were generated, but the production of the late-born islet-1:GFP+ motor neurons were severely affected. Immuno-labelling of motor axons showed unaffected primary motor axons such as CaP and MiP, and secondary motor axons that project ventrally in the CaP pathways. However, the rostral primary axons (RoP) that extend ventro-laterally, as well as dorsal secondary motor axon projections (MiP pathway) are absent. Together with the neuronal cell counts, these results hint that the generation of primary ventral and dorsal motor neurons and ventral subtype of secondary motor neurons are likely to be normal, but that the rostral primary motor neurons and the secondary motor neurons with dorsal projections (MiP pathways) and lateral projections (RoP pathway) are not formed. To study the possible causes for the lack of these motor neurons in #151 mutants, I examined the survival and differentiation of motor neuron progenitor cells. To investigate whether fewer islet-1:GFP motor neurons were due to the selective cell death in olig2:Dsred labelled progenitor cells and motor neurons, I applied cell death detection in both fixed tissues and in live embryos at 38 hpf and 48 hpf. I observed no significant increase of cell death in either method used, indicates the survival of

motor neuron progenitor cells and differentiated motor neurons are not compromised. I investigated whether fewer motor neurons were due to reduced progenitor cell proliferation, and observed a decrease in olig2:DsRed proliferation in the mutants. I detected proliferating *olig2*-expressing progenitor cells in #151mutants using PH3 to label cells in M phase, and observed a reduction in PH3 labelled olig2:DsRed cells in the mutant embryos. These results indicate that the proliferation of progenitor cells is compromised in the mutants. In addition to a reduced number of islet-1:GFP motor neurons, #151 mutants also showed other defects. For example, I found a failure in myelination and disorganized muscle fibres from early developmental stages. The generation of Pax2 interneurons is also affected in the mutant. These data suggest that the gene may have a significant impact on the generation of different neuronal types such as olig2:DsRed+ progenitor cells, islet-1:GFP^{+} motor neurons and Pax2+ interneurons. However, it is not clear whether the lack of motor neurons is secondary to the altered surrounding environment. Therefore, similar to #249, it is essential to examine whether the mutant phenotype is cell-autonomous for pMN progenitor cells.

Table 3.3 Characterizations of #151 mutant

Motor axons	Primary motor axons	CaP	Present
		MiP	Present
		RoP	Absent
	Secondary motor axons	CaP pathway	Present
		MiP pathway	Absent
		RoP pathway	Absent
Motor neurons	islet-1:GFP+ neurons		97% Reduction
	Anti-Islet-1 labelled neurons		17% Reduction
	Anti-Hb9 labelled neurons		19% Reduction
	Anti-ChAT labelled neurons		34% Reduction
Interneurons	Anti-pax2 labelled neurons		27% Reduction
Olig2:Dsred cells	Numbers of olig2:Dsred cells 38 & 48 hpf		11% & 18% Reduction
	Proliferation of olig2 progenitor cell (38hpf)		41% Reduction
	Cell death 38 & 48 hpf	Acridine orange	No increase
		TUNEL	No increase
Myelination	Anti-claudin K labelled myelin sheaths		No myelin detected
Muscle fibres	Fast muscle fibres		Affected
	Slow muscle fibres		Affected

For #151 mutant, I investigated a candidate gene *rbbp4* annotated from genome sequencing and bioinformatics analysis. A G-to-T substitute occurred in exon 13 of *rbbp4-201* transcript give rise to a pre-mature termination codon in coding sequence. I detected the expression of *rbbp4-201* mRNA and observed a broad expression pattern at 24 hpf wild-type embryos. I found no apparent changes in *rbbp4-201* mRNA expression examined in a pool of #151 embryos (+/+; +/m; m/m). Similar to #249, it could be that the mutation only affects protein synthesis, and western blot can be used to detect the change in protein level. Also, it is essential to apply *in situ* hybridization in olig2:GFP and Hb9:GFP transgenic embryos to evaluate whether *rbbp4-201* mRNA is expressed in the developing motor neuron progenitor cells and

differentiating motor neurons. In order to demonstrate that *rbbp4-201* is the causative mutation of the phenotype, I performed a gain-of-function experiment. However, by overexpressing *rbbp4-201* mRNA did not rescue the islet-1:GPF+ motor neuron phenotype in #151 mutant. The Failure of the rescue could be due to multiple reasons. For instance, it could be that *rbbp4-201* is not the phenotypic causative gene of #151 mutants. As the mutation occurs at the end of the last exon 13, it is possible that the mutation did not cause functional protein change that could contribute to a severe motor neuron phenotype. Also, some genes are expressed in a tissue specific manner. Rescue could fail because injected mRNA is ubiquitously expressed and prior to the endogenous RNA expression, which may not be transcribed and translated in accordance with the way that endogenous mRNA does. This inappropriate expression can lead to failure of the rescue. Therefore, to further verify the function of *rbbp4-201* in motor neuron generation, it is critical to conduct a loss-of-function experiment by using either CRISPR/Cas9 to knock-out or morpholino to knock-down *rbbp4-201*. Moreover, it is important to verify the other candidate gene identified. For example, a pre-mature stop codon is also occurred in another candidate gene *ankmy2b* (*ankyrin repeat and MYND domain containing 2b*) in the transcript ENSDART00000143494. Studies in mice have found that *ankmy2* regulates the Shh pathway through the interaction with another gene *FKBP38* (Saita et al. 2014). Shh is a secreted morphogen that plays a key role in embryonic development including central nervous system (Chen et al. 2001). It is required for both primary motor neuron and secondary motor neuron development. Preliminary results by genotyping #151 mutants and their siblings confirmed the existence of the nucleotide substitution (data not shown). To confirm if *ankmy2b* is causative mutation in #151, a loss-of-function experiment to either knock-down or knock-out the gene, and attempted rescue of the motor neuron phenotype by gain-of-function experiment have to be conducted.

As briefly discussed above, once the phenotype causing genes for both mutant lines are confirmed, a key study remains to test whether the genes are acting on the cell-autonomous or non-cell autonomous manner. Cell-autonomous function of the gene indicates mutant phenotype of interest is caused by the defects of the gene on mutant

cells independent from the surrounding environment (Li et al. 2011). Non-cell autonomous is the defect of neighbouring cells cause cells of interested to develop abnormally and therefore lead to a mutant phenotype (Li et al. 2011). To distinguish the two scenarios, a classic cell transplantation can be performed between mutants and wild-type embryos. Labelled donor cells from the mutant can be pulled and injected into wild type embryos, and vice versa, wild-type cells can be transplanted into mutant embryos. If mutant cells display a mutant phenotype regarding the wild-type environment, and wild-type cells remain their identity and grow normally, the gene is required in the cells of interest and considered to functions cell-autonomously. On the contrary, if wild-type cells are affected by the mutant environment, and mutant cells are able to develop properly by the influence of surrounding wild-type cells, means the gene is required not only in the cells of interest but also other cell types. In this situation, the gene acts non-cell autonomously. In the case of my research, cell transplantation could answer the question whether impaired dorsal axon growth in #249 is due to lack of ability in motor neurons or an unsupportive muscle environment. Similarly, in #151 mutant, whether the wild-type progenitor cells would be affected by the mutant environment, and fail to differentiate and grow motor axons.

3.4 Conclusion

I carried out a phenotype-driven screen and effectively screened 178 mutagenized genomes of the 222 genomes represented in the 111 F2 families. We successfully identified 6 mutants that display lack of islet-1:GFP motor neurons and/or their axons. I performed further phenotypic characterization for mutant #249, which showed a failure in dorsal islet-1:GFP+ motor axon outgrowth; and mutant #151, which displayed selective lack of islet-1:GFP+ motor neurons. For both mutants, functional analyses are necessary to determine genes that are responsible for the observed motor neuron and motor axon phenotypes. Genes identified from the screen will provide opportunities to dissect the mechanisms underlying the generation of motor neurons and path-finding of the motor axons, as well as the signalling pathway that may be involved.

Chapter 4 Spinal motor neurons are regenerated after mechanical lesion in zebrafish larvae

4.1 Introduction

4.1.1 Larval lesion induces local regeneration of motor neurons and shares similar mechanisms to that of the adult

In adult zebrafish, a mechanical lesion to the spinal cord leads to the proliferation of ependymo-radial glial cells (ERGs) which give rise to new born motor neurons, indicating a high degree of plasticity of spinal progenitors. The regeneration process has been found to be regulated by signals such as notch (Dias et al., 2012), serotonin (Barreiro-Iglesias et al., 2015) and dopamine signalling acting through its D4a receptor on the sonic hedgehog pathway (Reimer et al., 2013). From the previous study of my research group, Dr. Jochen Ohnmacht found that in zebrafish larvae, targeted ablation of motor neurons using metronidazole (MTZ) treatment, leads to motor neuron regeneration (Ohnmacht, Yang et al., 2016). Metronidazole is a prodrug that can be catalysed by bacterial Nitroreductase (NTR) to produce a cytotoxic product (Curado et al. 2008). This cytotoxic product interacts with DNA and induces cell death. In a zebrafish transgenic line expressing NTR under the *hb9* promotor, MTZ induces cell death exclusively within the NTR+ motor neurons. Dr. Ohnmacht also initiated the study of motor neuron regeneration in larvae and provided evidence that regenerative motor neurogenesis can be triggered by a mechanical lesion in the larval spinal cord at 3 dpf.

I continued the study of lesion-induced motor neuron regeneration in larvae and addressed the following questions: (1) whether motor neuron regeneration occurs at later stages in larvae after a lesion. This is interesting because the larval stage begins at 5dpf, which is also the time point that spinal progenitor proliferation and differentiation decrease to a level that remains stable for weeks (Park et al., 2007). Therefore, injury induced neurogenesis in larvae after 5 dpf would require progenitors to be reactivated. As the production of motor neurons concludes at around 51 hpf (Reimer et al., 2013), while oligodendrocytes are still being generated from pMN, I asked (2) whether pMN progenitors can switch from

oligodendrogenesis to motor neurogenesis after a mechanical injury; Also, given that a mechanical injury is sufficient to trigger pMN to regenerate motor neurons, I asked (3) whether a lesion is able to induce other progenitor cells to produce new neurons such as interneurons. Our findings were combined in the publication by Ohnmacht*, Yang* et al., 2016 (Development, * co-first authors) and are described below.

It has been shown that in zebrafish embryos, motor neurons are born from 9 hpf onwards, almost all motor neurons are generated from the motor neuron progenitor (pMN) domain up to 48-51 hpf and that progenitor cells remain relative quiescent at the adult stage (Reimer et al., 2013). Oligodendrocytes are also born from same *olig2*-expressing pMN progenitor zone, indicating pMN progenitor cells are multipotent. Oligodendrocyte progenitor cells are first specified at around 36 hpf (Kirby et al. 2006). Dr. Jochen Ohnmacht and Gianna Maurer first determined if motor neurons can be regenerated in larvae zebrafish, when their developmental generation has been completed. A mechanical lesion was inflicted on the larval spinal cord at 3 days post-fertilization (dpf), with the notochord and major blood vessels left intact. The proliferation marker EdU (5-ethynyl-2′-deoxyuridine) was injected into Hb9:GFP (also known as mnx1:GFP) transgenic animals directly after the lesion to label new-born motor neurons. Lesioned larvae showed a strong increase in the numbers of Hb9:GFP+/EdU+ cells at 5 dpf close to (<50 μm rostral and caudal), but not far from (100 μm>×>50 μm rostral and caudal) the lesion site. Injured larvae also showed an improvement of tissue integrity around the wound. This indicates that motor neuron regeneration is extremely quick in larvae compared to the adult, in which regenerative neurogenesis occurs at 2 weeks after a spinal cord lesion, and locomotor function recovers at 6 weeks post lesion (Reimer et al. 2008; Becker et al. 2004). The swim recovery was found correlate with regenerated axons across the spinal transection site (Becker et al. 2004).

During regeneration, embryonic signals such as sonic hedgehog and serotonin can be re-deployed within a period of time (Reimer et al., 2013; Barreiro-Iglesias et al., 2015). For example, Reimer et al. (2013) revealed dopamine synthesized by the rate limiting enzyme – tyrosine hydroxylase1 (TH1), promotes motor neuron

development in embryos as well as spinal motor neuron regeneration in adults. The study also shown TH1-positive axons from the diencephalon are the only detectable source of dopaminergic innervation in the spinal cord of embryos, and its projections into the spinal cord can be first be detected by immunohistochemistry at 33 hpf. To identify whether larval regeneration shares similar mechanisms with adult regeneration, Dr. Barreiro-Iglesias and Gianna Maurer analysed dopamine signalling by detecting the descending immunoreactive TH1+ axons. Results showed that lesioned larvae presented TH1+ axons rostral, but not caudal to the lesion site. Descending TH1+ axons were detected in control unlesioned larvae along the spinal cord, indicating dopaminergic innervation in the unlesioned spinal cord.

In adults, the dopamine agonist pergolide was found to accelerate pMN progenitor proliferation (Reimer et al. 2013). Therefore, we wondered whether larvae share similar mechanisms to that of the adult and would react to the dopamine agonist. Further study done by Gianna Maurer using pergolide incubation revealed a significant increase of numbers of newly generated Hb9:GFP+ motor neurons marked by EdU, suggest that motor neuron regeneration can be studied in larvae, as motor neuron regeneration in larval pMN reacts to similar signals to the adult after a lesion.

In adult fish, free swimming motor behaviour is largely restored 6 weeks after the lesion (Becker et al., 2004). To investigate if swimming capacity was recovered in lesioned larvae, my colleague Dr. Daniel Wehner measured the total distance moved after tail touch stimuli, as embryos remain immobile most of the time before they develop into activate predators at 5 dpf. Results showed a complete immobility immediately after the lesion at 3 dpf. However, touch stimulated swimming behaviour was quickly restored within 48 h after the injury, with the similar swimming distances as unlesioned control larvae, indicates the motor functional recovery is considerably faster at the larval stage than at the adult stage.

In Ohnmacht, Yang et al. (2016), my colleague Themis Tsarouchas also elucidated the role of immune system in regeneration. Lesion induces microglial cells and

macrophages to concentrate around the lesion site. However, suppression of the immune system led to decreased numbers of regenerated motor neurons, indicating a positive impact of the immune system on motor neuron regeneration.

4.1.2 Neuron-glia switch in the developing spinal cord

In ventral spinal cord, pMN progenitor cells that express Olig2 transcription factor generate first motor neurons and then oligodendrocytes. pMN progenitor cells give rise to motor neurons from 9 hpf to up to 51 hpf (Reimer et al., 2013). Co-expression of *olig2* and *nkx2.2* in progenitor cells induces *sox10* to specify oligodendrocytes precursor cells (OPCs) at 36 hpf, which later mature into oligodendrocytes and migrate to distribute in the spinal cord (Fig 4.1 A) (Kirby et al. 2006; Ravanelli & Appel 2015; Sun et al. 2001). Unlike motor neurons, generation of oligodendrocytes starts late during embryonic development and continues through larvae stages to adulthood (Park et al., 2007). In the spinal cord, P2 progenitor domain sits dorsally adjacent to the pMN domain and produces V2 interneurons (Stifani 2014). An *olig2*$^{-/-}$ mutant showed an expanded P2 domain and increased numbers of V2 interneurons instead of motor neurons and oligodendrocytes (Rowitch 2004). The switch in pMN progenitor cells from generating motor neurons to generating oligodendrocytes has been extensively studied (Kessaris et al., 2001; Rowitch 2004; Park et al., 2002; Anderson 1995; Ravanelli & Appel 2015; Zhou et al., 2001). Two model theories have been proposed (Fig 4.1 B): one is the "switching model", in which motor neurons and oligodendrocytes are derived from common Olig2+ progenitors, meaning the same neuroglioblasts divide asymmetrically to make first motor neurons and then OPCs (Rowitch 2004). For example, Park et al. (2002) used photoactivated fluorescein in combination with *olig2 in situ* hybridization, and the photoactivated fluorescein analysed was restricted to *olig2*-exprssing cells. They found photoactivated fluorescein in *islet-1* marked early born motor neurons at 19 hpf and *sox10* expressing oligodendrocytes progenitor cells at 48 hpf, suggesting that *olig2*-exprssing cells give rise to motor neurons or oligodendrocytes. Another theory is motor neurons and oligodendrocytes arise from fate-restricted progenitors, such as neuroblasts and glioblasts (Rowitch 2004). In this case, a subset of precursors differentiates into motor neurons first, and then later, another sub-population of

precursors develops into OPCs and then differentiates to mature oligodendrocytes. Ravanelli & Appel (2015) suggested that motor neurons and oligodendrocytes are generated from distinct lineage cells from pMN. By using time-lapse video their study found Olig2+ progenitor cells divide symmetrically to motor neurons without further dividing to oligodendrocytes progenitor cells, supporting the second "model" (Ravanelli & Appel 2015). In our larvae lesion paradigm, a mechanical lesion induces a re-production of motor neurons even after neurogenesis has largely ceased, while oligodendrocytes are still being generated. I would like to address the question whether pMN progenitors can switch from making oligodendrocytes to new motor neurons, by investigating the reaction of oligodendrocytes and their precursors after a lesion.

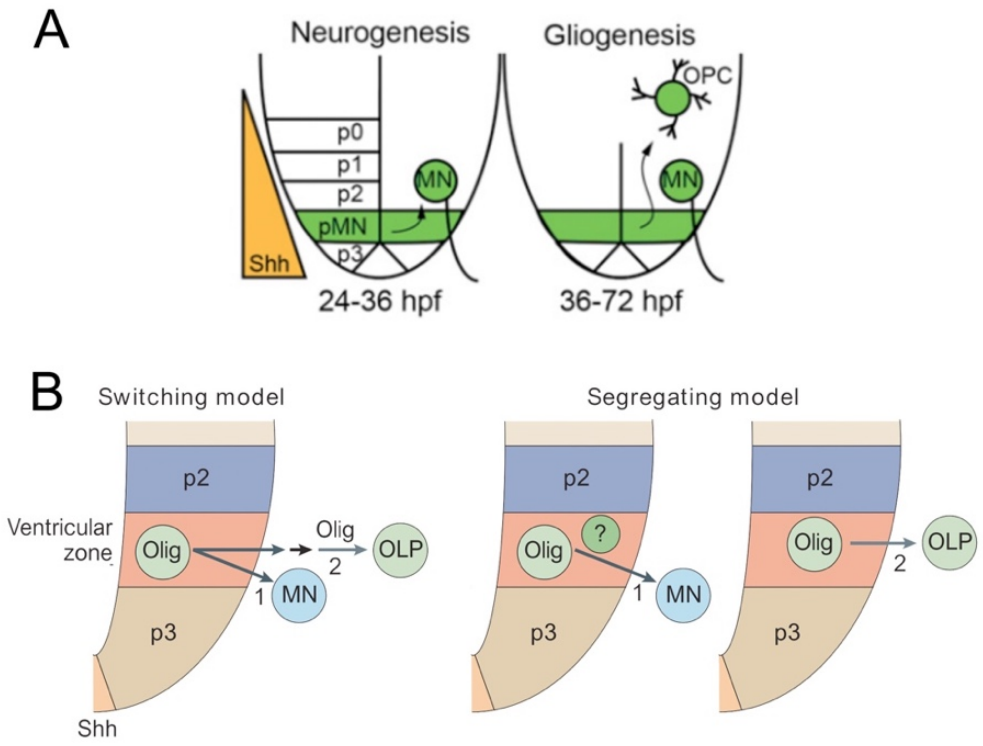

Fig 4.1 Illustrations of neuron-glia switch models. (A) Time points of neurogenesis and gliogenesis. **(B)** Two models of motor neuron and oligodendrocyte specification in ventral spinal cord. Adapted and modified from (Ravanelli & Appel 2015; Rowitch 2004).

4.2 Results

4.2.1 Regenerative neurogenesis also occurs at later stage in larvae

It has been found previously in our group that larvae zebrafish are able to produce new motor neurons after a mechanical lesion within 48 h. The lesion was done at 3 dpf, at which time developmental motor neuron generation had been completed. I was interested in testing whether motor neurons could also be regenerated if the lesion was inflicted at later stages, for instance, at the stage when larvae are behaving as predators. To do this, I shifted the injury paradigm to 5 dpf in Hb9:GFP transgenic larvae. In order to test whether new motor neurons were being produced, I needed to label the larvae spinal cord with markers for evidence of the generation of new cells. I used EdU as a cell proliferation marker in my study. Based on previously established lesion protocol, I applied EdU injection into the yolk sac of the larvae immediately after the spinal cord injury. Larvae were analysed 2 days post-lesion at 7 dpf and new born Hb9+ cells were detected by immunohistochemistry.

EdU is a modified thymidine analogue which incorporates into newly synthesized DNA during S phase. The labelling can be visualized with a florescence dye, with greater efficiency than the traditionally used BrdU (5–bromo–2′–deoxyuridine), for which a harsher treatment to denature the DNA is required (Kaiser et al. 2009). It is to be noted that the bioavailability (transportation and clearance in the body) of EdU has not been well established in zebrafish. Previous research of Zeng et al. (2010) injected EdU into adult mouse brains, and (Kaiser et al. 2009) injected EdU into the avian cochlea. These authors found EdU to incorporate into newly synthesized DNA during the 4-8 h following the injection. I used this time window as an indicator for the EdU analysis in my study.

As mentioned previously, motor neurons are regenerated close to (<50 μm rostral and caudal), but not far from (100 μm>×>50 μm rostral and caudal) the lesion site. I analysed double-labelled Hb9:GFP+/EdU+ neurons, 50 μm rostral and caudal adjacent to the lesion site; and 100 μm of unlesioned control spinal cord, as was done in 3 to 5 dpf standard protocol. The analysis showed hardly any new motor neurons labelled with EdU in the unlesioned control group However, I observed an increase

of 257% in the number of new motor neurons in lesioned animals (Fig 4.2 Unlesioned: 1.23 ± 0.38 cells, Lesioned: 4.40 ± 0.51 cells; 100 µm spinal cord, mean ± SEM, ****p < 0.0001; n = 13-10; Unpaired t test, two-tailed). This supports the previous finding that lesion induced local regeneration of motor neurons occurs within 48 h after the injury. The evidence indicates larvae are also capable of regenerating motor neurons after a lesion at later free-swimming predator stages, when their spinal cord is fully differentiated.

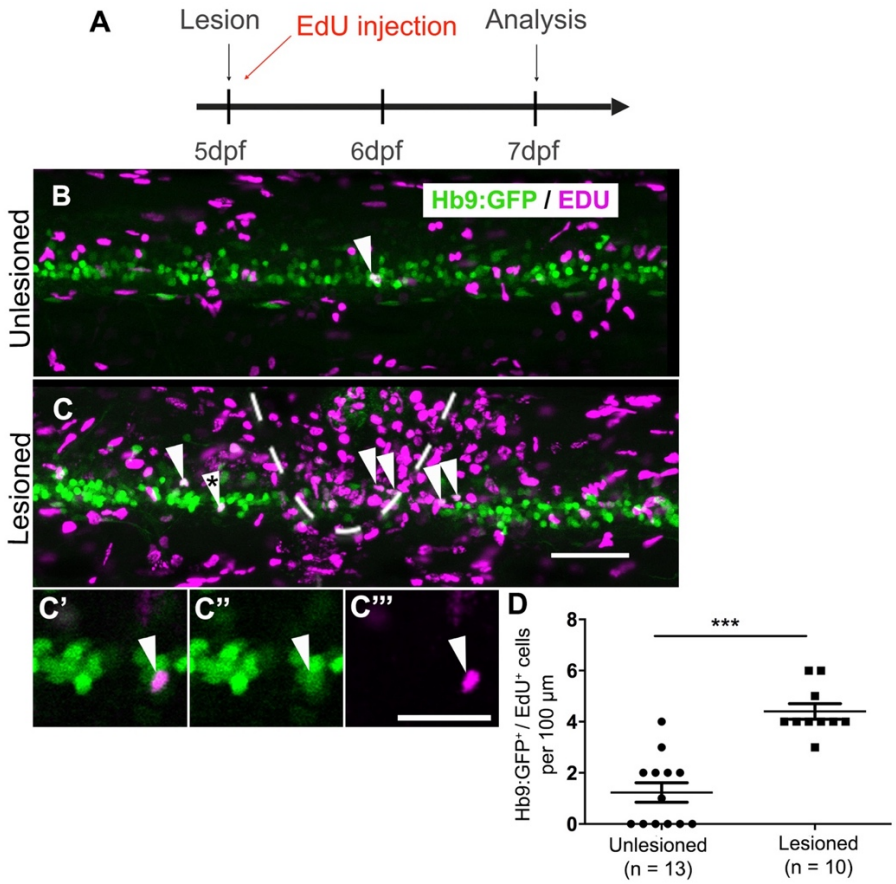

Fig 4.2 A lesion leads to motor neuron regeneration within 48 hours at later stage. (A) The timeline of the experiment. **(B,C)** Lateral views of larvae are shown, rostral is left, dorsal is up, lesion site is indicated by dashed line. The number of EdU labelled Hb9:GFP+ motor neurons (arrowheads) is strongly increased close to the lesion site (dotted line in B). **(C'-C''')** Single optical sections of the areas boxed in B and C, respectively, are shown in higher magnification. **(D)** Quantification shows a significant increase in motor neuron generation between 5 and 7 dpf (Unpaired t test, ****P < 0.0001). Scale bars = 50 µm. Adapted from Ohnmacht, Yang et al. (2016).

4.2.2 Lesion leads to increased proliferation of larval pMN progenitor cells

In the pMN domain, Olig2 transcription factor plays an important role in the development of motor neurons (Park et al., 2002). Lesion induces motor neurons to regenerate suggested that there may be an increased cell proliferation in the pMN domain, and the new born motor neurons are likely to be derived from those pMN progenitor cells. To test this hypothesis, I injected EdU into olig2:DsRed transgenic larvae, in which pMN progenitors and motor neurons contain DsRed protein. Taking into account that the possible bioavailability of EdU is 4-8 h (Kaiser et al. 2009), I chose an injury timeline in which the lesion was performed at 3 dpf and EdU was injected at 4 dpf. Larvae were allowed to survive for 4 h after the injection and then processed for analysis (Fig 4.3 A), in order to acutely label the proliferating cells in the pMN domain. I found that the number of olig2:DsRed+/EdU+ cells in lesioned fish was 8.83 ± 0.54, in comparison with 3.33 ± 0.92 in unlesioned control group (100 μm spinal cord, mean ± SEM, **p = 0.0049; n = 6 vs 6; Mann–Whitney test, two-tailed) (Fig 4.3 B-D). The analysis showed an increase of 165% in numbers of new pMN cells, suggesting that the pMN domain reacts to a lesion with increased proliferation.

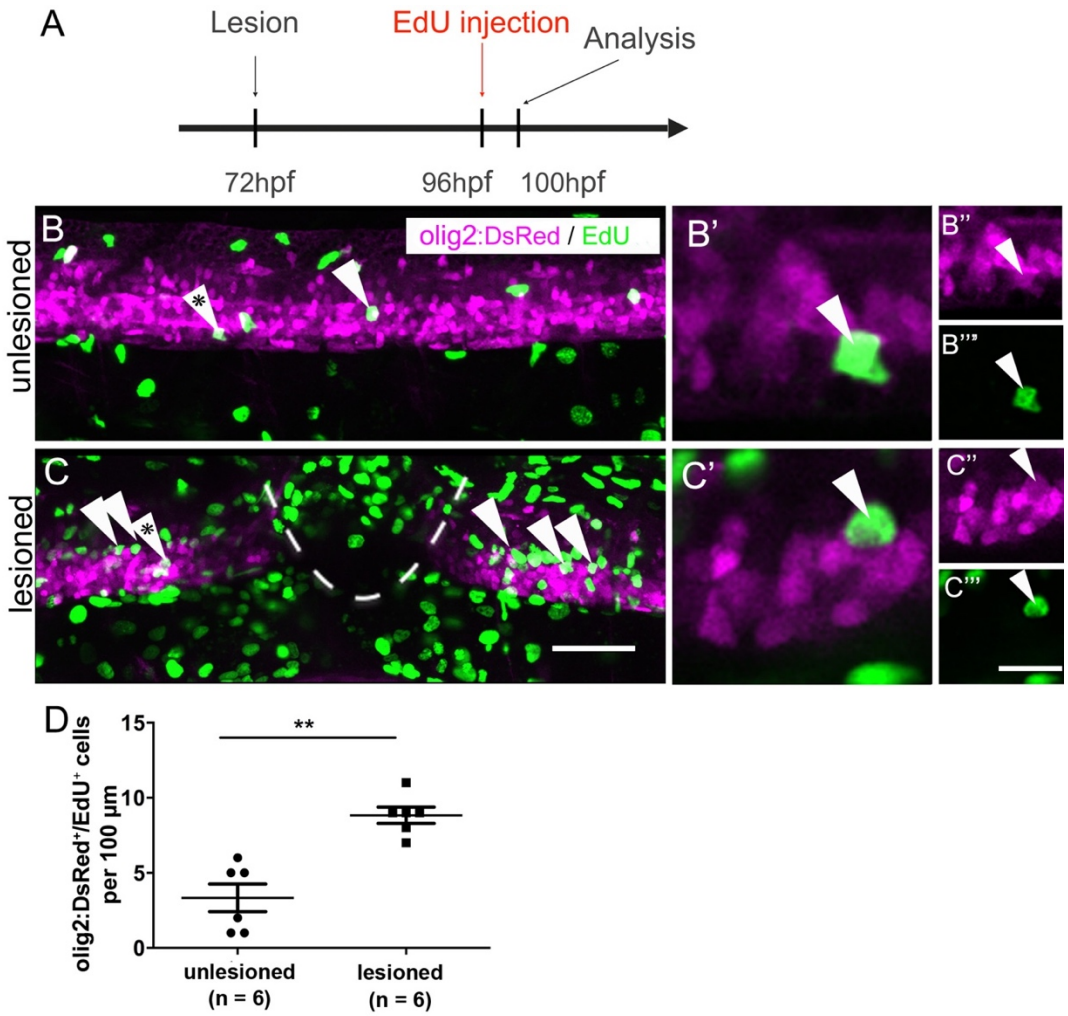

Fig 4.3 The pMN domain reacts to a lesion with increased proliferation. Lateral views are shown; rostral is left, dorsal is up. **(A)** Time line of the experiment. **(B,C)** olig2:DsRed+ cells (arrowheads) in the pMN domain that incorporated EdU within the last 4 h. **(B'-C''')** Higher magnifications of single optical sections of the cells indicated by asterisks in B and C, respectively, showing double labelling. **(D)** The number of proliferating cells in the pMN domain is significantly increased in the vicinity of the lesion site (Mann-Whitney test; **P=0.0049). Scale bars: 50 µm in C for B,C; 20 µm in C''' for B''-C''' and 10 µm for B',C'. Adapted from Ohnmacht, Yang et al. (2016).

It has been found that new motor neurons are likely to be derived from Olig2+ expressing ERGs in the adult pMN-like domain (Reimer et al. 2008; Reimer et al., 2009). These newly regenerated motor neurons first express the motor neuron-specific transcription factor Hb9 and later express the mature marker choline acetyltransferase (ChAT). However, it was not clear whether in lesioned larval spinal cord, proliferating Olig2+ progenitor cells are the source of newly regenerated motor neurons. By using Hb9:GFP x olig2:DsRed double transgenic larvae with EdU labelling, my colleague Gianna Maurer assessed whether newly generated motor neurons in larvae were derived from the *olig2*-expressing cells. Newly generated Hb9:GFP motor neurons derived from Olig2 progenitor would retain both GPF and DsRed protein, and would be positive for EdU labelling. Here DsRed protein acts as short-term lineage tracer. Results showed all newly generated motor neurons (Hb9:GFP+/EdU+; 23 neurons in 4 animals) were also positive for DsRed (Fig 4.4). This supports our hypothesis that newly generated motor neurons originate from *olig2*-expressing pMN progenitor cells after a lesion.

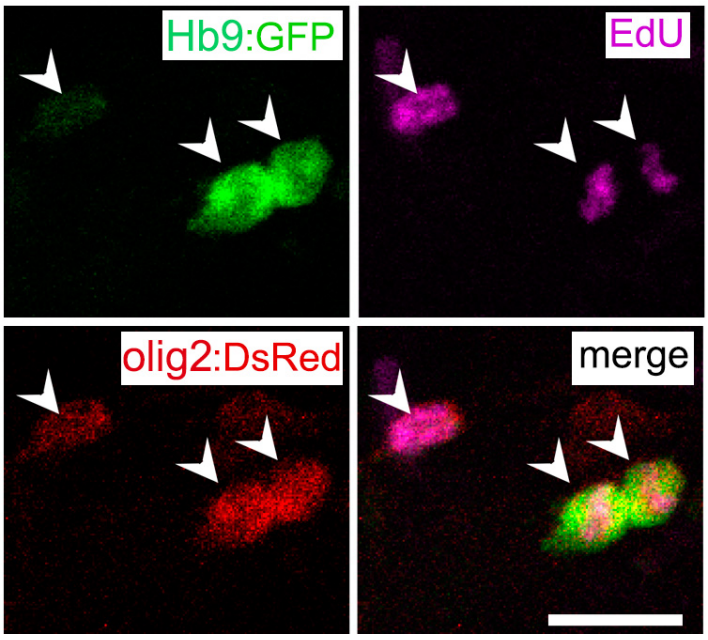

Fig 4.4 Regenerated motor neurons are derived from pMN progenitor cells after a lesion. In Hb9:GFP and olig2:DsRed double-transgenic larvae (lesion at 3 dpf and analysis at 5 dpf), Hb9:GFP+/EdU+ neurons retain DsRed protein are indicated by arrowheads. Scale bar 15 μm. Adapted from Ohnmacht, Yang et al. (2016).

4.2.3 Production of mature oligodendrocytes is affected by SC lesion

A mechanical lesion triggers motor neurons to regenerate even after developmental motor neuron generation has concluded. This raised another question of how would oligodendrocyte progenitor cells, which are still generating at the time, react to such an injury. To investigate if oligodendrocyte generation is altered after a lesion, I used the mbp:GFP transgenic line to assessed the number of newly generated differentiated oligodendrocytes (Almeida et al., 2011). In mbp:GFP transgenic larvae, oligodendrocytes are labelled under the regulatory sequences of the myelin basic protein a (*mbpa*) gene. *mbp* is exclusively expressed in mature oligodendrocytes and is an important protein for myelin formation (Zhou et al., 2001). EdU was applied after the lesion at 3 dpf and larvae were analysed at 5 dpf, consistent with the timeline of motor neuron regeneration. I observed fewer EdU double-labelled mbp:GFP+ cells in the lesioned group, with the mbp:GFP+/EdU+ number strongly reduced by 94% (unlesioned control 1.67 ± 0.37, in comparison with 0.10 ± 0.10 in lesioned group; mean ± SEM, ***P=0.0005; 100 μm spinal cord; n = 9-10; Mann–Whitney test, two-tailed) (Fig 4.5). In lesioned spinal cord, myelin sheaths caudal to the lesion site have degenerated, presumably because the axons they myelinated were descending degenerating axons. The result suggests that the generation of mature oligodendrocytes was reduced after the lesion. This could be due to the decreased production of oligodendrocytes precursor cells (OPCs) consequently resulting in fewer mature oligodendrocytes.

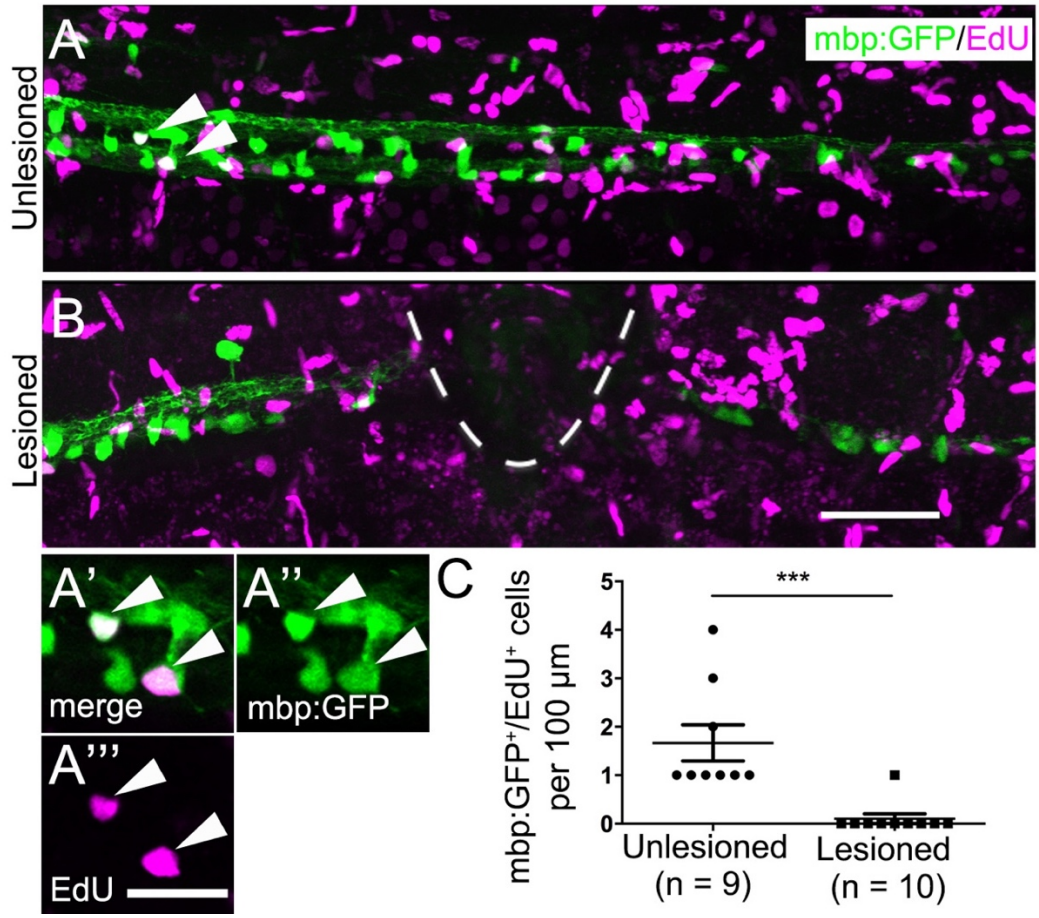

Fig 4.5 Generation of mature oligodendrocytes is affected by the lesion. Lesion is conducted at standard 3 to 5 dpf timeline. **(A,B)** Lateral views are shown; rostral is left, dorsal is up. The lesion site is indicated by a dashed line. mbp:GFP+ oligodendrocytes incorporate EdU (indicated by arrowheads) in unlesioned larvae. **(A'-A''')** Single optical section of two double-labelled neurons indicated in E showed in higher magnification. (B) Fewer mbp:GFP+/EdU+ cells are observed after a lesion. **(C)** The number of new oligodendrocytes is significantly reduced after a lesion (Mann–Whitney U-test; ***P=0.0005). Scale bars: 50 µm in B for A, B; 20 µm in A'''. Own figure plate, taken from Ohnmacht, Yang et al. (2016).

4.2.4 Oligodendrocyte progenitor differentiation is reduced in the lesioned spinal cord

Olig2 transcription factor is expressed during the early fate specification of oligodendrocytes which retain the expression throughout the differentiation stage into maturation (Liu et al., 2007). Olig2 progenitors co-express Sox10 in OPCs to promote oligodendrocyte differentiation (Takada et al. 2010). Therefore, Sox10 is used as an early marker for oligodendrocyte lineage cells. To assess whether the production of OPCs was altered after the lesion, I used olig2:GFP x sox10:mRFP double transgenic larvae. In the olig2:GFP transgenic line, GFP is expressed in pMN precursors including motor neurons and OPCs under the regulatory sequences of the *olig2* gene. In sox10:mRFP larvae, the expression of membrane-tethered monomeric red fluorescence protein (RFP) is under control of *sox10* regulatory sequence (Kirby et al., 2006). According to Kirby et al. (2006), the first specialization of OPCs in zebrafish ventral spinal cord is at 36 hpf, and myelination of axons by oligodendrocytes occurs at 72 hpf. Using our standard 3 to 5 dpf lesion paradigm, the number of olig2:GFP/sox10:mRFP/EdU triple-labelled cells was analysed. At this stage, triple-labelled cells are representing both newly generated oligodendrocytes and their precursors, hence we use the term oligodendrocyte lineage cells to indicate these cells. In the unlesioned group, the number of olig2:GFP+/sox10:mRFP+/EdU+ cells reached 9.30 ± 1.06, confirming previous evidence for continuous generation of oligodendrocytes in unlesioned larvae (Park et al., 2002). However, in the lesioned group, the number of triple labelled cells only reached 1.11 + 0.51 (mean ± SEM, ****P<0.0001; 100 μm spinal cord; n = 9-10; Unpaired t-test, two-tailed), with a significant reduction of 88% compared to control group (Fig 4.6). The results showed fewer OPCs and oligodendrocytes were produced, which is in agreement with my previous result that lower numbers of differentiated oligodendrocytes were newly generated after a lesion, and implies a reduction in the generation of OPCs. These analyses suggest that the pMN domain is able to switch from generating oligodendrocytes to making new motor neurons after a lesion.

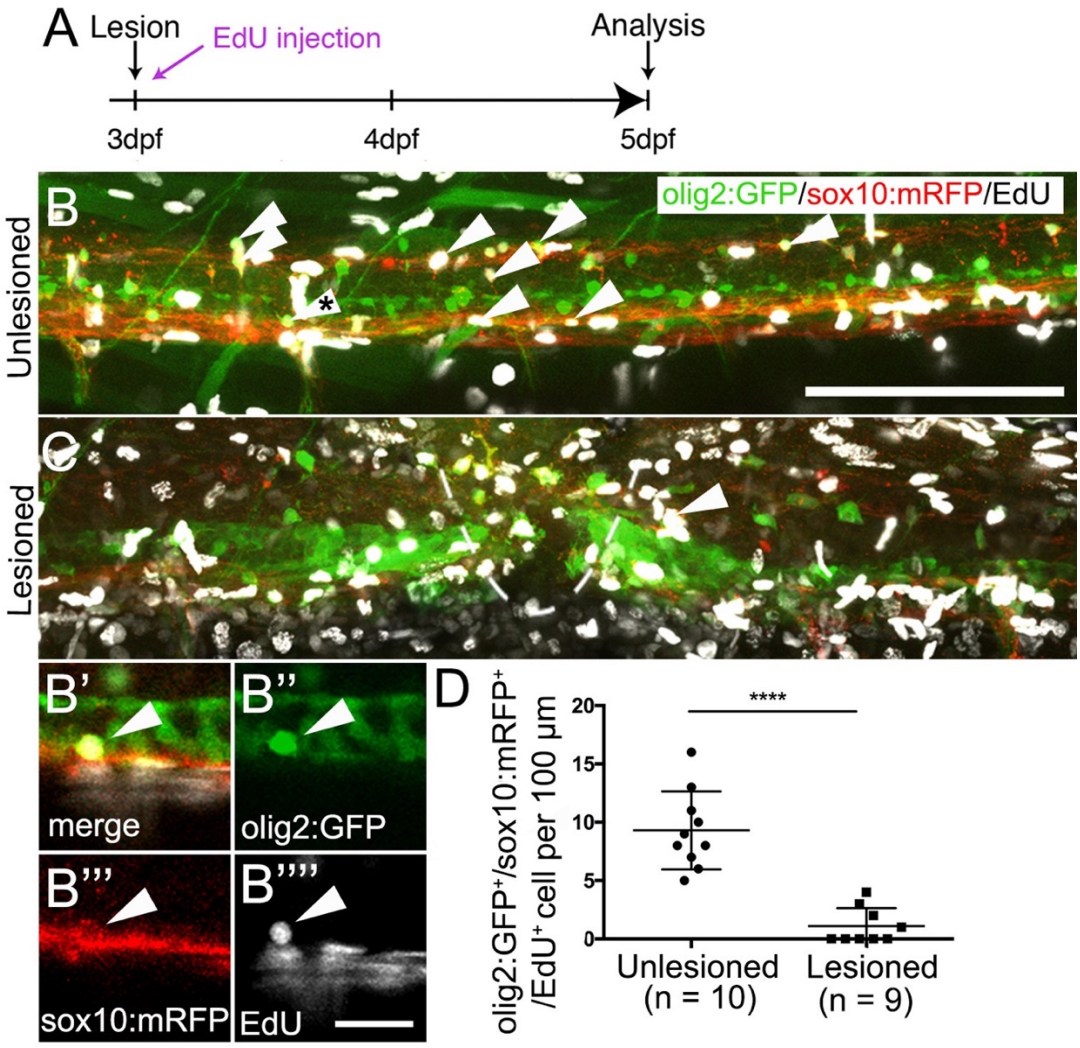

Fig 4.6 Generation of oligodendrocytes lineage cells is reduced after a spinal lesion. Lateral views are shown; rostral is left, dorsal is up. The lesion site is indicated by a dashed line. **(A)** Time line of the experiment. **(B,C)** Number of newly generated oligodendrocytes and their precursors (olig2:GFP, sox10:mRFP and EdU triple labelling (asterisk) are reduced in number after lesion. **(B'-B'''')** Single optical section of a triple-labelled cell (indicated with asterisk in B) at higher magnification. **(D)** The number of triple-labelled cells is reduced (Unpaired t-test, ****P<0.0001). Scale bars: 100 µm in B for B, C; 20 µm in B'''' for B'-B''''. Adapt from Ohnmacht, Yang et al. (2016).

4.2.5 No apoptotic cell death in oligodendrocyte progenitor cells

In order to investigate whether OPCs display selective cells death in the pMN domain, I used olig2:GFP/sox10:mRFP double-transgenic larvae. A standard 3 to 5 dpf lesion paradigm was applied followed by a TUNEL assay, which labels late cell death by detecting fragmented DNA (Kyrylkova et al. 2012). I first assessed the cell death in oligodendrocyte lineage cells by counting triple labelled olig2:GFP+/sox10:mRFP+/TUNEL+ cells. I did not observe any olig2:GFP+/sox10:mRFP+ that were labelled by the TUNEL reaction, suggesting that lower numbers of oligodendrocyte lineage cells were not due to increased cell death ($P>0.9999$; 100 μm spinal cord; $n = 13\text{-}9$; Mann–Whitney test, two-tailed) (Fig 4.7). Furthermore, I did not detect increased olig2:GFP/TUNEL double-labelled cells within the pMN domain, indicating that pMN progenitors did not go through selective cell death. Occasionally, I observed double-labelled cells outside the area of interest in both conditions, demonstrating that I am able to detect such cells. Taken together, these observations suggest that there is no increase in oligodendrocyte progenitor cell death after a lesion.

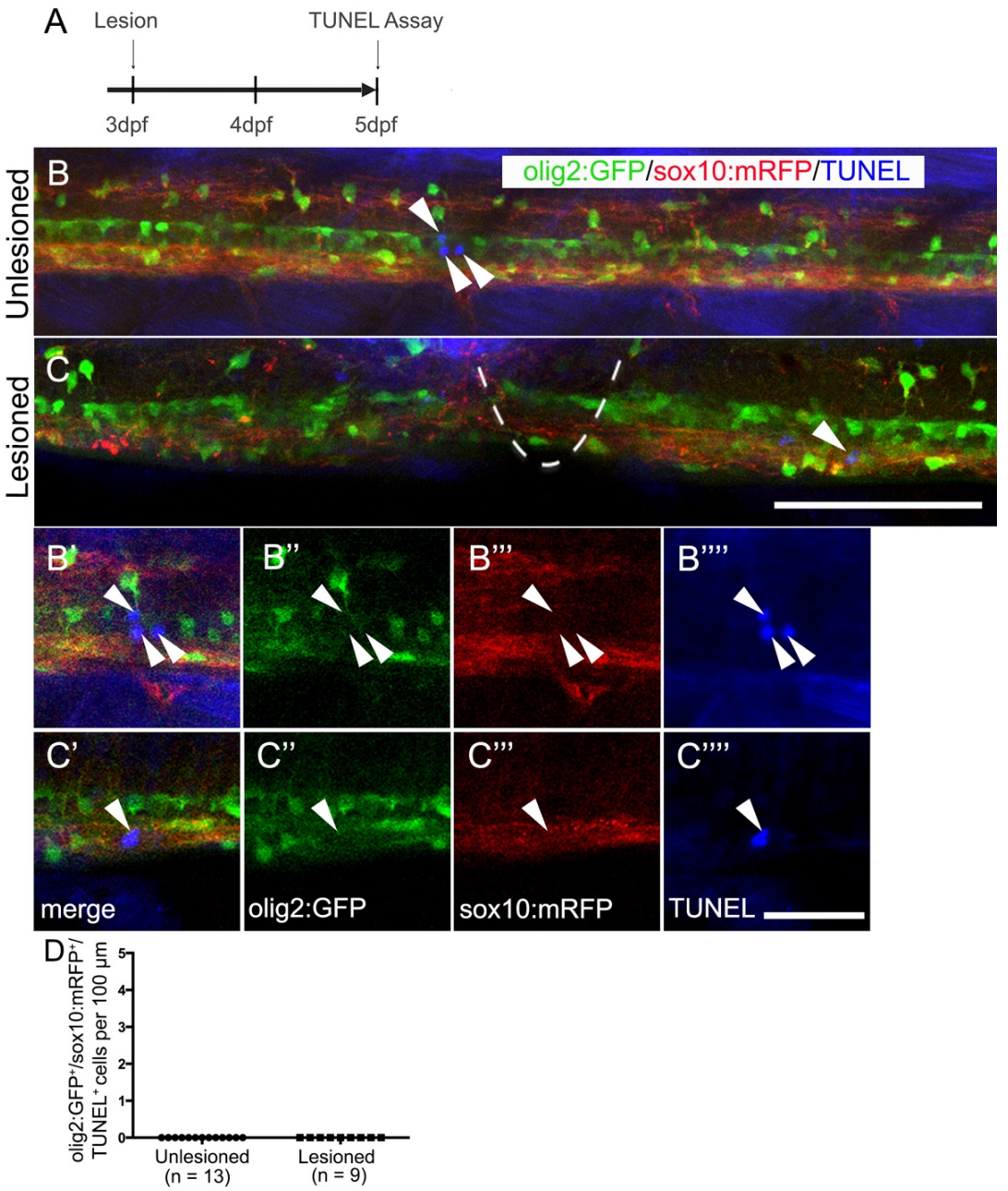

Fig 4.7 No apoptosis of oligodendrocyte generation is detected after a spinal lesion. (A) Time line of the experiment. **(B,C)** Lateral views are shown; rostral is left, dorsal is up. The lesion site is indicated by a dashed line. TUNEL positive cells (arrowheads). **(B'-C'''')** Single optical sections at higher magnification show a TUNEL positive but olig2:GFP/sox10:mRFP negative cell (indicated with arrowheads in B, C). **(D)** No increase in numbers of cell death (Student's t-test, P>0.9999). Scale bars: 100 µm in B for B, C; 20 µm in C'''' for B'-C''''. Adapted from Ohnmacht, Yang et al. (2016).

4.2.6 Pax2 expressing interneurons are not regenerated after SC lesion

In adult zebrafish, a spinal cord transection triggers cell proliferation not only in the pMN domain but also in the other progenitors such as P2 domain, which is dorsally adjacent to the pMN domain, and mainly generates V2 interneurons (Kuscha et al., 2012). Kuscha et al. (2012) found that undifferentiated V2 interneurons, marked by vsx1:GPF, as well as serotonergic interneurons, are regenerated at 2 weeks after a lesion in adult fish. The research also shown pax2a:GPF+ interneurons, which might be derived from a more dorsal progenitor domain distinct from the pMN domain, were not affected by the lesion at 2 weeks post-lesion (Kuscha et al., 2012). In larvae, genetic ablation of motor neurons also did not affect the generation of pax2a+ interneurons (Ohnmacht, Yang et al., 2016). In my study, I wanted to elucidate whether other progenitor cells are triggered to generate new neurons after SC lesion. I used pax2a:GPF transgenic larvae followed by EdU labelling and analysed the number of newly generated dorsal pax2a:GFP+ interneurons. The result showed low numbers of new born pax2a:GFP+/EdU+ cells in both unlesioned controls (0.25 ± 0.16 cells) and lesioned larvae (0.50 ± 0.34 cells), with no statistical difference between two groups ($P = 0.6839$; 100 μm spinal cord; $n = 8\text{-}6$; Mann-Whitney test, two-tailed) (Fig 4.8). This indicates that a lesion might not be sufficient to induce increased neuron generation for some dorsal progenitor zones.

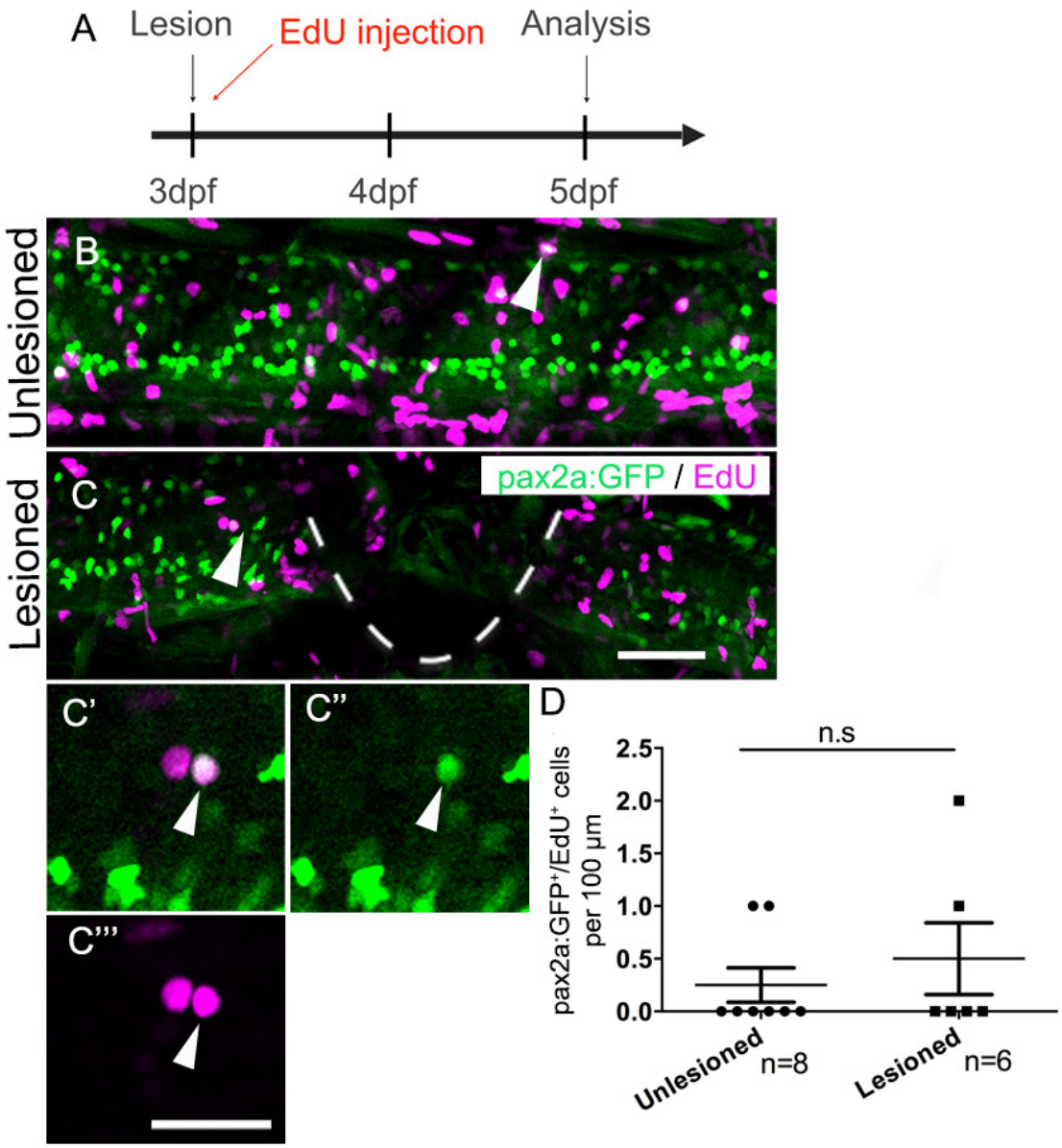

Fig 4.8 Generation of pax2a:GFP+ interneurons is not affected by a spinal lesion. Lateral views are shown; rostral is left, dorsal is up. **(A)** The timeline of the experiment is shown. **(B,C)** EdU+/pax2a:GFP+ cells (arrows) are present in unlesioned (B) and lesioned (C) larvae. The lesion site is indicated by dashed line. **(C'-C''')** Single optical section of the areas boxed in B and C, respectively, are shown at higher magnification. **(D)** Quantification shows no difference in pax2a:GFP+ neuron generation between 3 and 5 dpf (Mann-Whitney U test; P = 0.6839). Scale bar in C = 50 µm for B,C and in C' = 50 µm for B',C'. Own figure plate, taken from Ohnmacht, Yang et al. (2016).

4.3 Discussion

4.3.1 Zebrafish larvae is a rapid and robust model for the study of motor neuron regeneration

Unlike mammals, the adult zebrafish is capable of regenerating its spinal cord after an injury. Studies have demonstrated that adult zebrafish can replace neuronal loss by regenerating new neurons such as motor neurons (Reimer et al., 2008) and their progenitor cells, interneurons (Kuscha et al., 2012) and radial glia progenitor cells (Briona & Dorsky 2014). Although adult zebrafish has been a well-established model to study regenerative neurogenesis (Becker & Becker 2015), it takes 3-4 months for them to reach sexual maturity, and the analysis requires subsequent intervention such as surgery, perfusion, dissection and section for antibody staining, all limited by the number of animals that can be processed at a time. Moreover, the regeneration of motor neurons in adult takes place at 2-6 weeks after a lesion and adult fish have a motor functional recovery time of 6-8 weeks (Becker et al., 2004).

In contrast to adult, zebrafish larvae are transparent and small in size. Spinal cord transection can be inflicted with an injection needle and further analysis can be done in whole larvae. We have established larval zebrafish as a model for lesion induced motor neurogenesis, and have shown that zebrafish larvae have the ability to reclose the wound, regenerate motor neurons and restore swimming ability within 2 days post-injury (dpi), with a survival rate of 85%-90% after a lesion. We found that regeneration occurred at both early and relatively later stages. Our study is similar to a previous study of Briona & Dorsky (2014) that spinal cord injury in larvae displayed a neuronal replacement at 4 dpi as well as response to touch at 5 dpi. Lesioned larval showed a robust swimming behaviour at 9 dpi (Briona & Dorsky 2014). Other studies from Becker et al. (1997) and Reimer et al. (2008) found adult fish are able to repair disconnected axons and bridge the injury site with some degree of re-myelination, and a similar finding was described in Bhatt et al. (2007) that larvae regenerate fibres across the lesion site 24 h after a lesion without additional intervention. Combined with our finding, this research suggest larvae is an extremely rapid and robust tool for regenerative study.

We also showed that there is a recapitulation of signals in larval regeneration to that of the adult. Our study found that similar to the adult, Olig2 progenitor domain in larvae is highly plastic. Similar to the adult zebrafish, Olig2 progenitor cells are able to increase proliferation after an injury, and newly generated motor neurons in larvae are derived from *olig2*-expressing progenitor zone. Signals like dopamine, serotonin and notch react to a lesion in adult spinal cord and promote the re-generation of motor neurons from pMN domain (Kuscha et al., 2012; Barreiro-Iglesias et al., 2015; Reimer et al., 2013; Dias et al., 2012). By analysing the projection of TH1+ axons, which are the source of dopaminergic innervation in embryonic spinal cord, we confirmed there are dopaminergic projections down the spinal cord in 3 dpf larvae. Also, a dopamine agonist boosts the number of newborn motor neurons in lesioned larvae, indicating larval and adult regeneration share similar mechanisms. These findings strengthened zebrafish larvae as a model to study motor neuron regeneration after SC lesion. In addition to these, larvae have great accessibility for genetic modification as well as the ease of high-throughput screening for drug treatment and behaviour in lesioned animal.

Taken above, zebrafish larvae have great advantages and can be used as a model for the research of motor neuron regeneration.

4.3.2 pMN progenitors can switch from oligodendrogenesis to motor neurogenesis

Neurogenesis is relatively quiescent in the adult pMN domain (Reimer et al., 2008). However, motor neuron regeneration can be triggered by a mechanical transection of the spinal cord. Similarly, I found in larvae, a mechanical lesion could reactivate pMN progenitors to increase proliferation, and make new motor neurons after neurogenesis is completed, while oligodendrogenesis is on-going. New motor neurons are generated from the ventral spinal cord in the vicinity of lesion site, and retain DsRed expression controlled by *olig2* promoter, indicating they are likely to be derived from pMN progenitor cells. These new motor neurons could be generated from either a recruitment of new progenitor cells distinct from oligodendrocytes (Ravanelli & Appel 2015); or a change of nearby fate-restricted oligodendrocyte

progenitors during the embryonic development (Park et al., 2002). Interesting, I found a sharp decline of the generation of oligodendrocyte lineage cells, without detectable cell apoptosis of Olig2+ precursors, suggesting the number of a sub-population of Olig2+ cells are reduced. This is confirmed by my observation that fewer numbers of mbp+ mature oligodendrocytes are produced after a lesion. My findings are in favour of the first possibility, in which the lineage relationship of motor neuron and oligodendrocyte is "one or the other" – pMN precursors are required to make a decision to produce either motor neurons or oligodendrocytes. Here we provide evidence to show the highly plastic nature of pMN domain, and their progenitors are able to switch their fate from oligodendrogenesis to motor neuron generation after a mechanical lesion.

4.3.3 Progenitor domains present different potentials in regeneration

In my study, I did not detect an enhanced generation of pax2a+ interneurons. pax2a+ cells are mostly likely to be derived from a distinct progenitor pool dorsal to pMN domain (Kuscha, Frazer, et al. 2012), suggesting for some dorsal progenitor zones neither an ablation nor a mechanical lesion is sufficient to increase neuron generation. This finding is similar to the observation of Dr. Jochen Ohnmacht, in which pax2a+ interneurons did not regenerate after targeted motor neuron ablation in larvae. This shows that progenitor domains react differently to a lesion. For example, in adult fish, pax2a+ interneurons are newly generated after a lesion, and the generation of vsx1:GFP+ V2 interneurons from the P2 domain was enhanced (Kuscha et al., 2012). In the study of Kuscha et al. (2012), no change in numbers of dorsal parvalbuminergic interneurons were found up to 6 weeks post-lesion. In embryos, serotonin promotes motor neuron development but showed no impact on numbers of vsx1:GFP+ and pax2a:GFP+ interneuron produced (Barreiro-Iglesias et al., 2015). A dopamine agonist enhanced motor neuron generation at the expense of vsx1:GFP+ interneurons, while pax2a:GFP+ and glyt2:GFP+ glycinergic interneurons (Eklöf-Ljunggren et al., 2012) were unaffected (Reimer et al., 2013). In my study, further experiments can be done with other types of interneurons to test the regenerative variety of different progenitor domains. Together with my findings, we demonstrate

the potential of lesion-induced proliferation is different in progenitor domains and they may act on different mechanisms and signalling pathways.

4.4 Conclusion

Adult zebrafish are able to react to a lesion with increased numbers of Olig2+ progenitor cells to produce new motor neurons and re-gain swimming ability (Dias et al., 2012; Reimer et al., 2008; Becker et al., 2004). We showed that regenerative neurogenesis can be triggered by a mechanical lesion at the larval stage when motor neuron generation has ceased. pMN domain progenitors react with increased proliferation and differentiate into new born motor neurons. Motor neuron regeneration in larvae shares similar signals to that of the adult. Regeneration in larvae is considerably faster with both motor neuron and swimming ability restoration within 48 h. However, the link between new motor neurons and functional recovery still requires further investigation. More interestingly, we provide evidence that pMN domain progenitors can switch from making oligodendrocytes to making new motor neurons. We also showed that progenitor domains have different regenerative potentials after a lesion. The advantage of robust regenerative ability of larvae with the greater accessibilities for tools make it an excellent model for regeneration studies.

Chapter 5 General discussion

In my thesis I aimed to find mechanisms of motor neuron development and regeneration after a lesion. I will discuss in turn my efforts to find new mutants affecting motor neuron development (5.1) and my characterization of motor neuron progenitor behaviour after a spinal cord lesion in larval zebrafish (5.2). The latter part of my thesis has already been published with me as a co-first author (Ohnmacht and Yang et al., 2016)

5.1 Identify essential genes for spinal motor neuron and axon generation in zebrafish

In this part of the study, I presented an ENU-induced screen in zebrafish to identify genes that regulate the generation of secondary motor neurons and their axon development. I focused on 2 mutants discovered from the screen displaying defects in motor neuron generation (#151) and motor axon outgrowth (#249), and characterized the mutant phenotypes by using various molecular markers. I started the analysis of mutated genes that might be responsible for the observed phenotypes for both mutants, and obtained preliminary results showing that overexpression of the candidate gene *psmc2* partially rescued the dorsal secondary motor axon phenotype in the #249 mutants. However, in #151 mutants, overexpression of a candidate gene *rbbp4* did not promote islet-1:GFP motor neuron generation.

For decades, ENU mutagenesis screening has been widely used for novel gene identification. Mullins et al (1994) and Solnica-Krezel et al (1994) first established methods of performing large-scale mutagenesis screen in zebrafish, and demonstrated two most efficient mutagenic regimes and concentration that have been used as standardized methods for ENU treatment. Many studies have proved the reliability of ENU in generating point mutations and the utility of ENU screens in gene discovery across species (Acevedo-Arozena et al. 2008; Driever et al. 1996; Balling 2001; Nagy et al. 2003). This forward genetic approach requires no prior knowledge of the functions of the genes, hence allowed an unbiased phenotypic screening. As ENU induced mutations occurs at random, the identification of

phenotype of interest requires screening of a large numbers of animals. Therefore, when screening for specific phenotypes of interest, the parameters chosen for the screen must be robust and easy to be recognized by the investigators (Argmann et al. 2006; Moresco et al. 2013). This could largely avoid false positive results. In our screen, I used islet-1:GFP transgenic line as a readout, which allowed us to screen ~1200 embryos for motor neuron phenotype under a stereo-microscope equipped with a fluorescent lamp in a petri dish, and to evaluate fine motor axons of ~600-700 of flat-mounted embryos using a fluorescence microscope each week. I looked for abnormalities in the GFP expressed dorsal subset of secondary motor neuron and axons, and discarded mutants with general deformations and early developmental defects in order to minimize false positives and the influences of general physiological impairment when it comes to interpret the phenotype.

I investigated two mutant lines: #249, in which dorsal secondary motor axons were absent; and #151, which has fewer motor neurons. I applied neuronal, axonal and muscle fibre markers to further define their phenotype and found additional defects in muscle fibres and myelination. Therefore, it will be important to find out whether defects in motor neurons or their progenitors are cell-autonomous or a secondary consequence of the altered surrounding tissue. Understanding the cell-autonomous and non-cell-autonomous function of a gene could help to understand the interaction between genetic and environmental factors.

We used Next generation sequencing (NGS) technique (outsourced to Edinburgh Genomic) to identify mutated genes underlying the mutant phenotypes of #249 and #151. The strategy is to identify a chromosome interval linked to the mutation, and then search for single nucleotide polymorphisms (SNPs) within this defined region as potential causative mutations (Henke et al. 2013). The principal of the NGS is to fragment genomic DNA randomly into short sequences and ligate them with specialized adapters (primers). The generated short reads are amplified, sequenced, and then aligned to a reference genome using computational bioinformatics software in order to identify SNP variations. As sequencing reads can contain sequence errors, an accurate mutation detection requires higher genome coverage. Coverage refers to

the average number of times a base in the genome is sequenced (Sims et al. 2014). Reads with higher coverage contain fewer sequencing errors. However, higher coverage also means higher cost, therefore there is a need to balance the coverage and cost when it comes to NGS. A study of Voz et al. (2012) demonstrated that an 8x coverage of the zebrafish genome was sufficient to detect the phenotype-causing mutation. In our screen, we used ~19x coverage to sequence both mutants and their siblings. The first step for genetic mapping of a gene mutation is to create a mutant strain that is polymorphism to the mutagenized founder strain. This would provide high levels of polymorphism within the mutants to identify strain-specific variations and mutations. In our screen, I crossed F2 mutant carriers of #249 and # 151 with a mapping strain wild-type TL. The next step is to isolate mutants and their phenotypically wild-type siblings from the subsequent map-cross and extract gDNA for sequencing. It is important to ensure that mutants are phenotypically identifiable and no wild-type siblings were mis-sorted into the mutant pool, as it could decrease the homogeneity around the region containing the mutation and may yield false results (Henke et al. 2013). Although there is no defined rule of the numbers of mutants to be used, Henke et al. (2013) noted that using 20 fish and 3x coverage is enough to identify candidate mutations, and increasing the number of fish also increase the sensitivity of the mapping when sequencing with higher genome coverage. Voz et al. (2012) used a pool of 50 fish with 8x genome coverage for mutation identification. In our screen, as we are sequencing with ~19x coverage, I isolated 80-140 embryos for each mutant and wild-type sibling pool from each mutant family.

In #249 mutants, gain-of-function analysis of a candidate gene *psmc2* – a component of 26S proteasome that belongs to the Ubiquitin Proteasome System (UPS), showed promising preliminary results. I found that the overexpression of *psmc2* in mutants promoted the dorsal secondary motor axon outgrowth and improved the survival of the mutant embryos by following up to 4 dpf. Un-injected mutant embryos did not survive after 3 dpf. In future experiment, it is necessary to investigate whether the lack of *psmc2* mimic the dorsal motor axon phenotype, and whether the mutation in *psmc2* is associated with embryonic lethality. This can be done by using either

morpholino to knock-down *psmc2* (Imai et al. 2010) or CRISPR/Cas9 to knock-out *psmc2* gene. In addition, studied have shown that UPS plays a role in neurodegenerative diseases (Ciechanover & Kwon 2015; Kwon et al. 2013; Burnett et al. 2009; Tashiro et al. 2012). One could speculate that the finding may give not only new insights into the role of UPS in motor neuron and axon development, but also the link between UPS and neurodegenerative disease.

Meanwhile, confirming the causative mutation of the #151mutants in future experiments may provide opportunities to identify key molecular players in the development of motor neurons. To prioritize a candidate gene, I looked at the SNP that results in amino acid change and leads to altered protein product, as the change in protein function may influence the traits of interest. In addition, a gene is prioritized for further confirmation based on its relevance to the biological process underlying the phenotype of interest by reviewing through the literature to find whether there were previous studies connecting the gene with similar traits and signalling pathways (Kwon & Goate 2000). In #151 mutants, I first investigate *rbbp*4 as a potential phenotype causative gene. The single base substitution in *rbbp4-201* transcript result in a pre-mature stop in coding sequence, and study has shown that *rbbp4* knock-down reduces blastema progenitor cell proliferation and the re-differentiation of their daughter cells during the fin regeneration in zebrafish (Pfefferli et al. 2014). However, a gain-of-function experiment by overexpressing *rbbp4-201* in the mutants did not rescue the islet-1:GFP motor neuron phenotype. As discussed in Chapter 3, this could be due to that *rppb4* is not the gene responsible for #151 mutant phenotype, or the artificial overexpression of the target gene does not correspondent to the time and location of the endogenous mRNA expression. A loss-of-function experiment is necessary to test whether the lack of *rbbp4-201* leads to fewer islet-1:GPF motor neurons. In addition, a nonsense mutation was also present in the transcript ENSDART00000067165, coding for Ankmy2 (ankyrin repeat and MYND domain containing 2) protein. I have confirmed the existence of the nucleotide substitution in *ankmy2b* in #151 mutants by sequencing a fragment of DNA containing the mutation site. A study in mouse showed that a*nkmy2* plays a role in regulating Shh signalling (Saita et al. 2014). Therefore, *ankmy2* is another

potential causative gene for further confirmation, and similarly, by using a loss-of-function approach to either knock-down/knock-out the gene and a gain-of-function experiment to rescue the phenotype.

5.2 Regenerative neurogenesis larval zebrafish

In mammals, loss of motor neurons and axon connections in motor neuron diseases and spinal cord injuries are irreversible due to their inability to repair. Zebrafish, one the other hand, possess an excellent capacity to regenerate neuronal cells and restore locomotor function. In this part of the study, I showed that in the established larval zebrafish model, endogenous progenitor cells were recruited to give rise to new motor neurons at the expense of oligodendrocytes in response to an injury. The larval model allows us to compare the similarities and differences between larval and adult regeneration for their progenitor potential, how different cell populations are activated, and to understand the identity of progenitor cells that give rise to new neurons at different stages. It also expands our experimental possibilities in many aspects. External development and permeability to small molecules facilitate target drug screening in zebrafish larvae. They are genetically tractable as transgene can be expressed in specific cell types of interest and visualised in the intact transparent larva. This makes it possible to study the mechanisms involved in the activation of progenitor cells, differentiation and specification of regenerated neurons.

In the adult spinal cord, neurogenesis is rare across species, including primates, rodents, birds and fish (Alunni & Bally-Cuif 2016). A consequence of the spinal cord injury is the sudden loss of motor neurons and disconnection of axons. As part of the repair process, replenishing new motor neurons and a re-connection of axons may be necessary. This requires endogenous progenitors to exit from their quiescent stage to undergo active neurogenesis and cell proliferation. In the lesioned spinal cord of adult zebrafish, newly regenerated motor neurons are derived from the *olig2*-expressing ependymal radial glial cells (ERGs) that line in the central canal of the spinal cord (Reimer et al. 2008; Reimer et al. 2009). Transcription factors that define the progenitor zones in the neural tube of embryos, such as Olig2, Shh, Pax6 and Nkx6.1, were expressed in the ventrolateral ERGs around the central canal,

indicating that these ERGs are equivalent to pMN progenitor cells in the neural tube that give rise to motor neurons during the development (Reimer et al. 2009). Ependymal cell activation was also observed in mammals following the spinal cord injury, however, the newly generated ependymal cells mainly give rise to astrocytes that migrate to the lesion site to form the glia scar and prevent axon regeneration (Panayiotou & Malas 2013). Current interventions for the treatment of the spinal cord injury are focusing on protecting the surviving cells from secondary damage, replacing injured or dead cells, and promoting axon regeneration from the glial scar formed by reactive astrocytes that plays a crucial part in the regeneration failure. To achieve these goals requires to develop economical and powerful model organisms that could be used for real-time imaging of pathogenesis and to provide gene or drug target information. Similar to the adult zebrafish, neuronal replacement, axonal outgrowth and functional recovery also occurred in larval zebrafish. However, the neural repair is quicker as it happened within 48 hours as opposed to 6 weeks in adults. In this regard, larval zebrafish are amenable to study the intrinsic and extrinsic signals that control regeneration *in vivo* and to identify how the regenerated neurons integrate into the CNS circuit to restore neural function. The clinical relevance of the larval regeneration model is that it can be used for screening drugs in living animals and genetic manipulations that are not feasible in models such as mouse. Early drug screens for clinical use involves the identification of a protein or pathways that may result in a therapeutic effect, validation of the discovered development candidate in experimental models, and the screening of compounds that are likely to have activity at the target protein (Hughes et al. 2011). The transparency of zebrafish larvae enables small molecule screens that assay compound libraries against disease targets to identify drug-like compounds *in vivo*. The VAST (Vertebrate Automated Screening Technology) BioImager system, which is designed for high-resolution imaging of 2-7 dpf zebrafish larvae automatically, can be used for chemical screening in a more efficient manner to identify “hit” molecules that may have an effect during successful motor neuron and axon regeneration. Zebrafish larvae also allow genetic manipulations such as lineage tracing, transgenesis, and CRISPR/Cas9 mediated gene knock-out/knock-in in the whole animal organism, and

to perform direct observation to investigate the factors that regulate cell-fate decision during the regeneration.

5.3 Concluding remarks and future directions

In this thesis, I presented two pieces of work to study the role of developmental cues in motor neurogenesis and regeneration. I conducted an ENU-mutagenesis screen in searching for essential genes for the generation of motor neurons and correct pathfinding of their motor axons. I discovered mutants with motor neuron and motor axon defects, carried out phenotypic characterization and started candidate gene investigation. I also showed that zebrafish larvae can be used as a model for studying regeneration of motor neurons, and other cell types in the spinal cord. Genes identified from the screen can be used to dissect signals and pathways involved in the differentiation of motor neurons and the outgrowth of motor axons into their target muscle fibres. The findings can also be applied to lesioned zebrafish larvae to investigate the genes' potential in the promotion of the motor neuron regeneration. More importantly, identified mutants and the larval regeneration model offer opportunities for *in vivo* chemical compound screen for potential drugs that may ultimately lead to the identification of new therapeutic treatment for motor neuron disease and spinal cord injury.

Appendices

Appendix 1. Candidate gene list for #249 mutant line

Gene Name	Associated Transcript IDs	Position Chr4	Old codon/ New codon	Effect
psmc2	ENSDART00000019647	13992419	Caa/Taa	STOP
nell2b	ENSDART00000091151	13377119	aTc/aAc	Missense
	ENSDART00000133325	13377119	aTc/aAc	Missense
CCDC87	ENSDART00000067165	12681834	aAg/aGg	Missense
	ENSDART00000067165	12681750	aTc/aCc	Missense
exoc4	ENSDART00000101619	14724890	Cgc/Tgc	Missense
	ENSDART00000101619	14724862	ttA/ttT	Missense
	ENSDART00000101619	14724854	Cct/Tct	Missense
mdm1	ENSDART00000102010	12622355	gAa/gGa	Missense
	ENSDART00000132971	12622355	gAa/gGa	Missense
si:dkey-14k9.3	ENSDART00000137829	13961678	atC/atG	Missense
	ENSDART00000067036	13961678	atC/atG	Missense
plxnb2a	ENSDART00000048821	13542963	atT/atG	Missense
plxnb2	ENSDART00000145737	13711351	Aac/Tac	Missense
	ENSDART00000145737	13711341	aAt/aGt	Missense
	ENSDART00000145737	13711335	gCc/gTc	Missense
	ENSDART00000145737	13711326	aGg/aAg	Missense
	ENSDART00000067029	13711351	Aac/Tac	Missense
	ENSDART00000067029	13711341	aAt/aGt	Missense
	ENSDART00000067029	13711335	gCc/gTc	Missense
	ENSDART00000067029	13711326	aGg/aAg	Missense
	ENSDART00000145737	13711347	tCc/tTc	Missense
	ENSDART00000067029	13711347	tCc/tTc	Missense
	ENSDART00000145737	13711359	tCa/tTa	Missense
	ENSDART00000067029	13711359	tCa/tTa	Missense
	ENSDART00000145737	13711210	tAt/tTt	Missense
	ENSDART00000067029	13711210	tAt/tTt	Missense
	ENSDART00000145737	13712253	gAg/gTg	Missense

	ENSDART00000145737	13712284	Ggg/Agg	Missense
	ENSDART00000145737	13712243	agA/agT	Missense
	ENSDART00000145737	13712238	gAc/gTc	Missense
	ENSDART00000145737	13712237	gaC/gaA	Missense
	ENSDART00000114977	13703060	Ggt/Agt	Missense
	ENSDART00000145737	13711129	gGg/gCg	Missense
	ENSDART00000067029	13711129	gGg/gCg	Missense
	ENSDART00000145737	13711632	aAc/aGc	Missense
	ENSDART00000067029	13711632	aAc/aGc	Missense
	ENSDART00000145737	13711636	Ctc/Atc	Missense
	ENSDART00000067029	13711636	Ctc/Atc	Missense
	ENSDART00000145737	13712182	Acc/Gcc	Missense
	ENSDART00000145737	13712344	Atc/Gtc	Missense

Appendix 2. Candidate gene list for #151 mutant line

Gene Name	Associated Transcript IDs	Position Chr19	Old codon/ New codon	Effect
rbbp4	ENSDART00000130326	32244010	tCa/tAa	STOP
ankmy2b	ENSDART00000067165	32299687	tGg/tAg	STOP
	ENSDART00000143494	32290727	Ggt/Agt	Missense
	ENSDART00000143494	32293002	Gcc/Acc	Missense
	ENSDART00000143494	32290700	Gat/Aat	Missense
sync	ENSDART00000052169	32239570	gaG/gaT	Missense
	ENSDART00000134645	32239341	aGg/aAg	Missense
	ENSDART00000052169	32239341	aGg/aAg	Missense
	ENSDART00000134645	32238882	gAg/gGg	Missense
	ENSDART00000052169	32238882	gAg/gGg	Missense
meox2b	ENSDART00000088618	32429268	Cct/Tct	Missense
eif3i	ENSDART00000005119	31075389	gTc/gAc	Missense
abcf1	ENSDART00000048977	34724890	gaT/gaG	Missense
	ENSDART00000135128	31732354	Ctt/Ttt	Missense
	ENSDART00000135128	31740764	Tcc/Acc	Missense

bag6l	ENSDART00000135128	31745378	Cct/Tct	Missense
	ENSDART00000135128	31752111	gGc/gAc	Missense
	ENSDART00000088760	31752111	gGc/gAc	Missense
	ENSDART00000135128	31755649	gaA/gaC	Missense
	ENSDART00000088760	31755649	gaA/gaC	Missense
si:ch211-194e15.5	ENSDART00000137829	32142582	tGa/tAa	Silence
	ENSDART00000088573	32143584	AcT/aGt	Missense
	ENSDART00000137633	32143584	AcT/aGt	Missense
	ENSDART00000088573	32143946	atG/atT	Missense
	ENSDART00000137633	32143946	atG/atT	Missense
scin	ENSDART00000046609	32598253	gAa/gTa	Missense
si:dkeyp-120h9.1	ENSDART00000128391	33008206	Tct/Gct	Missense
	ENSDART00000103636	33008206	Tct/Gct	Missense
sostdc1b	ENSDART00000145971	32307181	caC/caA	Missense
	ENSDART00000145971	32307181	caC/caA	Missense
pag1	ENSDART00000078268	33308347	Gcc/Acc	Missense
	ENSDART00000078268	33319623	gCt/gTt	Missense
	ENSDART00000134934	33319623	gCt/gTt	Missense
C19H6orf136	ENSDART00000073704	31703209	Ctg/Atg	Missense
	ENSDART00000129742	31703209	Ctg/Atg	Missense
	ENSDART00000073704	31703138	aGa/aCa	Missense
	ENSDART00000129742	31703138	aGa/aCa	Missense
FAM8A1 (2 of 3)	ENSDART00000022667	33451722	aGg/aAg	Missense
	ENSDART00000022667	33448918	Gtc/Atc	Missense

Abbreviations

A	
AC	anterior commissure
AO	Acridine orange
AMPA	alpha-amino-3-hydroxy-5-methyl-4-isoxazole propionic acid
ALA52	Delta-aminolevulinate synthase 2
ALS	Amyotrophic lateral sclerosis
B	
bHLH	Basic helix-loop-helix
BSA	Bulked segregant analysis
βME	Beta-mercaptoethanol
BrdU	5–bromo–2′–deoxyuridine
BMP	Bone Morphogenetic Protein
C	
Calca	Calcitonin
Chodl	Chondrolectin
ChAT	Choline acetyltransferase
CNS	Central nervous system
CoPA	Commissural ascending primary interneurons
CaP	caudal primary
D	
des	deadly seven
dmd	dystrophy
dpf	days post-fertilization
dpi	days post-injury
DoLA	dorsal longitudinal ascending neuron
DVDT	dorsal-ventral diencephalic tract
E	

EdU	5-Ethynyl-2´-deoxyuridine
ENU	N-ethyl-N-nitrosourea
EMS	Ethylmethanesulfonate
ERGs	Ependymo-radial glial cells
EtBr	Ethidium bromide
F	
FF-subtype	fast-switch, fatigable
5-HT	Serotonin
5-HTP	5-hydroxytryptophan
G	
GFP	Green fluorescent protein
Gli3	Glioma-associated oncogene homolog 3
gDNA	genomic DNA
H	
HD	Homeodomain
hpf	hours post fertilization
HM	Horizontal myoseptum
HRP	horseradish peroxidase
I	
IHC	Immunohistochemistry
M	
Mag	Myelin-associated glycoprotein
mbpa	Myelin basic protein a
MiP	middle primary
MND	Motor neuron disease
Mnx1	Motor neuron and pancreas homeobox 1
MTZ	Metronidazole
mRNAs	Messenger RNAs
MOs	Morpholino oligonucleotides

N	
Neurog2	Neurogenin2
NGS	Next Generation Sequencing
NMD	nonsense-mediated RNA decay
NTR	Nitroreductase
NuRD	Nucleosome Remodeling and Deacetylase complex
O	
Omgp	Oligodendrocyte myelin glycoprotein
OH^8dG	8-hydroxy-2'-deoxyguanosine
OPCs	Oligodendrocytes precursor cells
OLPs	Oligodendrocyte progenitors
P	
PD	Parkinson's disease
PDE	phosphodiesterase
PDE5	phosphodiesterase 5
PC	posterior commissure
PCR	Polymerase chain reaction
PH3	Phospho-Histone H3
pMN	Motor neuron progenitor
POC	post-optic commissure
psmc2	proteasome 26S subunit, ATPase 2
ptc2	patched 2
R	
RA	Retinoic Acid
RB	Rohon-Beard
rbbp4	Retinoblastoma-binding protein 4
RoP	rostral primary
S	
Sau	sauternes

Sap	*sapje*
SC	Spinal cord
SCI	Spinal cord injury
SGZ	subgranular zone
shh	Sonic hedgehog signalling
SMA	Spinal muscular atrophy
SMN1	Survival of motor neuron 1
smo	smoothened
SNP	Single nucleotide polymorphism
SOD1	Superoxide dismutase 1
SVZ	subventricular zone
T	
tac1	tachykinin 1
TdT	Terminal deoxynucleotidyl transferase
TH	Tyrosine hydroxylase
TUNEL	Terminal deoxynucleotidyl transferase dUTP nick end labelling assay
U	
Ub	ubiquitin
UPS	ubiquitin proteasome system
V	
VeLD	ventral longitudinal interneuron
W	
WGS	Whole genome sequencing
wdo	where's waldo

References

Abrams, J.M. et al., 1993. Programmed death during Drosophila embryogenesis. *Development*, 117, pp.29–43.

Acevedo-Arozena, A. et al., 2008. ENU mutagenesis, a way forward to understand gene function. *Annual review of genomics and human genetics*, 9, pp.49–69.

Alibardi, L. & Toni, M., 2005. Wound keratins in the regenerating epidermis of lizard suggest that the wound reaction is similar in the tail and limb. *Journal of Experimental Zoology Part A: Comparative Experimental Biology*, 303A(10), pp.845–860.

Allan, D.W. & Thor, S., 2003. Together at Last: bHLH and LIM-HD regulators cooperate to specify motor neurons. *Neuron*, 38(5), pp.675–677.

Almeida, R.G. et al., 2011. Individual axons regulate the myelinating potential of single oligodendrocytes in vivo. *Development*, 138(20), pp.4443–4450. Available at: http://www.ncbi.nlm.nih.gov/pubmed/21880787.

Alunni, A. & Bally-Cuif, L., 2016. A comparative view of regenerative neurogenesis in vertebrates. *Development (Cambridge, England)*, 143(5), pp.741–53. Available at: http://www.pubmedcentral.nih.gov/articlerender.fcgi?artid=4813331&tool=pmcentrez&rendertype=abstract.

Alvarado, A.S. & Tsonis, P.A., 2006. Bridging the regeneration gap : genetic insights from diverse animal models. *NATURE REVIEWS GENETICS*, 7(November), pp.873–884.

Anderson, D.J., 1995. A molecular switch for the neuron-glia developmental decision. *Neuron*, 15(6), pp.1219–1222.

Appel, B. et al., 1995. Motoneuron fate specification revealed by patterned LIM homeobox gene expression in embryonic zebrafish. *Development (Cambridge, England)*, 121(12), pp.4117–4125. Available at: http://dev.biologists.org/content/121/12/4117%5Cnhttp://dev.biologists.org/content/121/12/4117.full.pdf%5Cnhttp://www.ncbi.nlm.nih.gov/pubmed/8575312.

Appel, B., Givan, L.A. & Eisen, J.S., 2001. Delta-Notch signaling and lateral inhibition in zebrafish spinal cord development. *BMC developmental biology*, 1,

p.13.

Araya, C. et al., 2016. Coordinating cell and tissue behavior during zebrafish neural tube morphogenesis. *Developmental Dynamics*, 245(3), pp.197–208.

Argmann, C. a, Dierich, A. & Auwerx, J., 2006. Uses of forward and reverse genetics in mice to study gene function. , Chapter 29, p.Unit 29A.1. Available at: http://eutils.ncbi.nlm.nih.gov/entrez/eutils/elink.fcgi?dbfrom=pubmed&id=18265381&retmode=ref&cmd=prlinks%5Cnpapers3://publication/doi/10.1002/0471142727.mb29a01s73.

Arvidsson, A. et al., 2002. Neuronal replacement from endogenous precursors in the adult brain after stroke. *Nat Med*, 8(9), pp.963–970. Available at: http://www.ncbi.nlm.nih.gov/entrez/query.fcgi?cmd=Retrieve&db=PubMed&dopt=Citation&list_uids=12692541.

Babin, P.J., Goizet, C. & Raldua, D., 2014. Zebrafish models of human motor neuron diseases: advantages and limitations. *Progress in neurobiology*, 118, pp.36–58.

Babin, P.J., Goizet, C. & Raldúa, D., 2014. Zebrafish models of human motor neuron diseases: Advantages and limitations. *Progress in Neurobiology*, 118, pp.36–58.

Baguna, J., 2001. Regeneration Model Systems : Invertebrate Epimorphic. *ENCYCLOPEDIA OF LIFE SCIENCES*.

Balling, R., 2001. ENU mutagenesis: analyzing gene function in mice. *Annual review of genomics and human genetics*, 2, pp.463–492.

Barnabé-Heider, F. et al., 2010. Origin of new glial cells in intact and injured adult spinal cord. *Cell Stem Cell*, 7(4), pp.470–482.

Barnes, M.R. & Gray, I.C., 2003. *Amino Acid Properties and Consequences of Substitutions* M. R. Barnes & I. C. Gray, eds.,

Barrallo-Gimeno, A. et al., 2004. Neural crest survival and differentiation in zebrafish depends on mont blanc/tfap2a gene function. *Development (Cambridge, England)*, 131, pp.1463–1477.

Barreiro-Iglesias, A. et al., 2015. Serotonin Promotes Development and Regeneration of Spinal Motor Neurons in Zebrafish. *Cell Reports*, 13(5), pp.924–932.

Barres, B.A. & Raff, M.C., 1999. Axonal Control of Oligodendrocyte Development. , 147(6), pp.1123–1128.

Bassett, D.I. & Currie, P.D., 2003. The zebrafish as a model for muscular dystrophy

and congenital myopathy. *Human molecular genetics*, 12 Spec No(2), pp.R265–R270.

Beattie, M.S. et al., 1986. Metamorphosis Alters the Response to Spinal Cord Transection in Xenopus Iaevis Frogs. *Journal of Neurobiology*, 21(7), pp.1108–1122.

Beck, C.W., Izpisu, J.C. & Christen, B., 2009. Beyond Early Development : Xenopus as an Emerging Model for the Study of Regenerative Mechanisms. *DEVELOPMENTAL DYNAMICS*, 238(March), pp.1226–1248.

Becker, C.G. et al., 2004. L1.1 Is Involved in Spinal Cord Regeneration in Adult Zebrafish. *Journal of Neuroscience*, 24(36), pp.7837–7842. Available at: http://www.jneurosci.org/cgi/doi/10.1523/JNEUROSCI.2420-04.2004.

Becker, C.G. & Becker, T., 2015. Neuronal Regeneration from Ependymo-Radial Glial Cells: Cook, Little Pot, Cook! *Developmental Cell*, 32(4), pp.516–527. Available at: http://dx.doi.org/10.1016/j.devcel.2015.01.001.

Becker, T. et al., 1997. Axonal regrowth after spinal cord transection in adult zebrafish. *Journal of Comparative Neurology*, 377(4), pp.577–595.

Bedford, L. et al., 2008. Depletion of 26S Proteasomes in Mouse Brain Neurons Causes Neurodegeneration and Lewy-Like Inclusions Resembling Human Pale Bodies. , 28(33), pp.8189–8198.

Bely, A.E. & Nyberg, K.G., 2010. Evolution of animal regeneration: re-emergence of a field. *Trends in Ecology and Evolution*, 25(3), pp.161–170.

Bhatt, D.H. et al., 2007. *Functional Regeneration in the Larval Zebrafish Spinal Cord*, Available at: http://doi.wiley.com/10.1002/9783527610365.ch9.

Bonanomi, D. & Pfaff, S.L., 2010. Motor axon pathfinding. *Cold Spring Harbor perspectives in biology*, 2(3), p.a001735.

Van Den Bosch, L. et al., 2000. Ca -permeable AMPA receptors and selective vulnerability of motor neurons. *Journal of the Neurological Sciences*, 180, pp.29–34. Available at: www.elsevier.com.

Bowne, S.J. et al., 2008. Why Do Mutations in the Ubiquitously Expressed Housekeeping Gene IMPDH1 Cause Retina-Specific Photoreceptor Degeneration? *Invest Ophthalmol Vis Sci*, 47(9), pp.3754–3765.

Briona, L.K. & Dorsky, R.I., 2014. Radial glial progenitors repair the zebrafish

spinal cord following transection. *Experimental Neurology*, 256, pp.81–92. Available at: http://dx.doi.org/10.1016/j.expneurol.2014.03.017.

Briscoe, J. & Novitch, B.G., 2008. Regulatory pathways linking progenitor patterning, cell fates and neurogenesis in the ventral neural tube. *Philosophical Transactions of the Royal Society B: Biological Sciences*, 363(1489), pp.57–70. Available at: http://rstb.royalsocietypublishing.org/cgi/doi/10.1098/rstb.2006.2012.

Brogna, S. & Wen, J., 2009. Nonsense-mediated mRNA decay (NMD) mechanisms. *Nature structural & molecular biology*, 16(2), pp.107–13. Available at: http://dx.doi.org/10.1038/nsmb.1550.

Burnett, B.G. et al., 2009. Regulation of SMN protein stability. *Molecular and cellular biology*, 29(5), pp.1107–15. Available at: http://www.pubmedcentral.nih.gov/articlerender.fcgi?artid=2643817&tool=pmcentrez&rendertype=abstract.

Burton, P.M. & Finnerty, J.R., 2009. Conserved and novel gene expression between regeneration and asexual fission in Nematostella vectensis. *Development Genes and Evolution*, 219(2), pp.79–87.

Carrier, L. et al., 2010. The ubiquitin-proteasome system and nonsense- mediated mRNA decay in hypertrophic cardiomyopathy. *Cardiovascular Research*, 85, pp.330–338.

Castro, D.S. et al., 2011. A novel function of the proneural factor Ascl1 in progenitor proliferation identified by genome-wide characterization of its targets. *GENES & DEVELOPMENT*, 25, pp.930–945.

Chablais, F. & Jaźwińska, A., 2012. Induction of Myocardial Infarction in Adult Zebrafish Using Cryoinjury. *Journal of Visualized Experiments*, (62), pp.2–6.

Chen, W., Burgess, S. & Hopkins, N., 2001. Analysis of the zebrafish smoothened mutant reveals conserved and divergent functions of hedgehog activity. *Development (Cambridge, England)*, 128, pp.2385–2396.

Cheriyan, T. et al., 2014. Spinal cord injury models: a review. *Spinal Cord*, 52(8), pp.588–595. Available at: http://www.ncbi.nlm.nih.gov/pubmed/24912546%5Cnhttp://0-search.ebscohost.com.library.ucc.ie/login.aspx?direct=true&db=s3h&AN=9731

6221&site=ehost-live.

Chernoff, E.A.G., 1996. Spinal cord regeneration: A phenomenon unique to urodeles? *International Journal of Developmental Biology*, 40(4), pp.823–831.

Chernoff, E.A.G. et al., 2003. Urodele spinal cord regeneration and related processes. *Developmental Dynamics*, 226(2), pp.295–307.

Cheroni, C. et al., 2005. Accumulation of human SOD1 and ubiquitinated deposits in the spinal cord of SOD1G93A mice during motor neuron disease progression correlates with a decrease of proteasome. *Neurobiology of Disease*, 18, pp.509–522.

Chitnis, a B. & Kuwada, J.Y., 1990. Axonogenesis in the brain of zebrafish embryos. *The Journal of neuroscience : the official journal of the Society for Neuroscience*, 10(6), pp.1892–1905.

Ciechanover, A. & Kwon, Y.T., 2015. Degradation of misfolded proteins in neurodegenerative diseases: therapeutic targets and strategies. *Experimental & Molecular Medicine*, 47(3), p.e147. Available at: http://www.pubmedcentral.nih.gov/articlerender.fcgi?artid=4351408&tool=pmcentrez&rendertype=abstract.

Clark, K.J., Voytas, D.F. & Ekker, S.C., 2011. A TALE of Two Nucleases: Gene Targeting for the Masses? *Zebrafish*, 8(3), pp.147–149. Available at: http://www.liebertonline.com/doi/abs/10.1089/zeb.2011.9993.

Conradi, S. & Ronnevi, L.O., 1993. Selective vulnerability of alpha motor neurons in ALS: Relation to autoantibodies toward acetylcholinesterase (AChE) in ALS patients. *Brain Research Bulletin*, 30(3–4), pp.369–371.

Curado, S., Stainier, D.Y.R. & Anderson, R.M., 2008. Nitroreductase-mediated cell/tissue ablation in zebrafish: a spatially and temporally controlled ablation method with applications in developmental and regeneration studies Silvia. *Nat Protoc*, 3(6), pp.948–954.

Davis-Dusenbery, B.N. et al., 2014. How to make spinal motor neurons. *Development (Cambridge, England)*, 141(3), pp.491–501. Available at: http://www.ncbi.nlm.nih.gov/pubmed/24449832.

Detrich, H.W., Westerfield, M. & Zon, L.I., 1999. *The Zebrafish: Genetics and Genomics*, San Diego: Academic Press 60: 407.

Devoto, S.H. et al., 1996. Identification of separate slow and fast muscle precursor cells in vivo , prior to somite formation. , 3380, pp.3371–3380.

Dias, T.B. et al., 2012. Notch signaling controls generation of motor neurons in the lesioned spinal cord of adult zebrafish. *The Journal of neuroscience : the official journal of the Society for Neuroscience*, 32(9), pp.3245–3252.

Dodd, A. et al., 2000. Zebrafish: bridging the gap between development and disease. *Human molecular genetics*, 9(16), pp.2443–2449.

Dooley, K. & Zon, L.I., 2000. Zebrafish: a model system for the study of human disease. *Current opinion in genetics & development*, 10(3), pp.252–256.

Driever, W. et al., 1996. A genetic screen for mutations affecting embryogenesis in zebrafish. *Development (Cambridge, England)*, 123, pp.37–46.

Echeverri, K. & Tanaka, E.M., 2002. Ectoderm to mesoderm lineage switching during axolotl tail regeneration. *Science*, 298(5600), pp.1993–6. Available at: http://www.ncbi.nlm.nih.gov/pubmed/12471259.

van Eeden, F.J. et al., 1996. Mutations affecting somite formation and patterning in the zebrafish, Danio rerio. *Development (Cambridge, England)*, 123, pp.153–164.

Eisen, J.S., 1994. Development of motoneuronal phenotype. *Annu. Rev. Neurosci*, pp.1–30.

Eisen, J.S., Paul Z. Myers & Westerfield, M., 1986. Pathway selection by growth cones of identified motoneurons in live zebra fish embryos. *Nature Publishing Group*.

Eisen, J.S. & Pike, S.H., 1991. The spf-1 Mutation Alters Segmental Arrangement and Axonal Development of Identified Neurons in the Spinal Cord of the Embryonic Zebrafish. , 6, pp.767–776.

Eklöf-Ljunggren, E. et al., 2012. Origin of excitation underlying locomotion in the spinal circuit of zebrafish. *Proceedings of the National Academy of Sciences of the United States of America*, 109(14), pp.5511–5516. Available at: http://www.pnas.org/content/109/14/5511.full.

Evans, A.E. et al., 2012. Molecular regulation of striatal development: a review. *Anat Res Int*, 2012(January), p.106529. Available at: http://www.ncbi.nlm.nih.gov/pubmed/22567304.

Fausett, B. V, Gumerson, J.D. & Goldman, D., 2008. The Proneural Basic Helix-Loop-Helix Gene Ascl1a Is Required for Retina Regeneration. *Journal of Neuroscience*, 28(5), pp.1109–1117.

Feldner, J. et al., 2007. PlexinA3 Restricts Spinal Exit Points and Branching of Trunk Motor Nerves in Embryonic Zebrafish. *The Journal of Neuroscience*, 27(18), pp.4978–4983. Available at: http://www.jneurosci.org/content/27/18/4978%5Cnhttp://www.jneurosci.org/content/27/18/4978.full.pdf%5Cnhttp://www.jneurosci.org/content/27/18/4978.long%5Cnhttp://www.ncbi.nlm.nih.gov/pubmed/17475806.

Ferrante, R.J. et al., 1997. Evidence of increased oxidative damage in both sporadic and familial amyotrophic lateral sclerosis. *Journal of neurochemistry*, 69, pp.2064–2074.

Filbin, M.T., 2003. Myelin-associated inhibitors of axonal regeneration in the adult mammalian CNS. *Nature reviews. Neuroscience*, 4(9), pp.703–13. Available at: http://www.ncbi.nlm.nih.gov/pubmed/12951563.

Fischer, A.J. & Reh, T.A., 2001. Müller glia are a potential source of neural regeneration in the postnatal chicken retina. *Nature Neuroscience*, 4, pp.247–252.

Francius, C. & Clotman, F., 2014. Generating spinal motor neuron diversity: a long quest for neuronal identity. *Cellular and molecular life sciences : CMLS*, 71(5), pp.813–829.

Gabrièle Piaton, Gould, R.M. & Lubetzki, C., 2010. Oligodendrocyte-axon interactions during development. *Journal of neurochemistry*, pp.1243–1260.

Gaete, M. et al., 2012. Spinal cord regeneration in Xenopus tadpoles proceeds through activation of Sox2-positive cells. *Neural Development*, 7(13), pp.1–17.

Gilbert, S.F., 2000. *Developmental Biology* 6th ed., Sunderland (MA): Sinauer Associates. Available at: http://www.ncbi.nlm.nih.gov/books/NBK10034/.

GrandPré, T. et al., 2000. Identification of the Nogo inhibitor of axon regeneration as a Reticulon protein. *Nature*, 403(6768), pp.439–444.

Grasl-Kraupp, B. et al., 1995. In situ detection of fragmented DNA (tunel assay) fails to discriminate among apoptosis, necrosis, and autolytic cell death: A cautionary note. *Hepatology*, 21(5), pp.1465–1468.

Griffiths, A.J.F. et al., 2005. *An Introduction to Genetic Analysis* 8th Editio., W.H.Freeman & Co Ltd.

Griffiths, I. et al., 1998. Axonal Swellings and Degeneration in Mice Lacking the Major Proteolipid of Myelin. *Science*, 280.

Haffter, P. et al., 1996. The identification of genes with unique and essential functions in the development of the zebrafish, Danio rerio. *Development*, 123, pp.1–36. Available at: http://dev.biologists.org/content/123/1/1.full.pdf.

Haffter, P. & Nusslein-Volhard, C., 1996. Large scale genetics in a small vertebrate, the zebrafish. *The International journal of developmental biology*, 40(1), pp.221–227.

Hamilton, A.M. & Zito, K., 2013. Breaking it down: the ubiquitin proteasome system in neuronal morphogenesis. *Neural plasticity*, 2013, p.196848. Available at: http://www.pubmedcentral.nih.gov/articlerender.fcgi?artid=3586504&tool=pmcentrez&rendertype=abstract.

Hardy, D. et al., 2016. Comparative Study of Injury Models for Studying Muscle Regeneration in Mice. *PloS one*, 11(1), p.e0147198. Available at: http://www.pubmedcentral.nih.gov/articlerender.fcgi?artid=4726569&tool=pmcentrez&rendertype=abstract.

Henke, K., Bowen, M.E. & Harris, M.P., 2013. *Identification of mutations in zebrafish using next-generation sequencing.*, Available at: http://www.ncbi.nlm.nih.gov/pubmed/24510885.

Henry, J.J. et al., 2008. *Animal Models in Eye Research*,

Higashijima, S., Hotta, Y. & Okamoto, H., 2000. Visualization of cranial motor neurons in live transgenic zebrafish expressing green fluorescent protein under the control of the islet-1 promoter/enhancer. *J Neurosci*, 20(1), pp.206–218. Available at: http://www.ncbi.nlm.nih.gov/pubmed/10627598.

Hitchcock, P.F. et al., 1996. Antibodies against Pax6 lmmunostain Amacrine and Ganglion Cells and Neuronal Progenitors , but not Rod Precursors , in the Normal and Regenerating Retina of the Goldfish. *Developmental Neurobiology*, 29(3), pp.399–413.

Hjorth, J. & Key, B., 2002. Development of axon pathways in the zebrafish central nervous system. *International Journal of Developmental Biology*, 46(4 SPEC.),

pp.609–619.

Hook, B. & Schagat, T., 2011. Integrating Functional Proteomics Techniques to Rapidly Isolate and Characterize the Human Proteasome. *Promega Corporation Web site*. Available at: http://www.promega.co.uk/resources/pubhub/functional-proteomics-techniques-to-isolate-and-characterize-the-human-proteasome/ Updated 2011.

Hsieh, P.C.H. et al., 2007. Evidence from a genetic fate-mapping study that stem cells refresh adult mammalian cardiomyocytes after injury. *Nature Medicine*, 13(8), pp.970–974.

Hughes, J.P. et al., 2011. Principles of early drug discovery. *British Journal of Pharmacology*, 162(6), pp.1239–1249.

Imai, F. et al., 2010. The ubiquitin proteasome system is required for cell proliferation of the lens epithelium and for differentiation of lens fiber cells in zebrafish. *Development (Cambridge, England)*, 137(19), pp.3257–3268. Available at: http://www.ncbi.nlm.nih.gov/pubmed/20724448.

Inoue, A. et al., 1994. Developmental regulation of islet-1 mRNA expression during neuronal differentiation in embryonic zebrafish. *Developmental dynamics : an official publication of the American Association of Anatomists*, 199(1), pp.1–11.

Jansen, A.H.P., Reits, E.A.J. & Hol, E.M., 2014. The ubiquitin proteasome system in glia and its role in neurodegenerative diseases. *Frontiers in molecular neuroscience*, 7(August), p.73. Available at: http://www.pubmedcentral.nih.gov/articlerender.fcgi?artid=4126450&tool=pmcentrez&rendertype=abstract.

Jessell, T.M., 2000. Neuronal specification in the spinal cord: inductive signals and transcriptional codes. *Nature reviews. Genetics*, 1(1), pp.20–29.

Jopling, C. et al., 2010. Zebrafish heart regeneration occurs by cardiomyocyte dedifferentiation and proliferation. *Nature*, 646, pp.606–609. Available at: http://www.nature.com/nature/journal/v464/n7288/full/nature08899.html.

Jopling, C., Boue, S. & Izpisua Belmonte, J.C., 2011. Dedifferentiation, transdifferentiation and reprogramming: three routes to regeneration. *Nature reviews. Molecular cell biology*, 12(2), pp.79–89. Available at: http://www.ncbi.nlm.nih.gov/pubmed/21252997.

Kaiser, C.L. et al., 2009. EdU Labeling Detects Proliferating Cells in the Regenerating Avian Cochlea. , 119(9), pp.1770–1775.

Kang, J.-S. & Krauss, R.S., 2010. Muscle stem cells in developmental and regenerative myogenesis. *Current Opinion in Clinical Nutrition & Metabolic Care*, 13(3), pp.243–248.

Karl, M.O. et al., 2008. Stimulation of neural regeneration in the mouse retina. *PNAS*, 105(49).

Kawahara, G. et al., 2011. Drug screening in a zebrafish model of Duchenne muscular dystrophy. *Proceedings of the National Academy of Sciences of the United States of America*, 108, pp.5331–5336.

Kawakami, Y. et al., 2006. Wnt/β-catenin signaling regulates vertebrate limb regeneration. *GENES & DEVELOPMENT*, 20(23), pp.3232–3237.

Kazakova, N. et al., 2006. A screen for mutations in zebrafish that affect myelin gene expression in Schwann cells and oligodendrocytes. *Developmental Biology*, 297(1), pp.1–13.

Kessaris, N., Pringle, N. & Richardson, W.D., 2001. Ventral neurogenesis and the neuron-glial switch. *Neuron*, 31(5), pp.677–680.

Key, B., 2016. *Regenerative Medicine - from Protocol to Patient*, Available at: http://link.springer.com/10.1007/978-3-319-27610-6.

Kimmel, C.B. et al., 1995. Stages of embryonic development of the zebrafish. *Developmental dynamics : an official publication of the American Association of Anatomists*, 203(3), pp.253–310.

Kirby, B.B. et al., 2006. In vivo time-lapse imaging shows dynamic oligodendrocyte progenitor behavior during zebrafish development. *Nature neuroscience*, 9(12), pp.1506–1511.

Kishimoto, N., Shimizu, K. & Sawamoto, K., 2012. Neuronal regeneration in a zebrafish model of adult brain injury. *Disease Models & Mechanisms*, 5(2), pp.200–209.

Knapik, E.W., 2000. ENU mutagenesis in zebrafish - From genes to complex diseases. *Mammalian Genome*, 11(7), pp.511–519.

Kolb, S.J. & Kissel, J.T., 2011. Spinal muscular atrophy: a timely review. *Archives of neurology*, 68(8), pp.979–84. Available at:

http://archneur.jamanetwork.com/article.aspx?articleid=1107831.

Korhonen, L. & Lindholm, D., 2004. The ubiquitin proteasome system in synaptic and axonal degeneration: A new twist to an old cycle. *Journal of Cell Biology*, 165(1), pp.27–30.

Koster, R.W. & Fraser, S.E., 2006. FGF Signaling Mediates Regeneration of the Differentiating Cerebellum through Repatterning of the Anterior Hindbrain and Reinitiation of Neuronal Migration. *The Journal of Neuroscience*, 26(27), pp.7293–7304.

Kuscha, V., Frazer, S.L., et al., 2012. Lesion-induced generation of interneuron cell types in specific dorsoventral domains in the spinal cord of adult zebrafish. *Journal of Comparative Neurology*, 520(16), pp.3604–3616.

Kuscha, V., Barreiro-Iglesias, A., et al., 2012. Plasticity of tyrosine hydroxylase and serotonergic systems in the regenerating spinal cord of adult zebrafish. *Journal of Comparative Neurology*, 520(5), pp.933–951.

Kuyinu, E.L. et al., 2016. Animal models of osteoarthritis: classification, update, and measurement of outcomes. *Journal of orthopaedic surgery and research*, 11(1), p.19. Available at: http://www.scopus.com/inward/record.url?eid=2-s2.0-84956823713&partnerID=tZOtx3y1.

Kwon, D.Y. et al., 2013. The E3 ubiquitin ligase mind bomb 1 ubiquitinates and promotes the degradation of survival of motor neuron protein. *Molecular biology of the cell*, 24, pp.1863–71. Available at: http://www.pubmedcentral.nih.gov/articlerender.fcgi?artid=3681692&tool=pmcentrez&rendertype=abstract.

Kwon, J.M. & Goate, a M., 2000. The candidate gene approach. *Alcohol research & health : the journal of the National Institute on Alcohol Abuse and Alcoholism*, 24(3), pp.164–168.

Kyrylkova, K. et al., 2012. Detection of apoptosis by TUNEL assay. *Methods in molecular biology (Clifton, N.J.)*, 887(41–7). Available at: http://link.springer.com/10.1007/978-1-61779-860-3.

Laugwitz, K. et al., 2005. Postnatal isl1 1 cardioblasts enter fully differentiated cardiomyocyte lineages. *Nature*, 433, pp.647–653.

Lepilina, A. et al., 2006. A Dynamic Epicardial Injury Response Supports Progenitor

Cell Activity during Zebrafish Heart Regeneration. *Cell*, 127(3), pp.462–464.

Lewcock, J.W. et al., 2007. The Ubiquitin Ligase Phr1 Regulates Axon Outgrowth through Modulation of Microtubule Dynamics. *Neuron*, 56(4), pp.604–620.

lez-Rosa, J.M.G.A. & Mercader, N., 2012. Cryoinjury as a myocardial infarction model for the study of cardiac regeneration in the zebrafish. *Nature protocols*, 7(4), pp.782–788. Available at: http://dx.doi.org/10.1038/nprot.2012.025%5Cnpapers2://publication/doi/10.1038/nprot.2012.025.

Li, P., White, R.M. & Zon, L.I., 2011. *Transplantation in Zebrafish* Third Edit., Elsevier Inc. Available at: http://dx.doi.org/10.1016/B978-0-12-381320-6.00017-5.

Lieschke, G.J. & Currie, P.D., 2007. Animal models of human disease: zebrafish swim into view. *Nature reviews. Genetics*, 8(5), pp.353–367.

Lin, G. & Slack, J.M.W., 2008. Requirement for Wnt and FGF signaling in Xenopus tadpole tail regeneration. *Developmental Biology*, 316(2), pp.323–335.

Liu, Z. et al., 2007. Induction of oligodendrocyte differentiation by Olig2 and Sox10: Evidence for reciprocal interactions and dosage-dependent mechanisms. *Developmental Biology*, 302(2), pp.683–693.

Lowery, L.A. & Sive, H., 2004. Strategies of vertebrate neurulation and a re-evaluation of teleost neural tube formation. *Mechanisms of Development*, 121(10), pp.1189–1197.

Lukovic, D. et al., 2015. Complete rat spinal cord transection as a faithful model of spinal cord injury for translational cell transplantation. *Scientific reports*, 5, p.9640.

Martino, G. et al., 2013. BRAIN REGENERATION IN PHYSIOLOGY AND PATHOLOGY : THE IMMUNE SIGNATURE DRIVING THERAPEUTIC PLASTICITY OF NEURAL STEM CELLS. *Physiological Reviews*, 91(4), pp.1281–1304.

Mchedlishvili, L. et al., 2012. Reconstitution of the central and peripheral nervous system during salamander tail regeneration. *PNAS*, 109(34), pp.E2258–E2266.

McWhorter, M.L. et al., 2003. Knockdown of the survival motor neuron (Smn) protein in zebrafish causes defects in motor axon outgrowth and pathfinding.

Journal of Cell Biology, 162(5), pp.919–931.

Mehta, N., Loria, P.M. & Hobert, O., 2004. A Genetic Screen for Neurite Outgrowth Mutants in Caenorhabditis elegans Reveals a New Function for the F-box Ubiquitin Ligase Component LIN-23. *Genetics*, 166(3), pp.1253–1267.

Menelaou, E. & Svoboda, K.R., 2009. Secondary motoneurons in juvenile and adult zebrafish: Axonal pathfinding errors caused by embryonic nicotine exposure. *Journal of Comparative Neurology*, 512(3), pp.305–322.

Mercola, M. et al., 2011. Cardiac muscle regeneration : lessons from development Cardiac muscle regeneration : lessons from development. *GENES & DEVELOPMENT*, 25, pp.299–309.

Minevich, G. et al., 2012. CloudMap: a cloud-based pipeline for analysis of mutant genome sequences. *Genetics*, 192(4), pp.1249–1269.

Mizuno, N. et al., 1999. Lens regeneration in Xenopus is not a mere repeat of lens development , with respect to crystallin gene expression. *Differentiation*, 64(3), pp.143–149. Available at: http://dx.doi.org/10.1046/j.1432-0436.1999.6430143.x.

Mokalled, M.H. et al., 2016. Injury-induced ctgfa directs glial bridging and spinal cord regeneration in zebrafish. *Science*, 354(6312), pp.630–634.

Moresco, E.M.Y., Li, X. & Beutler, B., 2013. Going forward with genetics: recent technological advances and forward genetics in mice. *The American journal of pathology*, 182(5), pp.1462–1473.

Mothe, A.J. & Tator, C.H., 2005. Proliferation, migration, and differentiation of endogenous ependymal region stem/progenitor cells following minimal spinal cord injury in the adult rat. *Neuroscience*, 131(1), pp.177–187.

Mullins, M.C. et al., 1994. Large-scale mutagenesis in the zebrafish: in search of genes controlling development in a vertebrate. *Curr Biol*, 4(3), pp.189–202. Available at: http://ac.els-cdn.com/S0960982200000488/1-s2.0-S0960982200000488-main.pdf?_tid=ad37d15e-360f-11e5-bf6f-00000aacb362&acdnat=1438187846_03a466a4c8466c6b5f5d10419f6ebde7.

Muneoka, K. et al., 2008. Mammalian Regeneration and Regenerative Medicine. *Birth Defects Res C Embryo Today*, 84(4), pp.265–280.

Muñoza, R. et al., 2015. Regeneration of Xenopus laevis spinal cord requires Sox2/3

expressing cells. *Developmental Biology*, 408(2), pp.229–243.

Münzel, E.J. et al., 2014. Zebrafish regenerate full thickness optic nerve myelin after demyelination, but this fails with increasing age. *Acta neuropathologica communications*, 2, p.77. Available at: http://www.pubmedcentral.nih.gov/articlerender.fcgi?artid=4164766&tool=pmcentrez&rendertype=abstract.

Myers, P.Z., Eisen, J.S. & Westerfield, M., 1986. Development and axonal outgrowth of identified motoneurons in the zebrafish. *The Journal of neuroscience : the official journal of the Society for Neuroscience*, 6(8), pp.2278–89. Available at: http://www.ncbi.nlm.nih.gov/pubmed/3746410.

Mysiak, K.S., 2015. *The role of monoamines in the development and regeneration of the zebrafish spinal cord*.

Nagy, A. et al., 2003. Tailoring the genome: the power of genetic approaches. *Nature genetics*, 33 Suppl, pp.276–284.

Nair, S. & Pelegri, F.J., 2011. Practical approaches for implementing forward genetic strategies in zebrafish. *Methods in molecular biology (Clifton, N.J.)*, 770, pp.185–209.

Nave, K., 2010. Myelination and support of axonal integrity by glia. *Nature*, pp.244–252.

Nelson, B.R. et al., 2004. NELL2 promotes motor and sensory neuron differentiation and stimulates mitogenesis in DRG in vivo. *Developmental Biology*, 270(2), pp.322–335.

Nguyen, N. et al., 2011. Random mutagenesis of the mouse genome: a strategy for discovering gene function and the molecular basis of disease. *American journal of physiology. Gastrointestinal and liver physiology*, 300(1), pp.G1-11.

Nijhawan, D. et al., 2012. Cancer Vulnerabilities Unveiled by Genomic Loss. *CELL*, 150(4), pp.842–854. Available at: http://dx.doi.org/10.1016/j.cell.2012.07.023.

Nusslein-Volhard, C., 2012. The zebrafish issue of Development. *Development*, 139(22), pp.4099–4103.

Nusslein-Volhard, C. & Dahm, R., 2002. *Zebrafish: A Practical Approach*, Oxford University Press, USA.

Ohnmacht, J. et al., 2016. Spinal motor neurons are regenerated after mechanical

lesion and genetic ablation in larval zebrafish. *Development*, pp.1–11. Available at: http://dev.biologists.org/cgi/doi/10.1242/dev.129155.

Ott, H. et al., 2001. Function of Neurolin (DM-GRASP/SC-1) in guidance of motor axons during zebrafish development. *Developmental biology*, 235(1), pp.86–97.

Palaisa, K. a & Granato, M., 2007. Analysis of zebrafish sidetracked mutants reveals a novel role for Plexin A3 in intraspinal motor axon guidance. *Development (Cambridge, England)*, 134(18), pp.3251–3257.

Panayiotou, E. & Malas, S., 2013. Adult spinal cord ependymal layer: a promising pool of quiescent stem cells to treat spinal cord injury. *Frontiers in physiology*, 4(November), p.340. Available at: http://www.pubmedcentral.nih.gov/articlerender.fcgi?artid=3842874&tool=pmcentrez&rendertype=abstract.

Panzer, J.A. et al., 2005. Neuromuscular synaptogenesis in wild-type and mutant zebrafish. *Developmental Biology*, 285(2), pp.340–357.

Park, H.-C. et al., 2002. olig2 Is Required for Zebrafish Primary Motor Neuron and Oligodendrocyte Development. *Developmental Biology*, 248(2), pp.356–368. Available at: http://www.sciencedirect.com/science/article/pii/S0012160602907384%5Cnhttp://www.sciencedirect.com/science/article/pii/S0012160602907384/pdf?md5=08e7f83a311c253adf7b3bfc61de28ba&pid=1-s2.0-S0012160602907384-main.pdf.

Park, H.C. et al., 2007. An olig2 reporter gene marks oligodendrocyte precursors in the postembryonic spinal cord of zebrafish. *Developmental Dynamics*, 236(12), pp.3402–3407.

Patestas, M. & Gartner, L.P., 2013. *A Textbook of Neuroanatomy*, John Wiley & Sons.

Percival, J.M. et al., 2012. Sildenafil reduces respiratory muscle weakness and fibrosis in the mdx mouse model of Duchenne muscular dystrophy. *The Journal of pathology*, 228(1), pp.77–87. Available at: http://www.pubmedcentral.nih.gov/articlerender.fcgi?artid=4067455&tool=pmcentrez&rendertype=abstract.

Pfaff, S. & Kintner, C., 1998. Neuronal diversification: development of motor neuron subtypes. *Current opinion in neurobiology*, 8(1), pp.27–36.

Pfefferli, C. et al., 2014. Specific NuRD components are required for fin regeneration in zebrafish. *BMC biology*, 12(1), p.30. Available at: http://www.pubmedcentral.nih.gov/articlerender.fcgi?artid=4038851&tool=pmcentrez&rendertype=abstract.

Pike, S.H., Melancon, E.F. & Eisen, J.S., 1992. Pathfinding by zebrafish motoneurons in the absence of normal pioneer axons. *Development*, 114(4), pp.825–831. Available at: http://dev.biologists.org/content/114/4/825%5Cnhttp://dev.biologists.org/content/114/4/825.full.pdf%5Cnhttp://www.ncbi.nlm.nih.gov/pubmed/1618146.

Plazas, P. V, Nicol, X. & Spitzer, N.C., 2013. Activity-dependent competition regulates motor neuron axon pathfinding via PlexinA3. *Proceedings of the National Academy of Sciences of the United States of America*, 110(4), pp.1524–9. Available at: http://www.pubmedcentral.nih.gov/articlerender.fcgi?artid=3557035&tool=pmcentrez&rendertype=abstract.

Porrello, E.R. et al., 2013. Regulation of neonatal and adult mammalian heart regeneration by the miR-15 family. *PNAS*, 110(1), pp.187–192.

Poss, K.D., 2010. Advances in understanding tissue regenerative capacity and mechanisms in animals. *Nat Rev Genet*, 11(10), pp.710–722.

Poss, K.D., Wilson, L.G. & Keating, M.T., 2002. Heart Regeneration in Zebrafish. *Science*, 298(5601), pp.2188–2190.

Puliti, A. et al., 2007. Teaching molecular genetics: Chapter 4 - Positional cloning of genetic disorders. *Pediatric Nephrology*, 22(12), pp.2023–2029.

Quarrie, S. a et al., 1999. Bulk segregant analysis with molecular markers and its use for improving drought resistance in maize. *Journal of Experimental Botany*, 50(337), pp.1299–1306. Available at: http://www.jexbot.oupjournals.org/cgi/doi/10.1093/jexbot/50.337.1299.

Ravanelli, A.M. & Appel, B., 2015. Motor neurons and oligodendrocytes arise from distinct cell lineages by progenitor recruitment. , pp.1–13.

Reimer, M.M. et al., 2013. Dopamine from the Brain Promotes Spinal Motor Neuron Generation during Development and Adult Regeneration. *Developmental Cell*, 25(5), pp.478–491. Available at: http://dx.doi.org/10.1016/j.devcel.2013.04.012.

Reimer, M.M. et al., 2008. Motor neuron regeneration in adult zebrafish. *The Journal of neuroscience : the official journal of the Society for Neuroscience*, 28(34), pp.8510–8516.

Reimer, M.M. et al., 2009. Sonic hedgehog is a polarized signal for motor neuron regeneration in adult zebrafish. *The Journal of neuroscience : the official journal of the Society for Neuroscience*, 29(48), pp.15073–15082.

Rinkevich, B. & Rinkevich, Y., 2013. The "Stars and Stripes" Metaphor for Animal Regeneration-Elucidating Two Fundamental Strategies along a Continuum. *Cells*, 2(1), pp.1–18. Available at: http://www.pubmedcentral.nih.gov/articlerender.fcgi?artid=3972663&tool=pmcentrez&rendertype=abstract.

Rodino-Klapac, L.R. & Beattie, C.E., 2004. Zebrafish topped is required for ventral motor axon guidance. *Developmental Biology*, 273(2), pp.308–320.

Rowitch, D.H., 2004. GLIAL SPECIFICATION IN THE VERTEBRATE NEURAL TUBE. , 5(May).

Saita, S. et al., 2014. Role of the ANKMY2-FKBP38 axis in regulation of the sonic hedgehog (Shh) signaling pathway. *Journal of Biological Chemistry*, 289(37), pp.25639–25654.

Sander, J.D. & Joung, J.K., 2014. CRISPR-Cas systems for editing, regulating and targeting genomes. *Nature biotechnology*, 32(4), pp.347–55. Available at: http://dx.doi.org/10.1038/nbt.2842.

Santoriello, C. & Zon, L.I., 2012. Hooked ! Modeling human disease in zebrafish. *Science in medicine*, 122(7), pp.2337–2343.

Schneeberger, K., 2014. Using next-generation sequencing to isolate mutant genes from forward genetic screens. *Nature reviews. Genetics*, 15(August), pp.662–676. Available at: http://www.nature.com/doifinder/10.1038/nrg3745%5Cnhttp://www.ncbi.nlm.nih.gov/pubmed/25139187.

Seredick, S.D. et al., 2012. Zebrafish Mnx proteins specify one motoneuron subtype and suppress acquisition of interneuron characteristics. *Neural development*, 7(1), p.35. Available at: http://www.pubmedcentral.nih.gov/articlerender.fcgi?artid=3570319&tool=pmc

entrez&rendertype=abstract.

Shaw, P.J., 1999. Motor neurone disease. *BMJ (Clinical research ed.)*, 318(7191), pp.1118–21. Available at: http://www.pubmedcentral.nih.gov/articlerender.fcgi?artid=1115517&tool=pmcentrez&rendertype=abstract.

Shen, C.-N. et al., 2003. Transdifferentiation of pancreas to liver. *Mechanisms of Development*, 120(1), pp.107–116.

Shimizu, I. et al., 1990. Anatomical and functional recovery following spinal cord transection in the chick embryo. *J Neurobiol*, 21(6), pp.918–937. Available at: http://www.ncbi.nlm.nih.gov/entrez/query.fcgi?cmd=Retrieve&db=PubMed&dopt=Citation&list_uids=2077104.

Shirasaki, R. & Pfaff, S.L., 2002. Transcriptional codes and the control of neuronal identity. *Annual review of neuroscience*, 25, pp.251–281.

Silva, N.A. et al., 2014. From basics to clinical: A comprehensive review on spinal cord injury. *Progress in Neurobiology*, 114, pp.25–57.

Simons, M. & Trajkovic, K., 2006. Neuron-glia communication in the control of oligodendrocyte function and myelin biogenesis.

Sims, D. et al., 2014. Sequencing depth and coverage: key considerations in genomic analyses. *Nature reviews. Genetics*, 15(2), pp.121–32. Available at: http://www.ncbi.nlm.nih.gov/pubmed/24434847.

Slack, J.M.W., Lin, G. & Chen, Y., 2008. The Xenopus tadpole : a new model for regeneration research. *Cell Mol Life Sci*, 65(1), pp.54–63.

Solnica-Krezel, L., Schier, A.F. & Driever, W., 1994. Efficient recovery of ENU-induced mutations from the zebrafish germline. *Genetics*, 136(4), pp.1401–1420.

Stewart, A.M. et al., 2014. Zebrafish models for translational neuroscience research: from tank to bedside. *Trends in neurosciences*, 37(5), pp.264–278.

Stifani, N., 2014. Motor neurons and the generation of spinal motor neuron diversity. *Frontiers in Cellular Neuroscience*, 8(October), pp.1–22. Available at: http://journal.frontiersin.org/article/10.3389/fncel.2014.00293/abstract.

Stoick-Cooper, C.L. et al., 2007. Distinct Wnt signaling pathways have opposing roles in appendage regeneration. *Development*, 134, pp.479–489.

Streisinger, G. et al., 1981. Production of clones of homozygous diploid zebra fish

(Brachydanio rerio). *Nature*, 291(5813), pp.293–296.

Sun, T. et al., 2001. Olig bHLH proteins interact with homeodomain proteins to regulate cell fate acquisition in progenitors of the ventral neural tube. *Current Biology*, 11(18), pp.1413–1420.

Takada, N., Kucenas, S. & Appel, B., 2010. Sox10 is necessary for oligodendrocyte survival following axon wrapping. *Glia*, 58(8), pp.996–1006.

Tanaka, E. & Reddien, P.W., 2011. The cellular basis for animal regeneration. *Dev Cell*, 21(1), pp.172–185.

Tanaka, E.M. & Ferretti, P., 2009. Considering the evolution of regeneration in the central nervous system. *Nature Reviews Neuroscience*, 10, pp.713–723. Available at: http://dx.doi.org/10.1038/nrn2707.

Taniguchi, Y. et al., 2008. Spinal cord is required for proper regeneration of the tail in Xenopus tadpoles. *Develop. Growth Differ*, 50, pp.109–120.

Tashiro, Y. et al., 2012. Motor neuron-specific disruption of proteasomes, but not autophagy, replicates amyotrophic lateral sclerosis. *Journal of Biological Chemistry*, 287(51), pp.42984–42994.

Thisse, C. & Thisse, B., 2008. High-resolution in situ hybridization to whole-mount zebrafish embryos. *Nature protocols*, 3(1), pp.59–69.

Thuret, S., Moon, L.D.F. & Gage, F.H., 2006. Therapeutic interventions after spinal cord injury. *Nature reviews. Neuroscience*, 7(8), pp.628–43.

Tierney, M.B. & Lamour, K.H., 2005. The Plant Health Instructor. *The Plant Health Instructor.*, pp.1–7. Available at: http://www.apsnet.org/edcenter/advanced/topics/Pages/ReverseGeneticTools.aspx.

Torkildsen, O. et al., 2008. The cuprizone model for demyelination. *Acta Neurologica Scandinavica*, 117(SUPPL. 188), pp.72–76.

Uemura, O. et al., 2005. Comparative functional genomics revealed conservation and diversification of three enhancers of the isl1 gene for motor and sensory neuron-specific expression. , 278, pp.587–606.

Vartanian, T., Fischbach, G. & Miller, R., 1999. Failure of spinal cord oligodendrocyte development in mice lacking neuregulin. , 96(January), pp.731–735.

Vervoort, M., 2011. Regeneration and Development in Animals. *Biological Theory*, 6(1), pp.25–35.

Voz, M.L. et al., 2012. Fast homozygosity mapping and identification of a zebrafish enu-induced mutation by whole-genome sequencing. *PLoS ONE*, 7(4), pp.1–10.

Wang, Y. et al., 2007. Nanos Function Is Essential for Development and Regeneration of Planarian Germ Cells. *Proc Natl Acad Sci U S A*, 104(14), pp.5901–5906. Available at: http://www.ncbi.nlm.nih.gov/entrez/query.fcgi?db=pubmed&cmd=Retrieve&dopt=AbstractPlus&list_uids=17376870.

Watts, R.J., Hoopfer, E.D. & Luo, L., 2003. Axon Pruning during Drosophila Metamorphosis : Evidence for Local Degeneration and Requirement of the Ubiquitin-Proteasome System. *Neuron*, 38, pp.871–885.

Westerfield, M., 1995. *THE ZEBRAFISH BOOK A guide for the Laboratory Use of Zebrafish (Danio rerio)*,

Whitehead, G.G. et al., 2005. Fgf20 Is Essential for Initiating Zebrafish Fin Regeneration. *Science (New York, N.Y.)*, 310(5756), pp.1957–1960.

Wilken, M.S. & Reh, T.A., 2016. Retinal regeneration in birds and mice. *Current Opinion in Genetics & Development*, 40, pp.57–64. Available at: http://dx.doi.org/10.1016/j.gde.2016.05.028.

Wu, S.M., Chien, K.R. & Mummery, C., 2008. Essay Origins and Fates of Cardiovascular Progenitor Cells. *CELL*, 132(4), pp.537–543.

Yaguchi, Y. et al., 2009. Fibroblast Growth Factor (FGF) Gene Expression in the Developing Cerebellum Suggests Multiple Roles for FGF Signaling During Cerebellar Morphogenesis and Development. *Developmental Dynamics*, 238(8), pp.2058–2072.

Yamada, T. et al., 1993. Control of cell pattern in the neural tube: Motor neuron induction by diffusible factors from notochord and floor plate. *Cell*, 73(4), pp.673–686.

Yamamoto, S. et al., 2001. Proliferation of parenchymal neural progenitors in response to injury in the adult rat spinal cord. *Experimental neurology*, 172(1), pp.115–27.

Yi, J.J. & Ehlers, M.D., 2007. Emerging roles for ubiquitin and protein degradation

in neuronal function. *Pharmacological reviews*, 59(1), pp.14–39.

Zeller, J. & Granato, M., 1999. The zebrafish diwanka gene controls an early step of motor growth cone migration. *Development (Cambridge, England)*, 126(15), pp.3461–3472.

Zeng, C. et al., 2010. Evaluation of 5-ethynyl-2′-deoxyuridine staining as a sensitive and reliable method for studying cell proliferation in the adult nervous system. , pp.21–32.

Zhang, J. et al., 2004. Zebrafish unplugged reveals a role for muscle- specific kinase homologs in axonal pathway choice. , 7(12), pp.1303–1309.

Zhang, J. & Granato, M., 2000. The zebrafish unplugged gene controls motor axon pathway selection. , 2111, pp.2099–2111.

Zhong, Z. et al., 2012. Chondrolectin mediates growth cone interactions of motor axons with an intermediate target. *The Journal of neuroscience : the official journal of the Society for Neuroscience*, 32(13), pp.4426–39. Available at: http://www.jneurosci.org/content/32/13/4426.

Zhou, Q., Choi, G. & Anderson, D.J., 2001. The bHLH transcription factor Olig2 Promotes oligodendrocyte differentiation in collaboration with Nkx2.2. *Neuron*, 31(5), pp.791–807.

Zhou, Y. & Zon, L.I., 2011. The Zon laboratory guide to positional cloning in zebrafish. *Methods in Cell Biology*, 104, pp.287–309.